OPTIMAL BATTERY SIZING FOR ELECTRIC VEHICLES CONSIDERING BATTERY AGEING TO MINIMIZE THE TOTAL COST OF THE POWER TRAIN COMPONENTS AND CONSUMED ENERGY

A THESIS SUBMITTED TO
THE GRADUATE SCHOOL OF NATURAL AND APPLIED SCIENCES
OF
MIDDLE EAST TECHNICAL UNIVERSITY

BY
ALİ GEZER

IN PARTIAL FULFILLMENT OF THE REQUIREMENTS
FOR
THE DEGREE OF MASTER OF SCIENCE
IN
ELECTRICAL AND ELECTRONICS ENGINEERING

AUGUST 2021

Approval of the thesis:

OPTIMAL BATTERY SIZING FOR ELECTRIC VEHICLES CONSIDERING BATTERY AGEING TO MINIMIZE THE TOTAL COST OF THE POWER TRAIN COMPONENTS AND CONSUMED ENERGY

submitted by **ALİ GEZER** in partial fulfillment of the requirements for the degree of **Master of Science in Electrical and Electronics Engineering Department, Middle East Technical University** by,

Prof. Dr. Halil Kalıpçılar
Dean, Graduate School of **Natural and Applied Sciences** _____

Prof. Dr. İlkay Ulusoy
Head of Department, **Electrical and Electronics Engineering** _____

Prof. Dr. Baki Zafer Ünver
Supervisor, **Electrical and Electronics Engineering** _____

Examining Committee Members:

Assist. Prof. Dr. Emine Bostancı
Electrical and Electronics Engineering, METU _____

Prof. Dr. Baki Zafer Ünver
Electrical and Electronics Engineering, METU _____

Prof. Dr. Işık Çadırcı
Electrical and Electronics Engineering, Hacettepe Üni. _____

Prof. Dr. Kemal Leblebicioğlu
Electrical and Electronics Engineering, METU _____

Assoc. Prof. Dr. Murat Göl
Electrical and Electronics Engineering, METU _____

Date: 04.08.2021

I hereby declare that all information in this document has been obtained and presented in accordance with academic rules and ethical conduct. I also declare that, as required by these rules and conduct, I have fully cited and referenced all material and results that are not original to this work.

Name, Surname : Ali Gezer

Signature :

ABSTRACT

OPTIMAL BATTERY SIZING FOR ELECTRIC VEHICLES CONSIDERING BATTERY AGEING TO MINIMIZE THE TOTAL COST OF THE POWER TRAIN COMPONENTS AND CONSUMED ENERGY

Gezer, Ali
MS, Department of Electrical and Electronics Engineering
Supervisor: Prof. Dr. Baki Zafer Ünver

August 2021, 143 pages

Due to environmental issues such as emission of carbon gases, massive energy consumption, depleting natural resources regarding the internal combustion engine (ICE) based vehicles, electric vehicles (EVs) have caught more and more attention. To make EVs feasible and common, the batteries' high cost and performance degradation problems have to be overcome. The degradation of the battery regarding both energy capacity and power capability is highly dependent on conditions of utilization. Inspired by the literature, an electric vehicle model and an energy utilization and battery ageing (both calendar ageing and cycle ageing) model are proposed. Then, these models are validated considering a battery electric vehicle (BEV) in the market. The models are used to optimize the battery size to decrease the total cost of the power train and consumed energy over the battery's lifespan considering Worldwide Harmonized Light Vehicles Test Procedure (WLTP). Finally, the effects of possible future improvements in the technology or alterations in user preferences regarding ageing mechanisms, annual distance, price of electricity, specific cost of the battery pack, specific mass of battery pack, specific cost of electric motor (EM) and inverter, specific mass of EM and inverter, and test procedures on the battery size optimization are investigated.

Keywords: Electric Vehicles, Li-ion Battery, Battery Ageing, Battery Size Optimization

ÖZ

ELEKTRİKLİ ARAÇLARDA TOPLAM GÜÇ AKTARMA BİLEŞENİ VE TÜKETİLEN ENERJİ MALİYETİNİ EN AZA İNDİRMEK İÇİN OPTİMUM BATARYA BOYUTUNUN BATARYA YAŞLANMASI GÖZETİLEREK BELİRLENMESİ

Gezer, Ali
MS, Department of Electrical and Electronics Engineering
Supervisor: Prof. Dr. Baki Zafer Ünver

Ağustos 2021, 143 sayfa

İçten yanmalı motor tabanlı araçlarda karbon gazı salınımı, yoğun enerji tüketimi, doğal kaynakların tükenmesi gibi çevresel sorunlar nedeniyle elektrikli araçlar giderek daha fazla ilgi görmektedir. Elektirikli araçları uygulanabilir ve yaygın hale getirmek için bataryaların yüksek maliyet ve performans düşüşü sorunlarının üstesinden gelinmesi gerekiyor. Bataryanın hem enerji kapasitesi hem de güç kapasitesi açısından yaşlanması, büyük ölçüde kullanım koşullarına bağlıdır. Literatürden esinlenerek, bir elektrikli araç modeli ve bir enerji kullanımı ve batarya yaşlanma (hem takvim yaşlanması hem de çevrim yaşlanması) modeli önerilmiştir. Daha sonra bu modeller piyasadaki bir elektrikli araç dikkate alınarak doğrulanır. Modeller, "Worldwide Harmonized Light Vehicles Test Procedure (WLTP)" dikkate alınarak güç aktarma sisteminin ve pil ömrü boyunca tüketilen enerjinin toplam maliyetini azaltmak için pil boyutunu optimize etmek için kullanılır. Son olarak, yaşlanma mekanizmaları, yıllık mesafe, elektrik fiyatı, batarya paketinin birim maliyeti, batarya paketinin birim kütlesi, elektrik motoru ve eviricinin birim maliyeti, elektrik motoru ve eviricinin birim kütlesi, ve test prosedürleri ile ilgili olarak teknolojideki olası gelişmelerin ve kullanıcı tercihlerindeki değişikliklerin batarya boyutu optimizasyonuna etkileri incelenmiştir.

Anahtar Kelimeler: Elektrikli Araçlar, Li-ion Bataryalar, Batarya Yaşlanması, Batarya Boyut Optimizasyonu

To My Family and My Friends

ACKNOWLEDGEMENTS

I would like to express my deepest gratitude to my supervisor Prof. Dr. Baki Zafer Ünver for his comments, support, advices, guidance, and encouragement throughout my research. I would also like to thank Asist. Prof. Dr. Emine Bostancı for helping me to gather, analyse, and prepare the necessary information to complete this work.

I wish to thank ASELSAN for enabling me to conduct this academic study together with my work at ASELSAN.

I wish to thank TÜBİTAK BİDEB for their supports during this thesis work.

I specially thank to my colleagues from Power and Control Systems Department in ASELSAN for their continuous support and encouragement, but most importantly for their sincere friendship.

I would like to extend my sincere thanks to the ZEYTİN family for guidance and encouragement at the beginning of my school life, and ongoing support throughout my life.

I wish to express my most profound appreciation to my family for their patience and support throughout my life.

My heartfelt thanks go to İrem Kül not only for her support, motivation and understanding during this thesis work but also for every moment she was in my life.

TABLE OF CONTENTS

LIST OF TABLES

TABLES

LIST OF FIGURES

FIGURES

CHAPTER 1

INTRODUCTION

Environmental issues such as emission of carbon gases, massive energy consumption, and depleting natural resources are public concern. Although factories and industries seem to be the main cause of these issues, the internal combustion engine that generates power by burning a mix of fuel and gases based vehicles are significant too [1]. Consequently, electric vehicles (EVs) have caught more and more attention due to environmental concerns, because they use electrical energy that can be generated by renewable sources. Moreover, EVs use energy more efficiently as compared to internal combustion engine-based vehicles (ICEVs). For example, EVs are so designed that the energy flows bidirectionally at the time of running and braking. By regenerative braking, some of the energy typically lost in ICEVs during braking is used to charge the internal battery.

EVs date back to the 1890s. In those days, they were powered by lead-acid batteries and were gaining popularity and holding a substantial share in the market. However, in the 1910s, EVs lost the share and popularity after the invention of electric starter which eliminated the need for hand crank used in ICEVs. Also, the initiation of mass production of ICEVs made them more affordable. After a long break, EVs have started to come into prominence in the 1970s due to growing environmental concerns, high oil prices resulting from the oil crises in 1973 and 1979, and improvements in semiconductor switch and battery technologies. In the 1990s, nickel-metal hydride (NiMH) batteries which have higher energy and power density than the formerly used lead-acid batteries have been used in EVs. Soon after, lithium-ion (Li-ion) batteries have appeared in EVs in the 2000s. Today, EVs are getting growing market share with further improvements on these technologies day by day.

EVs are basically classified into five types: hybrid electric vehicles (HEVs), plug-in hybrid electric vehicles (PHEVs), fuel cell electric vehicles (FCEVs), battery electric vehicles (BEVs), and range-extended electric vehicles (REEVs). In addition to the above types, there are trucks, autobuses and even flying cars [2] using electricity as the energy source.

Unlike ICEVs that use only fossil fuel, some EVs have a secondary energy source. HEVs and PHEVs operate using both internal combustion engines and electric motors (EMs). While fossil fuel is their primary energy source, the on-board battery is their secondary energy source. The main difference of PHEVs and standard HEVs is that PHEVs have greater batteries and can be charged from an electrical grid. Resourcing the HEVs (refueling) and PHEVs (refueling and plug-in) are similar to ICEVs (refueling), so these types of EVs have gotten significant share in the market faster than the other types.

FCEVs operate using EMs and are powered by hydrogen (primary source) and on-board batteries (secondary source). They emit no harmful gases, only warm air and water vapor, but it is very problematic to store hydrogen in acceptable volumes. That requires using very high-pressure storage techniques and exceptional and expensive tubes. Besides, the chemical reaction between the stored hydrogen and oxygen in the air is strongly dependent on ambient conditions. Therefore, the electrical energy generation from such a chemical reaction can be quite unstable. Although there are some FCEVs [3] in the market, because of the above mentioned problems, they cannot take a substantial place. More improvements are needed to be achieved by chemists and FCEV developers to make them more common.

BEVs operate using EMs, and the on-board batteries are their only energy source. BEVs mainly suffer from the high cost of power train (EM, inverter, and battery), limited stored energy, and long times for recharging. Due to recent improvements in Li-ion battery production and battery utilization techniques, BEVs are taking more

and more place in the market nowadays. However, some more studies are needed to be conducted to make them more feasible and common.

Operation of REEVs is similar to BEVs, but they also include small gasoline tanks and generators to charge the main batteries thereby extending the range of the vehicles.

In the market, there exist a variety of EVs with different specifications [4]. Commonly, the total mass of EVs range from 1300 kg to 2500 kg, acceleration from 2.6 sec to 16 sec, top speed from 130 km/h to 260 km/h, and energy consumption from 15 kWh/100 km to 25 kWh/100 km.

Batteries in EVs are formed by parallel and series connection of Li-ion cells. The standard nominal voltage of a Li-ion cell varies from 2 V to 3.65 V depending on the type of chemistry [5], and each chemistry type shines out in terms of different aspects such as specific energy, specific power, safety, cost, and lifespan. The expected energy capacity of a Li-ion cell used in EVs varies from a few Wh to higher values. It is highly dependent on the size and type of the package such as cylindrical, prismatic and pouch [6]. Li-ion cells are connected in series depending on the desired nominal battery voltage and in parallel depending on the desired nominal battery capacity, so the number of cells included in the battery may range from a few hundred to a few thousand. Common nominal battery voltages range from 100 V to 200 V for hybrid vehicles and from 300 V to 800 V for BEVs. Higher voltages offer more power to be transferred with less loss over the same copper cable while requiring higher voltage rated components in the entire system. Typical battery capacities range from 0.5 kWh to 2 kWh for standard HEVs, from 4 kWh to 20 kWh for PHEVs, and from 30 kWh to 100 kWh for BEVs [7]. The travel range of EVs varies from 90 km to 570 km according to the Worldwide Harmonized Light Vehicles Test Procedure (WLTP). The detailed explanation of this procedure is given in Section 2.1.

Some essential problems regarding BEVs are limited battery energy storage because of the limited energy density of the chemistry, battery ageing, and high battery cost. Even though Li-ion batteries come to the forefront with their high energy and power densities as compared to other battery types such as lead-acid, nickel cadmium (NiCd), and NiMH batteries, the both densities of Li-ion batteries need to be improved for mobile applications especially for BEVs. Also, batteries degrade in terms of energy and power capacities in time which are highly dependent on the conditions they are utilized. In battery terminology, a battery health is expressed in terms of its state of health (SOH). Basically, the SOH is the ratio of the current energy capacity to the nominal energy capacity and measured in percentage points. The lifespan of a battery for mobile applications is generally defined as the time passed until the SOH of the battery becomes less than 70% or 80% depending on the application. There exist buses that use supercapacitor packs instead of Li-ion packs in urban transportation [8]; because, even though supercapacitors have less energy density than Li-ion batteries and suitable only within short ranges, their lifespan is longer. The list price of a BEV is too high to make it competitive against an ICEV. The battery cost causes the high cost, and as a matter of fact, the battery price ratio may reach up to 45% of the BEV list price. Since the dependency of BEVs to the battery is crucial, the research on the battery becomes more and more critical. In particular, the optimization with the objective of prolonging the working life while decreasing the high cost of the battery per km over the lifespan of the battery is of primary importance.

BEVs are charged by electric vehicle supply equipment which communicate with vehicles under the standards (IEC, ISO) and supply the electrical energy in a controlled way. The AC type of equipment uses standard household cables and sockets. The on-board charger converts AC to DC. The power rating varies from a few kW to 22 kW depending on the number of phases and the line capability. The DC charging requires infrastructure investment, but the power rating is quite large (up to 100 kW). The DC charging stations are not common and are shared among

hundreds of users. Depending on the supply equipment type and the type and capacity of BEV battery, the charging times varies for AC types from ~4 h to ~20 h and for DC types from ~1 h to ~4 h. Another type of charging, which is not on the market yet, is inductive (wireless) charging where the energy transfer occurs through magnetic coupling. Half of a transformer is placed on the BEV while the other half is put in the station.

Charging is a critical problem for BEVs. It is longer to charge a BEV compared to refuel an ICEV, and the fast charging DC stations for BEVs are quite rare compared to gasoline stations for ICEVs. In this work, the problems regarding recharging of BEVs are not considered.

1.1 Problem Definition

In order to increase the working life and decrease the high cost of the battery per km over the lifespan, ageing of Li-ion batteries should be well understood. A battery has two main performance parameters: energy capacity and power capability. The energy capacity describes the total available charge/discharge capacity subject to degradation, and the power capability is a measure of the deliverability of power throughout the lifetime. The degradation occurs both during operation and during stationary periods (no current flow). Hence, there are two types of battery ageing: cycle ageing regarding operation and calendar ageing regarding time. Depth-of-Discharge (DOD), Middle State-of-Charge (Mid-SOC), cumulative release ampere-hours, and charge and discharge current rates are the main stress factors for the battery cycle ageing. On the other hand, storage temperature, storage State-of-Charge (SOC) (the ratio of the charge level to the current energy capacity which is measured in percentage points), and time are the main stress factors for the battery calendar ageing. These factors and how they affect ageing will be explained in detail in Chapter 2 and Appendix A. Considering some factors of the calendar and/or cycle ageing, many studies have been conducted to improve the battery usage in EVs [9],[10]. In this work, it is aimed to study the effect of battery size on cycle ageing of

an EV battery. Battery size alterations imply addition or subtraction of cells in parallel keeping the series cell number constant. Therefore, changing the battery size will make a difference only in “Ah (or kWh) capacity” while keeping the rated battery voltage constant. It is important to notice that the battery size alteration directly affects the charge and discharge current rates which are the main factors for cycle ageing.

Regarding battery size optimization, some studies have been conducted in the literature. In [11], minimization of the total cost of ownership of the electric bus fleet is investigated by choosing the optimal battery size, the number of charging stations, and charging power for a given schedule, vehicle characteristics, and environmental conditions. However, the system is investigated as one and only, and the maximum battery utilization over the years is not considered as the primary objective. The development mainly arises from the reduced battery pack capacity and the higher utilization ratio of the charging infrastructure. Moreover, Ostadi and Kazerani [12] study the optimal sizing of battery to minimize the overall cost to the electric drivetrain, test procedures, and performance specifications, but the ageing of battery is not taken into account. In [13] the battery ageing is studied. The work bases on a specific case, a 3.5 t light-duty commercial electric truck and a particular route. Besides, an intelligent recharging strategy is worked depending on the SOC control in the way of delayed recharge. Although authors claim that “For this particular segment, carmakers have to offer adaptive vehicle in accordance with customers’ needs and constraints”, it is the fact that it would not be feasible and realizable to go into mass production for too many types of vehicles. Only a few types of vehicles can come into use such as long-range type, short-range type, etc.

Paralleling more cells to the battery reduces the discharge rate, and consequently the battery ageing slows down. Obviously, it is not feasible to increase the battery size too much due to the high initial cost of the battery and some physical limits on the board. Moreover, increase of the battery size will cause an enlargement of EM and

power converter's capability to overcome the mass increase and maintain the required EV performance. The energy consumption per km will also increase because of the rise in the total mass. In conclusion, the battery sizing directly affects the cycle ageing (not the calendar ageing), and one should look for the optimum size which will reduce the power train cost per km over the lifespan of the battery. The BEV is utilized to reveal the maximum improvement by battery size optimization while maintain practicalness of the work. The SOC is kept in favorable conditions in terms of calendar ageing. Regarding cycle ageing, cumulative release ampere-hours is based on WLTP. Thus, a more general study than the one in [13] based on an automobile and a standard test procedure can be conducted, and this would be a contributive study.

Unlike the specific study in [13], in this work, an electric car and a route based on the WLTP are studied. In addition, a battery ageing model is reformed. In the literature, most of the battery ageing models are not shared clearly; therefore, they cannot be used directly. On the other hand, the battery ageing model in [14] that discusses optimal sizing and management of lithium-ion batteries for photovoltaic plants is clear. Noting that the battery ageing model does not depend on the application, this model is taken as reference in a BEV application in this work. Since the ageing of a battery is slow in the model, the model parameters are updated using the real ageing data. These issues are explained in detail in Chapter 2. Moreover, some scenarios for the battery size optimization are run considering the possible future improvements in the technology or alterations in user preferences regarding ageing mechanisms, annual distance, price of electricity, specific cost of battery pack, specific mass of battery pack, specific cost of EM and inverter, specific mass of EM and inverter, and test procedures. While determining possible future improvements in the technology, new targets in the technology roadmap reports that are published by governments and agencies in order to accelerate the proliferation of EVs are considered [15],[16],[17].

In this work, according to the desired BEV specifications such as maximum vehicle speed, maximum time for acceleration from zero to top speed, maximum time for acceleration from 0 to 100 km/h, and range in km for the WLTP; the battery size and other BEV design parameters are determined. The SOC value during the operation is limited using the battery ageing studies and models given in the literature [18], and it is assumed that the conditions are kept in these favorable points. The ambient temperature for calendar ageing calculations is determined considering the average temperature values over a year for Istanbul. Then, using the resulting parameters, the energy consumption per km, the battery life and the power train initial cost are calculated and recorded according to the utilization of BEV as explained in Section 3.2. Finally, the battery size is optimized. The resulting changes in the energy consumption per km, the battery life prolongation, and the initial cost considering the power train component updates are calculated and recorded. In summary, taking the battery ageing and the WLTP into consideration, the optimum battery size to minimize the ratio of the sum of the consumed energy cost per km and the initial cost of power train (EM, inverter, and battery) per km over the lifespan of the battery is determined. The improvements are presented and the effects of the possible future improvements in the technology or alterations in user preferences are given.

1.2 Thesis Organization

In Chapter 1, the importance of the battery system and the battery size optimization for EVs in terms of usability and cost are discussed. The studies regarding the battery size optimization in the literature are presented. In Chapter 2, the vehicle dynamic model and the battery ageing model are introduced and the modification of the battery ageing model in [14] is explained. The vehicle dynamic and battery ageing models are validated at the end of the Chapter. In Chapter 3, the battery size optimization algorithm, the physical limitations of the vehicle body and the effects of battery size optimization are presented. In Chapter 4, the effects of possible future improvements in the technology or alterations in user preferences on the battery size optimization

are presented. In Chapter 5, the benefits of battery size optimization are discussed. Some details regarding the main structure and battery ageing phenomena for Li-ion batteries are given in Appendix A.

CHAPTER 2

VEHICLE DYNAMIC AND BATTERY AGEING MODELS

2.1 The Worldwide Harmonized Light Vehicles Test Procedure (WLTP)

In the vehicle industry, there exist some test procedures that provide speed versus time data for vehicles to measure the fuel consumption and the CO2 emissions as well as the pollutant emissions. While the results of CO2 and pollutant emission measurements are checked by the authorities, the fuel consumption results are beneficial for comparing the vehicles in the market by consumers. These procedures introduce driving profiles which contain a variety of driving phases: stops, acceleration and braking phases. In Europe, the New European Driving Cycle (NEDC) had been in use from the 1980s to September 2018. Since the NEDC was set by considering a theoretical driving profile, it was criticized in the middle of 2010s for its practicableness and its impact on reducing the CO2 emissions. The WLTP is a new, more realistic test procedure introduced by the European Commission. It is developed considering the real driving data gathered from all around the world. Different CO2 values for individual vehicles, higher speeds, more dynamic and realistic acceleration and deceleration phases are considered in the WLTP as compared to the NEDC. The WLTP includes low, medium, high, and extra high-speed parts to simulate urban, suburban, rural and highway scenarios, respectively. However, it still cannot account for driving behaviors, traffic conditions, weather conditions, vehicle loads, vehicle maintenance conditions, road bends, and road gradients [19]. Since September 2018, all new car registrations in Europe must use the WLTP [20]. There are different test procedures in some countries, for example, JC08 in Japan, SRC&SBC in USA and CUEDC&SPC240 in Australia, but the WLTP is widely admitted all over the world. Although fuel consumption and emission considerations of test procedures seem to be related only to ICEVs, EVs also use these procedures especially to express their driving ranges.

The WLTP classifies the vehicles according to their power to mass ratios (PMR): Class 1, PMR $\leq$ 22 W/kg; Class 2, 22 W/kg $<$ PMR $\leq$ 34 W/kg; Class 3, PMR $>$ 34 W/kg [21].

In this study, the PMRs of BEVs under consideration are in between 72 W/kg and 80 W/kg as can be calculated by using Table 3.1. Hence, they belong to Class 3. The speed versus time graph considered in this study is given in Figure 2.1, where the range is 23.27 km, the duration is 30 minutes, and the average and maximum speeds are 46.5 km/h and 131.3 km/h, respectively.

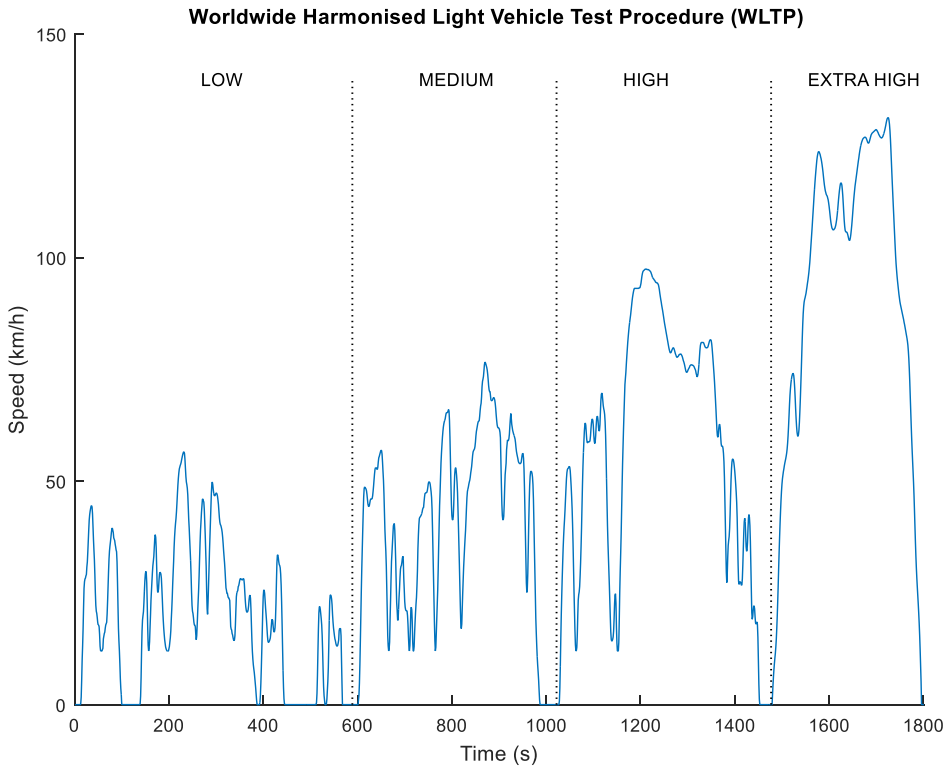

Figure 2.1. Speed vs time graph regarding WLTP [21]

2.2 The Vehicle Dynamic Model

The forces acting on a vehicle must be known in order to understand its dynamic characteristics. Basically, there are four types of forces affecting a vehicle: vertical, lateral, yaw (change of direction), and longitudinal forces [18]. In this study, the vehicle dynamic model is used not only to define the specifications of the vehicle components but also to calculate the power flow during the given test procedures. The WLTP does not account for vehicle loads and road bends. The longitudinal forces have the main effect on the power flow characteristics. Therefore, in this study, for simplicity, the vehicle is assumed to be a rigid body and only the longitudinal forces are considered when developing the vehicle dynamic model.

There are five types of longitudinal forces: aerodynamic drag, rolling friction, grading resistance, tractive, and braking forces[22]. The motive force generated by the engine (for ICEVs) or the EM (for EVs) must surpass all the other forces resisting the motion of the vehicle. Consequently, the longitudinal vehicle movement can be expressed by Equation 2.1 where F_t, F_{rt}, δ, M, and dV/dt stand for the tractive force, the resistive force, the mass factor, the vehicle mass and the linear acceleration respectively:

$$F_t - F_{rt} = \delta M \frac{dV}{dt} \quad \textbf{(2.1)}$$

In the above equation, F_t - F_{rt} is the net force on the vehicle. dV/dt is limited by the adhesion capability of the vehicle to the ground surface. This limitation should be investigated considering the adhesive coefficient of tires to the ground surface, whether the vehicle is front/all/rear-wheel drive and the load distribution during both braking and acceleration.

F_{rt} is the sum of the rolling resistance force, F_r, the aerodynamic drag force, F_w, and the grading resistance force, F_g:

$$F_{rt} = F_r + F_w + F_g \quad \textbf{(2.2)}$$

Since climbing is not considered in this study, F_g is set to zero when developing the vehicle dynamic model.

F_r can be expressed as in Equation 2.3 where f_r, M, g, and a stand for the coefficient of rolling resistance, the vehicle mass, the gravitational acceleration, and the road angle, respectively:

$$F_r = f_r M g cos(a) \quad \textbf{(2.3)}$$

Note that $cos(a)$ equals 1 since there is no climbing.

F_w can be expressed as in Equation 2.4 where ρ, A_f, C_d, V, and V_w stand for the air density, the frontal area, the coefficient of aerodynamic drag, the vehicle speed, and the wind speed, respectively:

$$F_w = \frac{1}{2} \rho A_f C_d (V + V_w)^2 \quad \textbf{(2.4)}$$

A vehicle is modelled according to the assumed set of requirements given in Table 2.1. The requirements on the maximum vehicle speed, the maximum time for acceleration from 0 to 100 km/h, and the maximum time for acceleration from 0 to the maximum vehicle speed are determinative for the rated power and torque values of the power train components. The requirement on the minimum range for the WLTP is determinative for the rated energy capacity of the battery.

Table 2.1. Vehicle Performance Requirements

Parameters	**Required Values**
Max. vehicle speed	180 km/h
Max. time for acceleration from 0 to max. vehicle speed	40 sec
Max. time for acceleration from 0 to 100 km/h	7.6 sec
Min. range for the WLTP	300 km

When modelling, more assumptions regarding the vehicle and component characteristics are required as given in Table 2.2.

Table 2.2. Vehicle and Component Characteristics

Parameters	**Assumed Values**
Body mass without powertrain	1500 kg
Initial value for maximum acceleration at top speed	0.49 m/sec^2
Driver mass	75 kg
Mass factor (mass increase due to acceleration of rotating masses)	1.05
Gravitational acceleration	9.8 m/sec^2
Frontal area	3.15 m^2
Aerodynamic drag coefficient	0.29
Air density	1.25 kg/m^3
Friction coefficient of tires	0.006
Radius of wheels	0.38 m
Gear ratio (EM to wheels	9.0478
Accessories consumption (fixed)	750 W
Adhesive coefficient of tires to ground surface	0.9
Load distribution during acceleration, Wfront/Wtotal	0.5
Load distribution during braking, Wfront/Wtotal	0.65
Efficiency of EM & inverter	92%
Efficiency of gearbox & differential	97%
Efficiency of battery pack	95%

The model gives the specifications on the power train components, i.e., the torque and power capability of the electric machine, the power capability of the inverter and the energy capacity and the power capability of the battery as outputs according to the given requirements. By using the specifications on the power train components, the mass, volume and cost of these components are obtained according to the expressions given in Table 2.3 [23]. Following most of the reference sources, the costs are presented in dollars.

Table 2.3. Expressions Regarding Powertrain Components

Parameters	**Expressions**
Specific cost of EM + inverter	$30/kW
Specific mass of EM + inverter	1.1 kW/kg
Battery pack specific cost	$250/kWh
Battery pack specific mass	(200 - 3 x Pbatt/Ebatt) Wh/kg +120 kg

The battery pack specific cost can be set to $(200 + 13 x P_{batt}/E_{batt})/kWh [23]. Since P_{batt}/E_{batt}, is generally in between 3.5 and 4 for BEVs, it can be approximately taken as $250/kWh not only for simplicity but also for compatibility with the scenarios explained in Chapter 4.

In the light of the above information regarding the longitudinal behavior of a vehicle and the aforementioned assumptions, a BEV with front-wheel drive is modelled considering the given requirements. The flowchart of modelling is provided in Figure 2.2, and the explanations regarding the main blocks in the flowchart are given in Sections 2.2.1, 2.2.2, 2.2.3, 2.2.4 and 2.2.5.

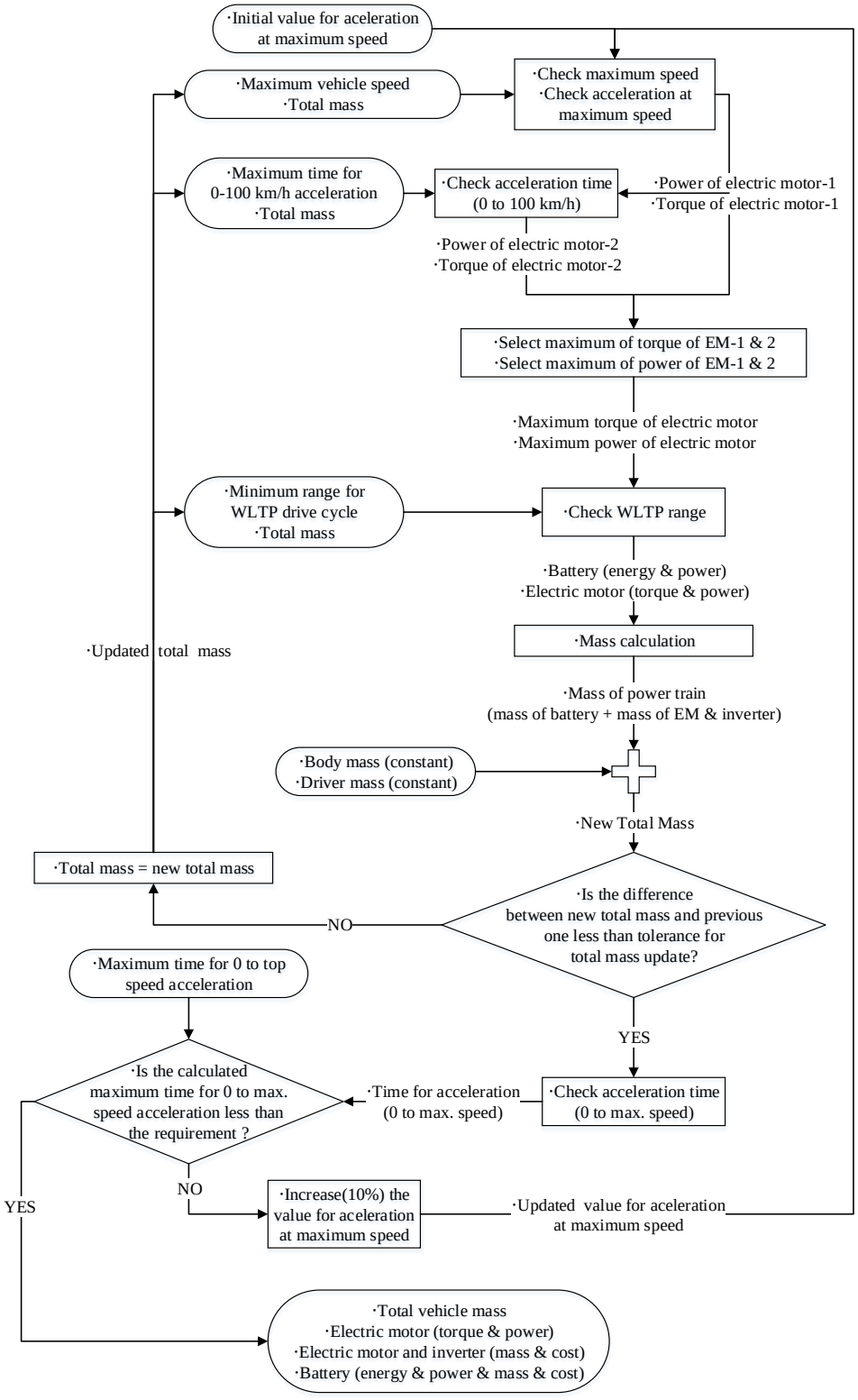

Figure 2.2. BEV Modelling

2.2.1 Maximum Vehicle Speed and Acceleration at Top Speed

It is desired to reach the top speed swiftly, i.e., in seconds, in BEVs. Thus, the requirement of maximum time for acceleration from 0 to maximum vehicle speed is defined in this work as in Table 2.1. This requirement can be satisfied only by having acceleration capability at top speed. Note that the top speed of BEVs is limited by software due to some rotation limitations of EM and connection pieces although power and torque capabilities of power train components are able to accelerate the BEV further. In this sense, a virtual parameter, acceleration at top speed, is defined to meet the requirement of maximum time for acceleration from 0 to maximum vehicle speed although there is no actual acceleration at top speed in this work.

Using the initial value or updated value for maximum acceleration at top speed given in Table 2.2, the minimum net force on the wheels is calculated by considering not only total mass but also mass factor given in Table 2.2. Total mass is initially assumed as summation of body mass and driver mass. In addition, the resistive forces, i.e., the rolling friction force and the aerodynamic drag force, are calculated as explained in Equations 2.3 and 2.4, respectively. Then, the required tractive force on the wheels is calculated using Equations 2.1 and 2.2. Finally, rated torque and power requirements for EM are calculated using maximum speed requirement in Table 2.1, wheel radius, gear ratio, efficiency of gearbox & differential assumptions in Table 2.2. The values are ended up as power of EM-1 and torque of EM-1.

2.2.2 Acceleration Time (0 to 100km/h)

Firstly, the limit values for maximum force and torque on the wheels are calculated using adhesive coefficient of tires to ground surface in Table 2.2. The limitation is reflected to define maximum rated torque value of EM using gear ratio, efficiency of gearbox & differential assumptions in Table 2.2. Then, an initial torque value of 150 Nm for EM is assumed and increased step by step with a size, 1 Nm, until the torque value for EM is enough to meet the maximum time requirement for 0 to 100 km/h

acceleration in Table 2.1. If the increase in torque continues up to the maximum torque limit for EM and the torque value of EM is not enough to meet the maximum time requirement for 0 to 100 km/h acceleration, the maximum time requirement for 0 to 100 km/h acceleration cannot met. For every step of torque of EM, acceleration profile of the vehicle is calculated in an inner loop. This acceleration loop runs with a timestep of 0.01 seconds and continues up to the maximum time requirement for 0 to 100 km/h acceleration. The value of power of EM-1 is used as initial value for rated power calculations of EM. In an EM, the base speed is defined as the speed where the torque just starts to decrease and the power just reaches its maximum. The base speed of EM is calculated using rated power and rated torque value of EM. Compared to base speed, the operation region of the EM (constant power or constant torque) is determined depending on the current speed. If the current speed is less than the base speed, the EM operates in constant (maximum) torque region. In constant torque region, the torque of EM is reflected to wheels and the traction force is calculated. The acceleration is calculated for the given time interval with using Equations 2.1, 2.2, 2.3 and 2.4. On the other hand, if the current speed is greater than or equal to the base speed, the EM operates in constant (maximum) power region. In constant power region, the power of EM and current speed are used to calculate the torque of EM. Then, the torque of EM is reflected to wheels and the traction force is calculated. The acceleration is calculated for the given time interval with using Equations 2.1, 2.2, 2.3 and 2.4. After getting acceleration for the given time interval for the operation regions, the current speed is increased as the multiplication of time step size and acceleration. The torque of EM is increased in the outer loop if the final speed value at the end of the inner loop does not reach 100 km/h. When the final speed reaches 100km/h in the time requirement for 0 to 100 km/h acceleration for the first time, the torque and power of EM in the outer loop are ended up as power of EM-2 and torque of EM-2.

2.2.3 The WLTP Range

After selecting the maximum of the values regarding power and torque of EM as rated, the energy and power of the battery are calculated considering the requirement of minimum range for WLTP in Table 2.1. For this purpose, power flow of the battery is calculated for a single WLTP while the current BEV speed follows the reference speed data of the WLTP in Figure 2.1. At every time step, 1 second, of the WLTP, the difference between the current speed of the BEV and the reference speed is calculated. That is, the required acceleration for the given time interval is calculated. Then, the movement (acceleration, deceleration or constant speed) until the next time step is determined. Like in Section 2.1.2, the base speed, the EM operation region, maximum torque limitation regarding adhesive coefficient of tires to the ground surface, efficiency of the battery pack and efficiency of EM & inverter and the required acceleration amount are used to calculate how much power the battery sinks (regeneration) or sources. At the end of a single WLTP, the total net power consumption is divided by the distance of a single WLTP. That is, the average power consumption per km based on WLTP is gotten. Multiplying this average power consumption and the requirement of minimum range for WLTP in Table 2.1, the minimum energy capacity of the battery is calculated. On the other hand, the rated power of the battery is determined considering the rated power of EM, power of accessories, efficiency of the battery pack and efficiency of EM & inverter.

2.2.4 Determination of the Components in the BEV

As shown in Figure 2.2, the masses of components are calculated after the specifications of components are determined. Then, the masses of components are summed with body mass and driver mass, and the new total mass is obtained. If the difference between the new total mass and the previous total mass is greater than the tolerance of 5 kg, the loop updates the total mass and continues its operation. After the difference stays in tolerance, a BEV model that meets the requirements of

maximum vehicle speed, maximum time for acceleration from 0 to 100 km/h and minimum range for the WLTP is obtained.

2.2.5 Acceleration Time (0 to Top Speed)

Using the same logic explained in Section 2.2.2, the BEV is accelerated up to top speed. Unlike Section 2.2.2, the torque or power rating of power train components are not modified to meet the requirement of maximum time for acceleration from 0 to maximum vehicle speed. Only the time passed for this acceleration period is calculated. As can be seen at the end of the flowchart in Figure 2.2, the value for acceleration at top speed is increased if the calculated acceleration time does not satisfy the requirement of maximum time for acceleration from 0 to maximum vehicle speed. Then, previous steps are repeated with updated value for acceleration at top speed in a loop. After the requirement of maximum time for acceleration from 0 to maximum vehicle speed is satisfied, the BEV model ends up with the outputs presented in Table 2.4. That is, the minimum values of the BEV's parameters that meet all requirements in Table 2.1 are given in Table 2.4.

Table 2.4. BEV modeling outputs

Parameters	Outputs
EM (torque – power)	401 Nm-168 kW (225 HP)
Battery (energy - power)	48 kWh - 193 kW
Initial Cost for EM & Inv - Batt - Total	5042 $ - 11941 $ - 16983 $
Mass for EM & Inv - Batt - Total BEV	153 kg - 374 kg - 2102 kg

2.3 The Battery Ageing Model

In EVs, batteries affect total mass, acceleration capability and travel range. These features highly depend on the type of battery. Batteries are energy storage devices and are classified into two types, primary and secondary. Primary batteries can be

only discharged. For example, Zinc-Carbon, alkaline-manganese dioxide, Lithium Iron Disulfide are the main primary batteries. Secondary batteries can be charged and discharged multiple times. Thus, secondary batteries are preferred in applications that require numerous cycling, such as cellphones, smartwatches, and EVs. For example, Lead Acid, Nickel Cadmium (Ni-Cd), Nickel-Metal Hydride (Ni-MH) and Lithium-Ion (Li-ion) are the main secondary batteries. The Li-ion batteries dominate the EV market because of their higher specific power and higher specific energy than other secondary battery family members. Thus, this work is based on Li-ion batteries.

The main structure, types, and ageing mechanisms of Li-ion batteries are investigated and presented in the appendices. It is essential to emphasize that one of the main limitations regarding Li-ion batteries is degradation. To overcome degradation, chemists and material engineers study the ageing mechanisms. On the other hand, system designers who use Li-ion batteries should try to model ageing phenomena and integrate this model into their system model. Thus, the system designers can optimize the design and utilization of their systems considering the battery ageing. In other words, they can use the battery in the best way for their systems being aware of the ageing effects.

Before going into details, note that battery health is expressed with its SOH and battery charge level is expressed with its state of charge (SOC) in battery terminology. Basically, SOH is the ratio of the current energy capacity to the nominal energy capacity, and SOC is the ratio of the charge level to the current energy capacity.

2.3.1 An Ageing Model of Li-ion Batteries[14]

Batteries have two main performance parameters: energy capacity and power capability. Regarding these performance parameters, battery degrades depending on the utilization of the battery and time. The energy capacity is a measure of the total available charge/discharge capacity, and degradation of the energy capacity is stated

as capacity fade (ΔC). The power capability can be considered as deliverability of power, and degradation of the power capability is expressed as impedance rise (ΔR_i). Degradation on these performance parameters is modelled to get the ability to consider ageing effects in users' systems. The parameters of the model should be appropriately assigned for utilization. Thus, ageing phenomena are generally modelled considering cycling and storage. That is, ageing is modelled into two parts, cycle ageing and calendar ageing. In [14], energy capacity and power capability degradation are modelled considering cycle ageing and calendar ageing as in Equations 2.5, 2.6, 2.7, 2.8 and 2.9.

Capacity fade and impedance rise occur regarding time (t) and the number of equivalent cycles (Q) as stated in Equations 2.5 and 2.6, where α and β are ageing parameters for calendar and cycle, respectively. t expresses the elapsed time in days, and Q represents equivalent full cycles. For example, if a battery with SOC=1 (fully charged) is discharged to SOC=0.5 and then charged up to SOC=1, Q would be equal to 0.5. If the cycle is repeated ten times, Q would be equal to 5.

Capacity Fade

$$\frac{\Delta C(t,Q)}{C(t)} = -(a_C * \boldsymbol{t} + \beta_C * \boldsymbol{Q}) \quad \textbf{(2.5)}$$

Impedance Rise

$$\frac{\Delta R_i(t,Q)}{R_i(t)} = \left(a_{R_i} * \boldsymbol{t} + \beta_{R_i} * \boldsymbol{Q}\right) \quad \textbf{(2.6)}$$

Calendar ageing occurs over time with a battery being stored while there is no charging or discharging. Calendar ageing mainly depends on the time (t), cell voltage (v_{cell}) and temperature (T). v_{cell} expresses the open circuit voltage of a cell at rest, i.e., there is no external current flow throughout the battery and unit of v_{cell} is volts. v_{cell} highly depends on the current SOC. T expresses cell temperature in kelvin.

Cycle ageing occurs while the cell is being charged or operates under load. Cycle ageing mainly depends on the number of equivalent cycles (*Q*), average cell voltage (v_{cyc}), depth of discharge (*DOD*) and *C-rate*. v_{cyc} expresses the average voltage of a cell during cycling in volts. For example, if a battery with 4V is discharged to 3V and then charged up to 4V, v_{cyc} would be equal to 3.5V. Discharged depth is expressed with its depth of discharge (*DOD*) in battery terminology. Basically, *DOD* is the ratio of the released energy to the current energy capacity. Notice that sum of *DOD* and SOC of a battery is equal to 1. *C-rate* is the rate of discharge (or charge) compared to the battery's current energy capacity. For example, if a battery with 10Ah capacity is discharged (or charged) with 1A, *C-rate* would be equal to 0.1.

Capacity fade and impedance rise are investigated with calendar ageing and cycle ageing. The term, *j*, in Equations 2.7 and 2.8 stands for capacity, C or impedance, R_i. The four parameters α_C, α_{Ri}, β_C and β_{Ri}, are not constant because calendar ageing becomes fast with higher v_{cell} and *T*, and cycle ageing becomes fast with higher v_{cyc}, *DOD* and *C-rate*. These four parameters change as stated in Equations 2.7 and 2.8.

<u>*Calendar Ageing*</u> - State of Charge (SOC) and Temperature (T)

$$a_j = a_{v,j} * \left(\boldsymbol{v_{cell}} - a_{0,j}\right) * \exp\left(-\frac{a_{T,j}}{\boldsymbol{T}}\right) \qquad \textbf{(2.7)}$$

<u>*Cycle Ageing*</u> - $\boldsymbol{v_{cyc}}$, DOD and C-rate

$$\beta_j = b_{0,j} + b_{v,j} * \left(\boldsymbol{v_{cyc}} - b_{v0,j}\right)^2 + b_{DOD,j} * \boldsymbol{DOD} + b_{I,j} * \exp\left(b_{exp,j} * \frac{|\boldsymbol{i_{bat}}|}{\boldsymbol{C}}\right) \qquad \textbf{(2.8)}$$

In Equation 2.7, the cell voltage affects calendar ageing linearly, and the effect of temperature is modelled by an Arrhenius expression [24]. In Equation 2.8, cycle ageing has a quadratic dependence on v_{cyc}, *DOD* affects cycle ageing linearly [24], and *C-rate* affects cycle ageing exponentially [25]. In [14], these variables are used for modelling the calendar and cycle ageing with the parameters in Table 2.5.

The time and number of equivalent cycle dependency on ageing is linear in this model. Therefore, this ageing model is only suitable for a linear region of the battery ageing when capacity fade and impedance rise is below 30% [26]. Both capacity fade and impedance rise processes accelerate after 30%, and battery life is usually considered to be over. This model works well in this study because SOH limit for working life is considered 70%. In this context, ΔSOH is expressed as in Equation 2.9.

$$\Delta SOH = -max\left(\left|\frac{\Delta C}{C}\right|, \left|\frac{\Delta R_i}{R_i}\right|\right) \quad \textbf{(2.9)}$$

In this study, the battery ageing model in [14] is used but not as is because the ageing is slow in the model. The parameters of the battery ageing model in [14] are given in Table 2.5. Note that these parameters are used for calculation of α_C, α_{Ri}, β_C and β_{Ri} using Equations 2.7 and 2.8.

Table 2.5. Ageing model parameters in [14] for ΔC and ΔR_i calculation

	Parameters	**Unit**	**Parameters (ΔC) @** [14]	**Parameters (ΔR_i)@** [14]
Calendar	a_v	-	271600	9486
	a_0	V	3.1482	3.0960
	a_T	K	6976	5986
Cycle	b_0	-	2.7100e-05	2.2800e-05
	b_v	V^{-1}	3.1400e-04	3.2080e-04
	b_{v0}	V	3.6830	3.7410
	b_{DOD}	-	1.6100e-06	3.4040e-06
	b_I	-	1.5600e-05	1.5600e-05
	b_{exp}	h	1.8000	1.8000

The parameters in Table 2.5 are updated according to the real ageing data given in the first four subsections of Section 2.3.2. The resulting parameters are shown in Section 2.3.2.5.

2.3.2 Updating the parameters in the Ageing Model[14] with using the real ageing data

While trying to use the ageing model given in the work by [14], it is realized that ageing of the battery is very slow and limited. Since the ageing model is vital for this work, it is desired to check the model in the [14] by some real ageing data. For that purpose, some ageing data is asked from either industrial facilities or manufacturers. After some negotiations, a small set of ageing data of a Lithium Nickel Manganese Cobalt (NMC) cell is gotten. This special data set is presented in four main parts: capacity loss due to calendar ageing, resistance growth due to calendar ageing, capacity loss due to cycle ageing and resistance growth due to cycle ageing. When the conditions specified in the data set are applied to the ageing model in the [14], it is observed that ageing of the battery by the model is very slow compared to real data. After this observation, the respective parameters of the ageing model in the [14] are optimized using each of the data parts. In addition, a scaling factor multiplication is included in each formula part separately to get fast convergence while optimizing the parameters. All the details, results and comparisons are presented below.

2.3.2.1 Capacity Loss due to Calendar Ageing

In the capacity loss formula given in the [14], only the calendar ageing part is considered. Also, a scaling factor (SF) multiplication named as SF_C_cal is included to get fast convergence in optimization.

$$\frac{\Delta C\_calendar(t,Q)}{C\_calendar(t)} = -(SF\_\text{C\_cal}) * \left(a_{v,C} * \left(\boldsymbol{v_{cell}} - a_{0,C}\right) * \exp\left(-\frac{a_{T,C}}{\boldsymbol{T}}\right) * \boldsymbol{t}\right) \qquad \textbf{(2.10)}$$

For each condition specified in the data set, the capacity loss is calculated by the ageing model. Then, the absolute value of the differences between the calculation and real ageing data is summed. In this way, the total error is calculated. Pseudo-code of total error calculation is given below:

err_total = 0;

for i=1 to <(numberofdata)>

*err_s (i) = <**Capacity Loss(Calculated)**(i)> - <**Capacity Loss(byManufacturer)**(i)>;*

err_total = err_total + absolute of <(err_s(i))>;

end

This error calculation method is used during parameter optimization. The main objective is to minimize the total error by updating the parameters one by one. In Table 2.6, the effect of parameter optimization on error minimization can be seen:

Table 2.6. Effect of parameter optimization in capacity loss due to calendar ageing

State info \ Parameters	**SF**	a_v	a_0	a_T	**Error**
All is in the initial state	Not Included	Initial	Initial	Initial	1.6706
Only SF is included	Included	Initial	Initial	Initial	0.7776
SF is included and a_v is optimized	Included	Optimized	Initial	Initial	0.5977
SF is included and a_v & a_0 are optimized	Included	Optimized	Optimized	Initial	0.5910
SF is included and a_v, a_0& a_T are optimized	Included	Optimized	Optimized	Optimized	*0.5677*

The real capacity loss for the specified conditions given by the manufacturer, the capacity loss calculated by the formula with parameters in the [14] and the capacity loss calculated by the formula with optimized parameters are presented in Table 2.7 and Figure 2.3.

Table 2.7. Comparison of capacity loss calculations due to calendar ageing

Specified Conditions	*Vcell*	*Temperature*	*time(years)*	***Capacity Loss (by Manufacturer)***	**Capacity Loss (by** [14]**)**	**Capacity Loss (in this work)**
1	*3.64*	*24*	*0.35*	*0.018*	0.001087492	0.005085705
2	*3.83*	*24*	*0.35*	*0.021*	0.001507629	0.006638546
3	*4*	*24*	*0.35*	*0.04*	0.001883542	0.00802793
4	*4.1*	*24*	*0.35*	*0.039*	0.002104667	0.008845214
5	*4.2*	*24*	*0.35*	*0.033*	0.002325792	0.009662499
6	*3.64*	*24*	*0.71*	*0.027*	0.002206056	0.010316716
7	*3.83*	*24*	*0.71*	*0.03*	0.003058334	0.013466764
8	*4*	*24*	*0.71*	*0.052*	0.003820899	0.016285229
9	*4.1*	*24*	*0.71*	*0.052*	0.004269467	0.017943149
10	*4.2*	*24*	*0.71*	*0.041*	0.004718034	0.01960107
11	*3.64*	*40*	*0.35*	*0.033*	0.003608777	0.01704416
12	*3.83*	*40*	*0.35*	*0.04*	0.005002977	0.022248329
13	*4*	*40*	*0.35*	*0.064*	0.006250419	0.026904691
14	*4.1*	*40*	*0.35*	*0.056*	0.006984209	0.029643728
15	*4.2*	*40*	*0.35*	*0.046*	0.007717998	0.032382764
16	*3.64*	*40*	*0.71*	*0.05*	0.007320662	0.034575296
17	*3.83*	*40*	*0.71*	*0.056*	0.010148896	0.045132325
18	*4*	*40*	*0.71*	*0.08*	0.012679422	0.054578088
19	*4.1*	*40*	*0.71*	*0.075*	0.014167966	0.060134419
20	*4.2*	*40*	*0.71*	*0.062*	0.015656511	0.06569075
21	*3.64*	*55*	*0.35*	*0.078*	0.009990776	0.047583589
22	*3.83*	*55*	*0.35*	*0.086*	0.013850571	0.062112498
23	*4*	*55*	*0.35*	*0.095*	0.017304073	0.075112048
24	*4.1*	*55*	*0.35*	*0.082*	0.019335544	0.082758842
25	*4.2*	*55*	*0.35*	*0.08*	0.021367015	0.090405636
26	*3.64*	*55*	*0.71*	*0.115*	0.020267003	0.096526709
27	*3.83*	*55*	*0.71*	*0.126*	0.028096873	0.125999639
28	*4*	*55*	*0.71*	*0.137*	0.035102547	0.152370154
29	*4.1*	*55*	*0.71*	*0.141*	0.039223532	0.167882222
30	*4.2*	*55*	*0.71*	*0.18*	0.043344517	0.18339429

Note that the value of "SF_C_Cal" is calculated corresponding to the condition, 18th, in Table 2.7. This condition is selected because it states the environment at an intermediate level.

SF_C_Cal = ***Capacity Loss (byManufacturer)(18^{th})*** **/ Capacity Loss (by**[14]**)** ***(18^{th})***
= *0.08* / 0.012679422 = 6.3094

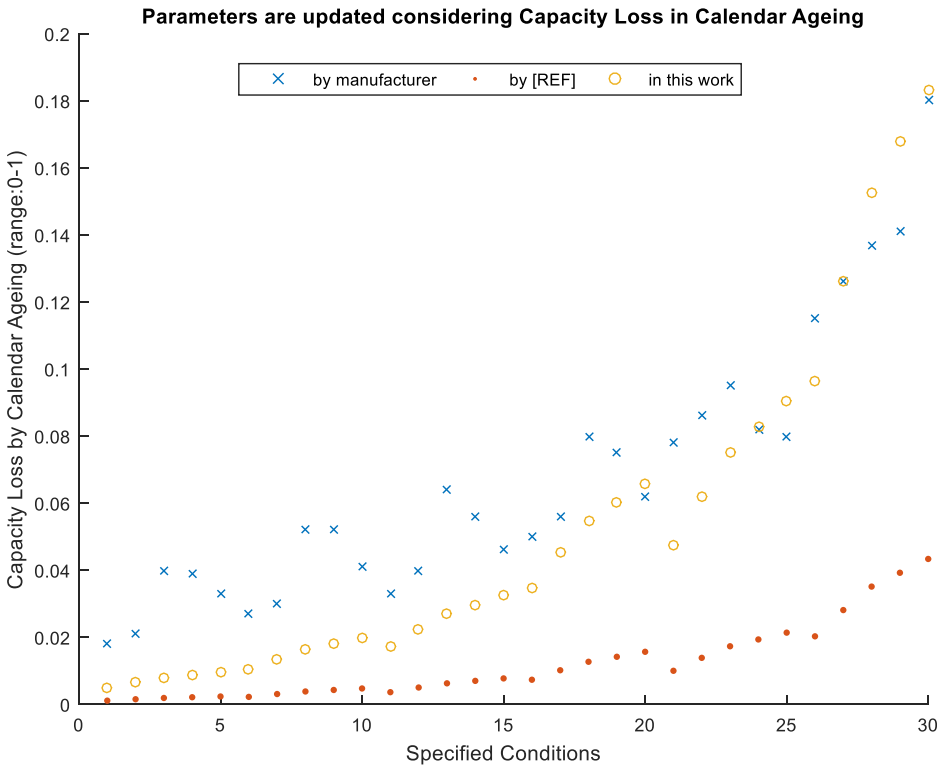

Figure 2.3. Comparison of capacity loss calculations due to calendar ageing

The points named as "in this work" are closer to the points named "by manufacturer" compared to the points named as "by [REF]" in Figure 2.3. That is, the parameter optimization makes the model more realistic. These optimized parameters are presented in Table 2.8.

Table 2.8. Updating the parameters for ΔC calculation regarding calendar ageing

	Parameters	Unit	Parameters (ΔC) @ [14]	Parameters (ΔC) in this work for Equation 2.10		Parameters (ΔC) in this work for Equation 2.7
Calendar	a_v	-	271600	SF_C_Cal = 6.3094	1.9304e+05	6.3094*1.9304e+05 = *1.2180e+06*
	a_0	V	3.1482		3.0177	*3.0177*
	a_T	K	6976		7.0335e+03	*7.0335e+03*

2.3.2.2 Resistance Growth due to Calendar Ageing

In the resistance growth formula given in the [14], only the calendar ageing part is considered. Also, a scaling factor multiplication (SF_Ri_Cal) is included to get fast convergence in optimization.

$$\frac{\Delta R_i\_calendar(t,Q)}{R_i\_calendar(t)} = (SF\_\text{Ri\_Cal}) * \left(a_{v,Ri} * \left(\boldsymbol{v_{cell}} - a_{0,Ri}\right) * \exp\left(-\frac{a_{T,Ri}}{\boldsymbol{T}}\right) * \boldsymbol{t}\right) \qquad \textbf{(2.11)}$$

For each condition specified in the data set, resistance growth is calculated by the ageing model. Then, the absolute value of the differences between the calculation and real ageing data is summed. In this way, the total error is calculated. Pseudo-code of total error calculation is given below:

err_total = 0;

for i=1 to <(numberofdata)>

err_s (i) = < ***Resistive Growth(Calculated)****(i)> - <* ***Resistive Growth(byManufacturer)****(i)>;*

err_total = err_total + absolute of <(err_s(i))>;

end

This error calculation method is used during parameter optimization. The main objective is to minimize the total error by updating the parameters one by one. In Table 2.9, the effect of parameter optimization on error minimization can be seen:

Table 2.9. Effect of parameter optimization in resistance growth due to calendar ageing

State info \ Parameters	**SF**	a_v	a_0	a_T	**Error**
All is in the initial state	Not Included	Initial	Initial	Initial	2.9680
Only SF is included	Included	Initial	Initial	Initial	0.4739
SF is included and a_v is optimized	Included	Optimized	Initial	Initial	0.3067
SF is included and a_v & a_0 are optimized	Included	Optimized	Optimized	Initial	0.3068
SF is included and a_v, a_0& a_T are optimized	Included	Optimized	Optimized	Optimized	*0.3068*

The real resistance growth for the specified conditions given by the manufacturer, the resistance growth calculated by the formula with parameters in the [14] and the resistance growth calculated by the formula with optimized parameters are presented in Table 2.10 and Figure 2.4.

Table 2.10. Comparison of resistance growth calculations due to calendar ageing

Specified Conditions	*Vcell*	*Temperature*	*time(years)*	***Resistance Growth (by Manufacturer)***	**Resistance Growth (by** [14]**)**	**Resistance Growth (in this work)**
1	*3.64*	*24*	*0.35*	*0.027*	0.001175729	0.01256915
2	*3.83*	*24*	*0.35*	*0.027*	0.00158637	0.016958817
3	*4*	*24*	*0.35*	*0.02*	0.001953786	0.020886414
4	*4.1*	*24*	*0.35*	*0.023*	0.002169912	0.023196764
5	*4.2*	*24*	*0.35*	*0.037*	0.002386039	0.025507115
6	*3.64*	*24*	*0.71*	*0.033*	0.002385051	0.025497419
7	*3.83*	*24*	*0.71*	*0.031*	0.003218065	0.034402171
8	*4*	*24*	*0.71*	*0.029*	0.003963394	0.042369582
9	*4.1*	*24*	*0.71*	*0.041*	0.004401822	0.047056294
10	*4.2*	*24*	*0.71*	*0.057*	0.004840251	0.051743006
11	*3.64*	*40*	*0.35*	*0.038*	0.003290886	0.03518146
12	*3.83*	*40*	*0.35*	*0.049*	0.004440277	0.047468281
13	*4*	*40*	*0.35*	*0.061*	0.005468679	0.058461752
14	*4.1*	*40*	*0.35*	*0.083*	0.006073621	0.064928499
15	*4.2*	*40*	*0.35*	*0.102*	0.006678563	0.071395247
16	*3.64*	*40*	*0.71*	*0.063*	0.006675798	0.071368105
17	*3.83*	*40*	*0.71*	*0.082*	0.009007418	0.096292798
18	*4*	*40*	*0.71*	*0.106*	0.011093605	0.118593839
19	*4.1*	*40*	*0.71*	*0.133*	0.012320774	0.131712098
20	*4.2*	*40*	*0.71*	*0.16*	0.013547943	0.144830358
21	*3.64*	*55*	*0.35*	*0.089*	0.007884817	0.084293619
22	*3.83*	*55*	*0.35*	*0.12*	0.010638705	0.113732435
23	*4*	*55*	*0.35*	*0.138*	0.013102711	0.140072429
24	*4.1*	*55*	*0.35*	*0.157*	0.014552125	0.155566543
25	*4.2*	*55*	*0.35*	*0.196*	0.01600154	0.171060657
26	*3.64*	*55*	*0.71*	*0.171*	0.015994914	0.170995627
27	*3.83*	*55*	*0.71*	*0.227*	0.021581373	0.230714369
28	*4*	*55*	*0.71*	*0.257*	0.026579784	0.284146928
29	*4.1*	*55*	*0.71*	*0.309*	0.029520026	0.315577845
30	*4.2*	*55*	*0.71*	*0.397*	0.032460267	0.347008762

Note that the value of "SF_Ri_Cal" is calculated corresponding to the condition, 18th, in Table 2.10. This condition is selected because it states the environment at an intermediate level.

SF_Ri_Cal = ***Resistive Growth (byManufacturer) (18th)*** **Resistive Growth (by**[14]**)** ***(18th)***
= *0.106* / 0.011093605 = 9.5551

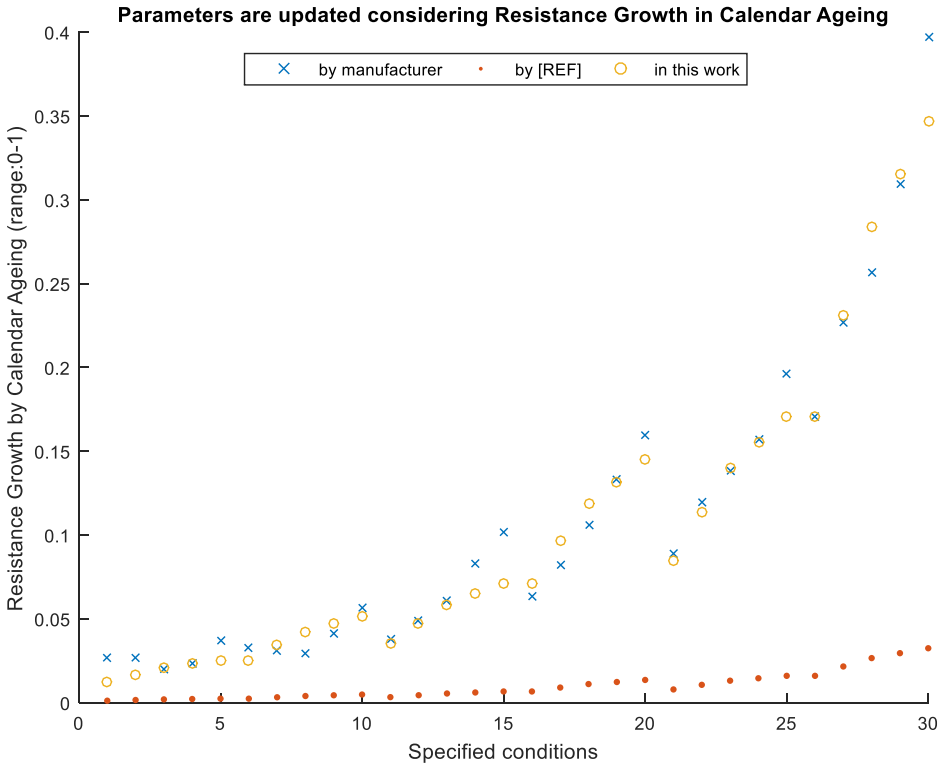

Figure 2.4. Comparison of resistance growth calculations due to calendar ageing

The points named as "in this work" are closer to the points named "by manufacturer" compared to the points named as "by [REF]" in Figure 2.4. That is, the parameter optimization makes the model more realistic. These optimized parameters are presented in Table 2.11.

Table 2.11. Updating the parameters for ΔRi calculation regarding calendar ageing

	Parameters	Unit	Parameters (ΔR_i)@ [14]	Parameters (ΔR_i) in this work for Equation 2.11		Parameters(ΔR_i) in this work for Equation 2.7
Calendar	a_v	-	9486	SF_Ri_Cal = 9.5551	1.0614e+04	9.5551*1.0614e+04= *1.0142e+05*
	a_0	V	3.0960		3.0960	*3.0960*
	a_T	K	5986		5986	*5986*

2.3.2.3 Capacity Loss due to Cycle Ageing

In the capacity loss formula given in the [14], only the cycle ageing part is considered. Also, a scaling factor multiplication (SF_C_cycle) is included to get fast convergence in optimization.

$$\frac{\Delta C_{cycle(t,Q)}}{C_{cycle(t)}} = -(SF\_C\_cycle) * \left(b_{0,C} + b_{v,C} * \left(\boldsymbol{v_{cyc}} - b_{v0,C}\right)^2 + b_{DOD,C} * \boldsymbol{DOD} + b_{I,C} * \exp\left(b_{exp,C} * \frac{|\boldsymbol{i_{bat}}|}{\boldsymbol{C}}\right) * \boldsymbol{Q} \right) \quad \textbf{(2.12)}$$

For each condition specified in the data set, the capacity loss is calculated by the ageing model. Then, the absolute value of the differences between the calculation and real ageing data is summed. In this way, the total error is calculated. Pseudo-code of total error calculation is given below:

err_total = 0;

for i=1 to <(numberofdata)>

*err_s (i) = <**Capacity Loss(Calculated)**(i)> - <**Capacity Loss(byManufacturer)**(i)>;*

err_total = err_total + absolute of <(err_s(i))>;

end

This error calculation method is used during parameter optimization. That the main objective is to minimize the total error by updating the parameters one by one. In Table 2.12, the effect of parameter optimization on error minimization can be seen. “I” stands for “Initial” and “O” stands for “Optimized”.

Table 2.12. Effect of parameter optimization in capacity loss due to cycle ageing

State info \ Parameters	SF	b_0	b_v	b_{v0}	b_{DOD}	b_I	b_{exp}	Error
All is in the initial state	Not Included	I	I	I	I	I	I	1.1377
Only SF is included	Included	I	I	I	I	I	I	0.3694
SF is included and $b_0$is optimized	Included	O	I	I	I	I	I	0.3364
SF is included and b_0 & b_v are optimized	Included	O	O	I	I	I	I	0.3364
SF is included and b_0, b_v& b_{v0} are optimized	Included	O	O	O	I	I	I	0.3358
SF is included and b_0, b_v b_{v0} & b_{DOD} are optimized	Included	O	O	O	O	I	I	0.3358
SF is included and b_0, b_v b_{v0} b_{DOD} & b_I are optimized	Included	O	O	O	O	O	I	0.3358
SF is included and b_0, b_v b_{v0} b_{DOD}, b_I & b_{exp} are optimized	Included	O	O	O	O	O	O	*0.3358*

The real capacity loss for the specified conditions given by the manufacturer, the capacity loss calculated by the formula with parameters in the [14] and the capacity loss calculated by the formula with optimized parameters are presented in Table 2.13 and Figure 2.5.

Table 2.13. Comparison of capacity loss calculations due to cycle ageing

Specified Conditions	*Vcyc*	*DOD*	*Crate*	*Q_eqvfullcycle*	***Capacity Loss (by Manufacturer)***	**Capacity Loss (by** [14]**)**	**Capacity Loss (in this work)**
1	*3.7*	*1*	*0.3*	*100*	*0.035*	0.005557045	0.014910195
2	*3.7*	*1*	*0.3*	*200*	*0.055*	0.011114091	0.02982039
3	*3.7*	*1*	*0.3*	*300*	*0.07*	0.016671136	0.044730584
4	*3.7*	*1*	*0.3*	*400*	*0.075*	0.022228181	0.059640779
5	*3.7*	*1*	*0.3*	*500*	*0.09*	0.027785227	0.074550974
6	*3.7*	*1*	*0.3*	*600*	*0.1*	0.033342272	0.089461169
7	*3.7*	*1*	*0.3*	*700*	*0.105*	0.038899317	0.104371363
8	*3.7*	*1*	*0.3*	*800*	*0.11*	0.044456362	0.119281558
9	*3.7*	*1*	*0.3*	*900*	*0.115*	0.050013408	0.134191753
10	*3.7*	*1*	*0.3*	*1000*	*0.12*	0.055570453	0.149101948
11	*3.65*	*0.9*	*0.4*	*90*	*0.045*	0.005484609	0.014281754
12	*3.65*	*0.9*	*0.4*	*180*	*0.06*	0.010969219	0.028563509
13	*3.65*	*0.9*	*0.4*	*270*	*0.07*	0.016453828	0.042845263
14	*3.65*	*0.9*	*0.4*	*360*	*0.075*	0.021938437	0.057127018
15	*3.65*	*0.9*	*0.4*	*450*	*0.08*	0.027423047	0.071408772
16	*3.65*	*0.9*	*0.4*	*540*	*0.095*	0.032907656	0.085690527
17	*3.65*	*0.9*	*0.4*	*630*	*0.1*	0.038392266	0.099972281
18	*3.65*	*0.9*	*0.4*	*720*	*0.11*	0.043876875	0.114254036
19	*3.65*	*0.9*	*0.4*	*810*	*0.115*	0.049361484	0.12853579
20	*3.65*	*0.9*	*0.4*	*900*	*0.12*	0.054846094	0.142817545

Note that the value of "SF_C_cycle" is calculated corresponding to the condition, 16th, in Table 2.13. This condition is selected because it states the environment at an intermediate level.

SF_C_cycle = ***Capacity Loss (byManufacturer)*** **(16th)/ Capacity Loss (by**[14]**)** ***(16th)***
= *0.095* / 0.032907656 = 2.8869

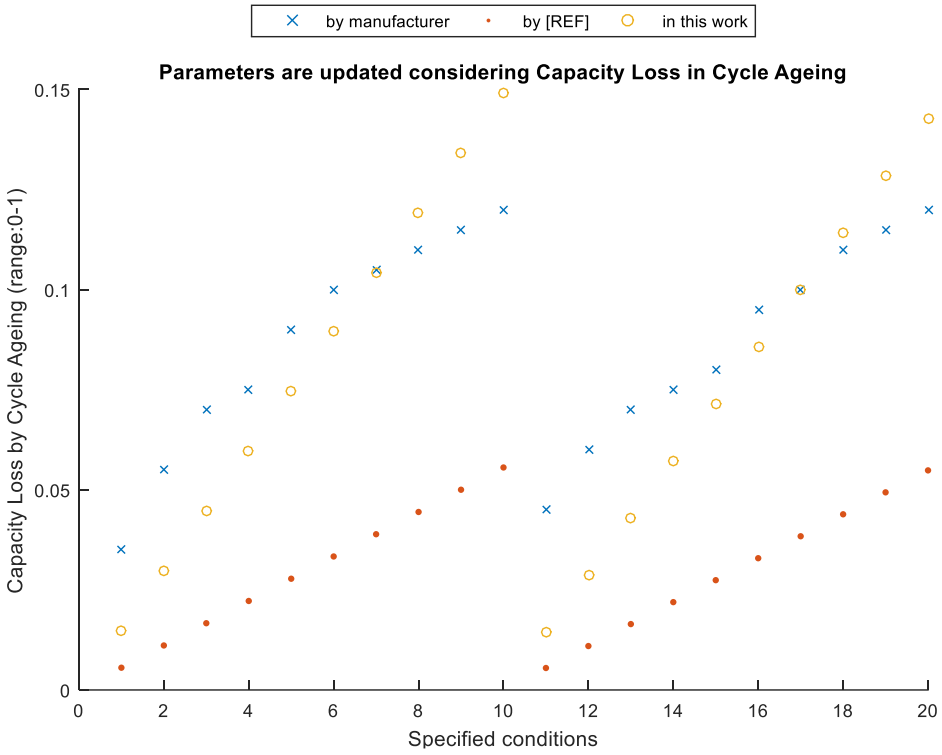

Figure 2.5. Comparison of capacity loss calculations due to cycle ageing

The points named as “in this work” are closer to the points named “by manufacturer” compared to the points named as “by [REF]” in Figure 2.5. That is, the parameter optimization makes the model more realistic. These optimized parameters are presented in Table 2.14.

Table 2.14. Updating the parameters for ΔC calculation regarding cycle ageing

	Parameters	**Unit**	**Parameters (ΔC) @ [14]**	**Parameters (ΔC) in this work for Equation 2.12**		**Parameters (ΔC) in this work for Equation 2.8**
Cycle	b_0	-	2.7100e-05	SF_C_cycle = 2.8869	2.1148e-05	2.8869*2.1148e-05= *6.1052e-05*
	b_v	V^{-1}	3.1400e-04		3.0992e-04	2.8869*3.0992e-04= *8.9471e-04*
	b_{v0}	V	3.6830		3.6171	3.6171
	b_{DOD}	-	1.6100e-06		1.6113e-06	2.8869*1.6113e-06= *4.6517e-06*
	b_I	-	1.5600e-05		1.5596e-05	2.8869*1.5596e-05= *4.5024e-05*
	b_{exp}	h	1.8000		1.7995	1.7995

2.3.2.4 Resistance Growth due to Cycle Ageing

In the resistance growth formula given in the [14], only the cycle ageing part is considered. Also, a scaling factor multiplication (SF_Ri_cycle) is included to get fast convergence in optimization.

$$\frac{\Delta R_i\_calendar(t,Q)}{R_i\_calendar(t)} = (SF\_\text{Ri\_cycle}) * \left(b_{0,Ri} + b_{v,Ri} * \left(\boldsymbol{v_{cyc}} - b_{v0,Ri}\right)^2 + b_{DOD,Ri} * \boldsymbol{DOD} + b_{I,Ri} * \exp\left(b_{exp,Ri} * \frac{|\boldsymbol{i_{bat}}|}{\boldsymbol{C}}\right) * \boldsymbol{Q}\right) \quad \textbf{(2.13)}$$

For each condition specified in the data set, resistance growth is calculated by the ageing model. Then, the absolute value of the differences between the calculation and real ageing data is summed. In this way, the total error is calculated. Pseudo-code of total error calculation is given below:

err_total = 0;

for i=1 to <(numberofdata)>

*err_s (i) = < **Resistive Growth(Calculated)**(i)> - < **Resistive Growth(byManufacturer)**(i)>;*

err_total = err_total + absolute of <(err_s(i))>;

end

This error calculation method is used during parameter optimization. The main objective is to minimize the total error by updating the parameters one by one. In Table 2.15, the effect of parameter optimization on error minimization can be seen. “I” stands for “Initial”, and “O” stands for “Optimized”.

Table 2.15. Effect of parameter optimization in resistance growth due to cycle ageing

State info \ Parameters	SF	b_0	b_v	b_{v0}	b_{DOD}	b_I	b_{exp}	Error
All is in the initial state	Not Included	I	I	I	I	I	I	0.8909
Only SF is included	Included	I	I	I	I	I	I	0.3951
SF is included and $b_0$is optimized	Included	O	I	I	I	I	I	0.3556
SF is included and b_0 & b_v are optimized	Included	O	O	I	I	I	I	0.3388
SF is included and b_0, b_v& b_{v0} are optimized	Included	O	O	O	I	I	I	0.3333
SF is included and b_0, b_v b_{v0} & b_{DOD} are optimized	Included	O	O	O	O	I	I	0.3333
SF is included and b_0, b_v b_{v0} b_{DOD} & b_I are optimized	Included	O	O	O	O	O	I	0.3145
SF is included and b_0, b_v b_{v0} b_{DOD}, b_I & b_{exp} are optimized	Included	O	O	O	O	O	O	*0.3110*

The real resistance growth for the specified conditions given by the manufacturer, the resistance growth calculated by the formula with parameters in the [14] and the resistance growth calculated by the formula with optimized parameters are presented in Table 2.16 and Figure 2.6.

Table 2.16. Comparison of resistance growth calculations due to cycle ageing

Specified Conditions	*Vcyc*	*DOD*	*Crate*	*Q_eqvfullcycle*	***Resistance Growth (by Manufacturer)***	**Resistance Growth (by** [14]**)**	**Resistance Growth (in this work)**
1	*3.7*	*1*	*0.3*	*100*	*0.017*	0.005351297	0.012393858
2	*3.7*	*1*	*0.3*	*200*	*0.034*	0.010702594	0.024787716
3	*3.7*	*1*	*0.3*	*300*	*0.051*	0.016053892	0.037181574
4	*3.7*	*1*	*0.3*	*400*	*0.068*	0.021405189	0.049575433
5	*3.7*	*1*	*0.3*	*500*	*0.085*	0.026756486	0.061969291
6	*3.7*	*1*	*0.3*	*600*	*0.102*	0.032107783	0.074363149
7	*3.7*	*1*	*0.3*	*700*	*0.119*	0.03745908	0.086757007
8	*3.7*	*1*	*0.3*	*800*	*0.136*	0.042810377	0.099150865
9	*3.7*	*1*	*0.3*	*900*	*0.153*	0.048161675	0.111544723
10	*3.7*	*1*	*0.3*	*1000*	*0.17*	0.053512972	0.123938581
11	*3.65*	*0.9*	*0.4*	*90*	*0.01*	0.005451237	0.011047758
12	*3.65*	*0.9*	*0.4*	*180*	*0.02*	0.010902475	0.022095516
13	*3.65*	*0.9*	*0.4*	*270*	*0.03*	0.016353712	0.033143274
14	*3.65*	*0.9*	*0.4*	*360*	*0.04*	0.021804949	0.044191032
15	*3.65*	*0.9*	*0.4*	*450*	*0.05*	0.027256186	0.055238789
16	*3.65*	*0.9*	*0.4*	*540*	*0.06*	0.032707424	0.066286547
17	*3.65*	*0.9*	*0.4*	*630*	*0.07*	0.038158661	0.077334305
18	*3.65*	*0.9*	*0.4*	*720*	*0.08*	0.043609898	0.088382063
19	*3.65*	*0.9*	*0.4*	*810*	*0.09*	0.049061135	0.099429821
20	*3.65*	*0.9*	*0.4*	*900*	*0.1*	0.054512373	0.110477579

Note that the value of "SF_Ri_cycle" is calculated corresponding to the condition, 16th, in Table 2.16. This condition is selected because it states the environment at an intermediate level.

SF_Ri_cycle = ***Resistance Growth (byManufacturer)*** **(16th)/ Resistance Growth (by**[14]**)** ***(16th)***
= *0.06* / 0.032707424 = 1.8344

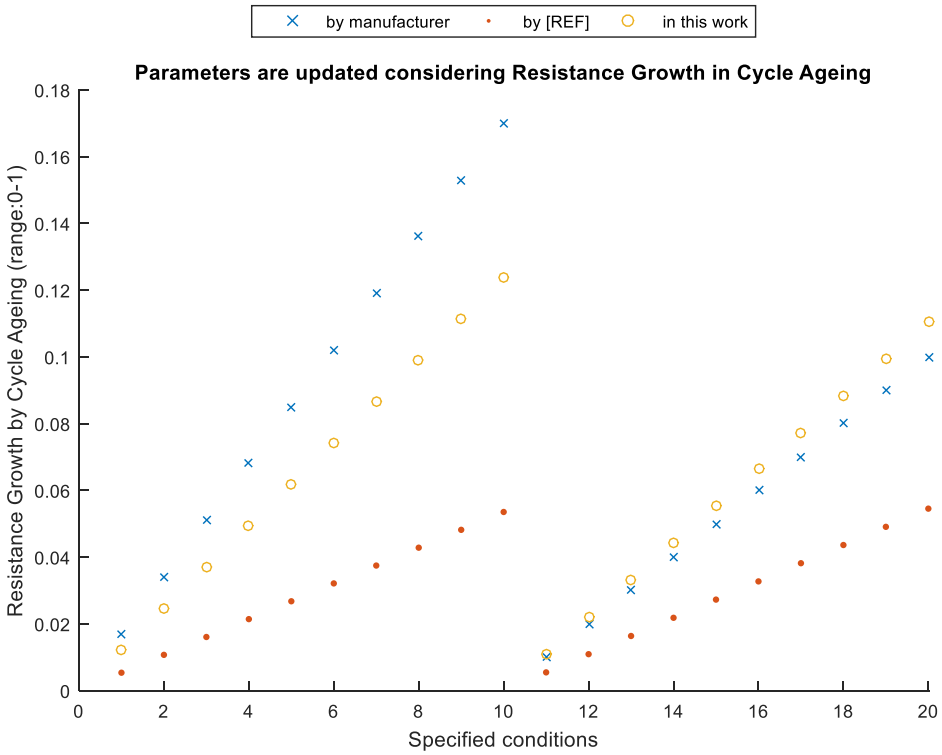

Figure 2.6. Comparison of resistance growth calculations due to cycle ageing

The points named as “in this work” are closer to the points named “by manufacturer” compared to the points named as “by [REF]” in Figure 2.6. That is, the parameter optimization makes the model more realistic. These optimized parameters are presented in Table 2.17.

Table 2.17. Updating the parameters for ΔRi calculation regarding cycle ageing

	Parameters	Unit	Parameters (ΔR_i)@ [14]	Parameters (ΔR_i) in this work for Equation 2.13		Parameters(ΔR_i) in this work for Equation 2.8
Cycle	b_0	-	2.2800e-05	SF_Ri_cycle = 1.8344	6.1957e-05	1.8344*6.1957e-05= *1.1365e-04*
	b_v	V^{-1}	3.2080e-04		3.2250e-05	1.8344*3.2250e-05= *5.9159e-05*
	b_{v0}	V	3.7410		3.5707	3.5707
	b_{DOD}	-	3.4040e-06		3.4042e-06	1.8344*3.4042e-06= *6.2447e-06*
	b_I	-	1.5600e-05		1.5734e-06	1.8344*1.5734e-06= *2.8862e-06*
	b_{exp}	h	1.8000		0.1815	0.1815

2.3.2.5 Resulting parameters

As stated above, the parameter optimization makes the model more realistic. These optimized parameters are presented in Table 2.18.

Table 2.18. Updating the parameters for ΔC and ΔRi calculation regarding calendar and cycle ageing

	Parameters	Unit	Parameters (ΔC) @ [14]	Parameters (ΔC) in this work for Equations 2.7 and 2.8	Parameters (ΔR_i)@ [14]	Parameters(ΔR_i) in this work for Equations 2.7 and 2.8
Calendar	a_v	-	271600	*1.2180e+06*	9486	*1.0142e+05*
	a_0	V	3.1482	*3.0177*	3.0960	*3.0960*
	a_T	K	6976	*7.0335e+03*	5986	*5986*
Cycle	b_0	-	2.7100e-05	*6.1052e-05*	2.2800e-05	*1.1365e-04*
	b_v	V^{-1}	3.1400e-04	*8.9471e-04*	3.2080e-04	*5.9159e-05*
	b_{v0}	V	3.6830	3.6171	3.7410	3.5707
	b_{DOD}	-	1.6100e-06	*4.6517e-06*	3.4040e-06	*6.2447e-06*
	b_I	-	1.5600e-05	*4.5024e-05*	1.5600e-05	*2.8862e-06*
	b_{exp}	h	1.8000	1.7995	1.8000	0.1815

2.4 Validation of the Vehicle Dynamic and Battery Ageing Models

A BEV is modelled with the same performance as Volkswagen ID4. In Table 2.19, the performance parameters that the manufacturer of VW ID4 shares are shown [27], [28], [29]. The requirement that the manufacturer of VW ID4 does not share is assumed as in Tables 2.1.

Table 2.19. Vehicle Performance Requirements by VW ID4

Parameters	Required Values
Max. vehicle speed	160 km/h
Max. time for acceleration from 0 to 100 km/h	8.5 sec
Min. range for the WLTP	495 km

As stated in Section 2.2, some more assumptions regarding vehicle and component characteristics are necessary for modelling. In Table 2.20, the parameters that the manufacturer of VW ID4 shares are shown. The parameters that the manufacturer of VW ID4 does not share are assumed as in Tables 2.2.

Table 2.20. Vehicle and Component Characteristics by VW ID4

Parameters	Assumed Values
Body mass without powertrain	1458 kg
Frontal area	3.0317 m^2
Aerodynamic drag coefficient	0.28
Radius of wheels	0.3815 m
Gear ratio (EM to wheels	12.9944

For the calculation of mass of components, the expressions in Table 2.3 are used.

Then, a BEV is formed using the vehicle dynamic model explained in Section 2.2. The modelled BEV is utilized as will be presented in Section 3.2, and the life of the battery is calculated using the battery ageing model explained in Section 2.3. In Figures 2.7 and 2.8, the data regarding the BEV that is modelled considering VW

ID4 are presented. In Figure 2.7, the SOC, status and SOH alterations of the battery are visualized for the first few cycles. The SOC, SOH and temperature alterations of the battery are visualized over the lifespan of the battery as in Figure 2.8. In Table 2.21, results of the models are given and are compared with the real VW ID4 parameters. The lifespan of the battery is defined as the time passed until SOH of the battery is less than 70% by VW ID4. That is, the end of life criteria regarding SOH (EOL) for the battery of the model is assumed as 70%.

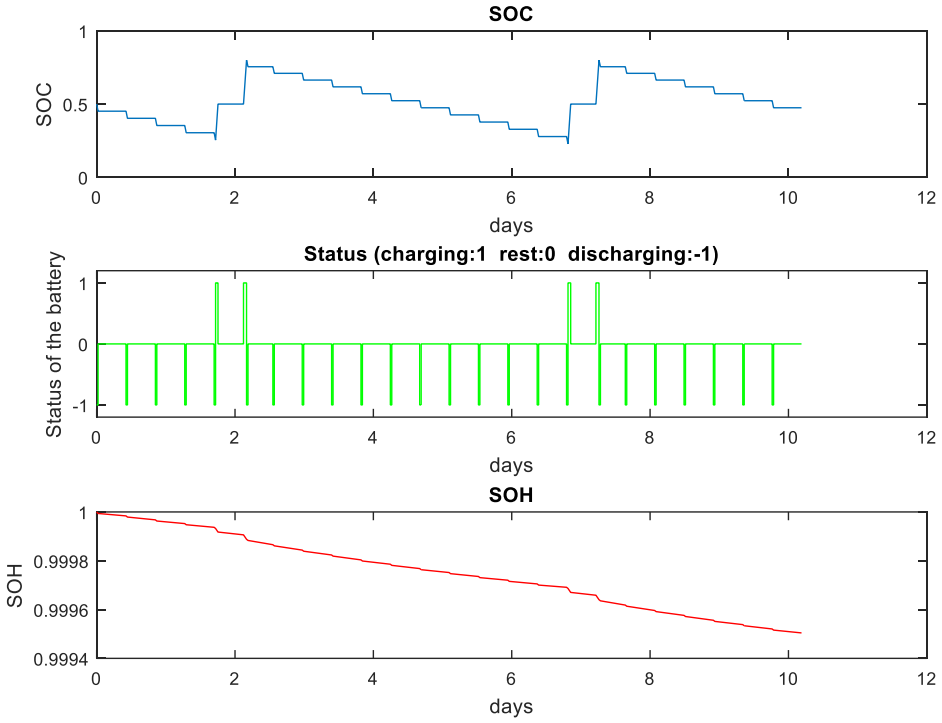

Figure 2.7. SOC, Status and SOH alterations regarding the BEV that is modelled considering VW ID4

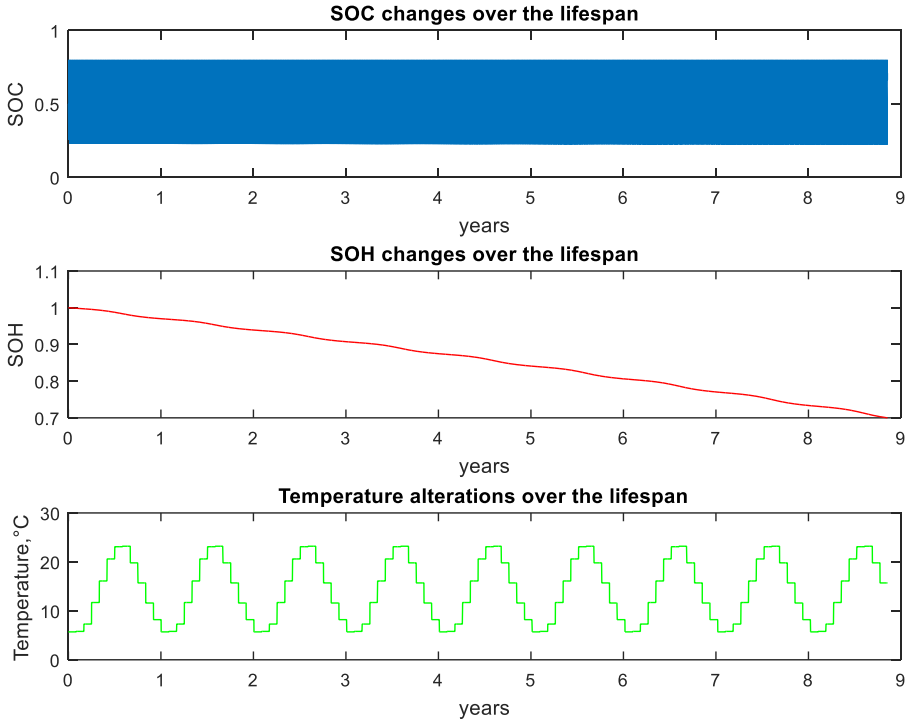

Figure 2.8. SOC, SOH and Temperature alterations over lifespan regarding the BEV that is modelled considering VW ID4

Table 2.21. Comparison of VW ID4 and the modelled BEV

Parameters	**VW ID4**	**The modelled BEV**	**Difference**
Torque of EM, Nm	310	291	6 %
Power of EM, kW	150	141,54	6 %
Battery Energy Capacity, kWh	77	76,99	0 %
Total Mass with driver, kg	2199	2179	1 %
Life of Battery (EOL=70%), years	8	8,85	11 %
Life of Battery (EOL=70%), km	160000	173200	8 %

As can be seen in Table 2.21, differences are pretty low. Thus, it can be claimed that the models are valid and suitable for this study. Note that differences may be caused by the assumptions are made for the parameters unspecified by the manufacturer.

CHAPTER 3

BATTERY SIZE OPTIMIZATION

In this study, C-rate, which causes faster cycle ageing as it gets higher, is focused on minimizing the battery's ageing since it affects ageing exponentially, as seen in Equation 2.8. Note that C-rate states the rate of discharge (or charge) compared to the battery's energy capacity. One can reduce the C-rate by decreasing the discharge (or charge) current and/or increasing the battery's energy capacity. Since the discharge (or charge) current highly affects the performance of BEV and depends on how the BEV is utilized, we should not restrict current drawn in order to keep meeting the requirements in Table 2.1. Therefore, increasing the energy capacity of the battery is the only way to reduce the C-rate. Energy capacity can be increased by adding some more parallel cells into blocks. In that way, the ampere-hour (Ah) capacity is increased while the nominal battery voltage is kept constant. However, increasing energy capacity causes an increase in total battery mass. Thus, other power train components, i.e., EM and inverter, should also be improved for neutralizing the added mass by the battery while continuing to meet the requirements in Table 2.1. It is evident that adding cells to the battery and improving EM and inverter raise the initial cost for these power train components and BEV. Therefore, optimization should be conducted to decide how much the energy capacity will be increased. Notice that, if the minimum range requirement for the WLTP given in Table 2.1 is too high, i.e. the initial cost of the power train components is too high, it may not be necessary to increase the battery's energy capacity for optimization. Besides, the battery's energy capacity may be decreased for optimization in a case that the minimum range requirement for the WLTP given in Table 2.1 is too high but the requirement is waivable. That is, battery sizing for BEV should be optimized considering battery ageing, requirements and restrictions for BEV. In this study, battery size is optimized according to the algorithm given in Figure 3.1. Explanations regarding the main blocks of the algorithm are given in Sections 3.1, 3.2, 3.3 and 3.4.

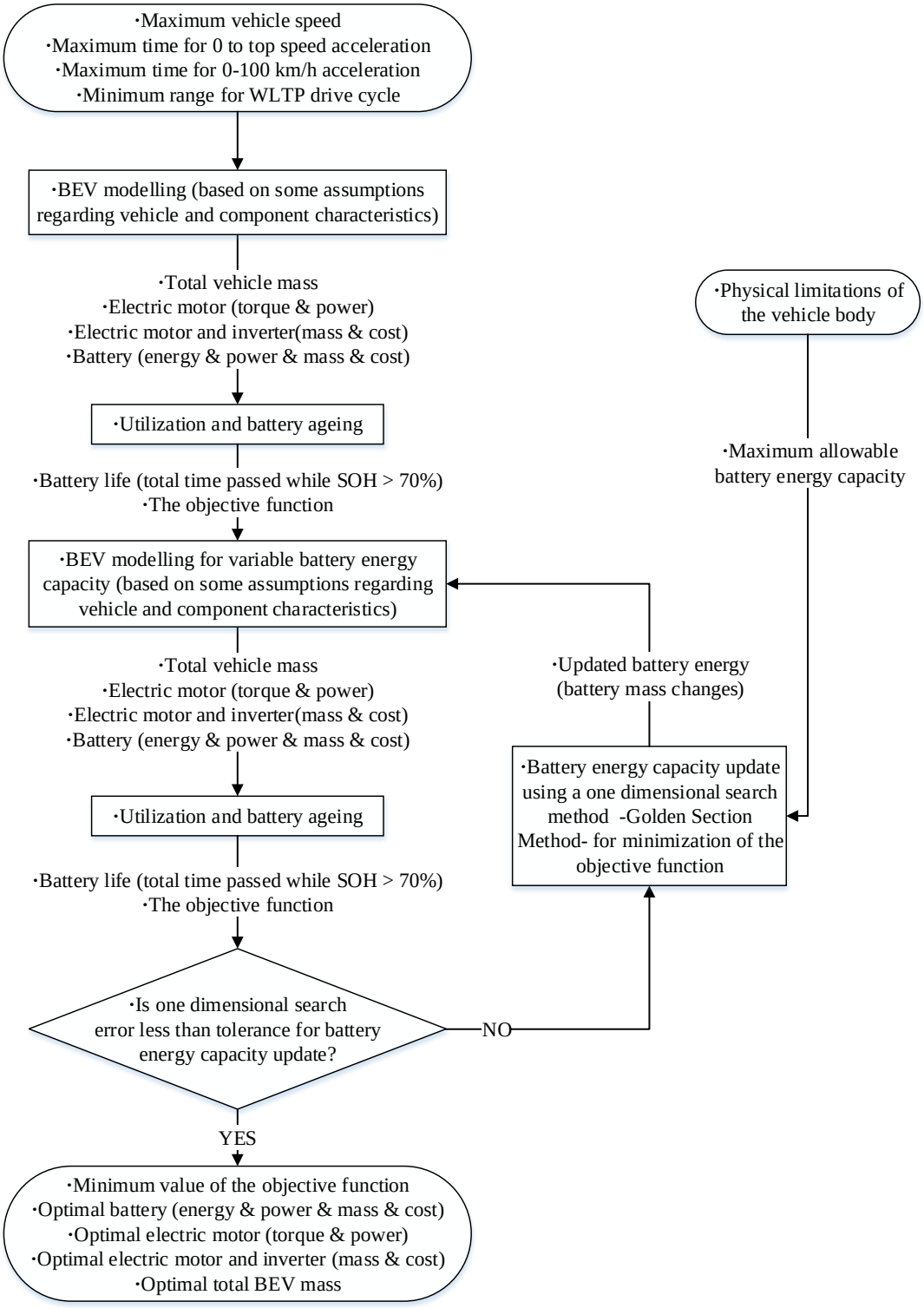

Figure 3.1. The Battery Size Optimization Algorithm

To be able to conduct an optimization, assumptions, objective function and restrictions must be well defined. In this study, the following assumptions have been made to make the problem solvable while keeping this work realistic and purposeful:

- The BEV is utilized in the WLTP. Although the WLTP has been criticized as mentioned in chapter 2, the WLTP was developed regarding real driving data gathered from all around the world, and it is the most suitable and widely accepted test procedure.
- The annual distance travelled is considered as 20000 km. Many of the leading brands in the industry state that the battery warranty is limited to 8 years or 160000 km (100000 miles) whichever comes first[30][31]. That is, travelling 20000 (=160000/8) km per year is a realistic way of utilization.
- Cost of electricity is considered as 0.11 $/kWh [32].
- SOC limits are introduced for both cycle ageing and calendar ageing. It is desirable to keep the SOC between 0.2 and 0.8 during charging and discharging, and to sustain the SOC at 0.5 while the battery is at rest [18] to reduce the ageing effects on a Li-ion battery.
- In addition, the average temperature values [33] of the city, Istanbul-Turkey, are considered for the calendar ageing calculations, and it is assumed that the BEV is started to be used at the beginning of January.
- An AC standard (32A, 3 phase socket) household charger of 22kW is used, and C-rate is calculated considering energy capacity of the battery. Maximum C-rate during charging is limited to 0.7C since the cell producer restricts it. In the cases of low energy capacity, charging power is decreased accordingly.
- The efficiency of the charger (EVSE) is considered as 90%.

In this study, minimizing the cost of ownership of a BEV is aimed by optimizing the size of the battery. Thus, the objective function is defined as in Equation 3.1. It is assumed that the maintenance cost per km and the initial cost of all the components except power train ones of the BEV, such as chassis, tires etc., are not affected by an

alteration in the energy capacity of the battery. On the other hand, it is considered that increasing the battery mass requires improvements on the EM and inverter. Thus, the initial costs of these power train components are also increased depending on the amount of increase in the energy capacity of the battery. Since these power train components are used over the lifespan of the battery, their total initial cost is divided by the total distance travelled over the lifespan of the battery. Thus, the first term of the objective function is formed. In addition, it is considered that consumed energy per km increases with the increase in the total mass of the BEV. The BEV is utilized in WLTP, and the energy consumption is not constant over WLTP. Therefore, the cost of total energy consumption over one WLTP is divided by the total distance travelled over one WLTP. The second term of the objective function that states the average energy consumption per km is formed. It is important to emphasize that the objective function does not express the total cost of ownership of the BEV. The objective function displays only the sum of cost of items that changes depending on the variation of battery size.

$$Objective\ Function = \left(\frac{Initial\ Cost\ of\ Power\ Train\ (Batt\&EM\&Inv)}{Total\ distance\ travelled\ over\ lifespan\ of\ the\ battery} + \frac{Consumed\ Energy\ Cost\ over\ one\ WLTP}{WLTP\ range}\right), \$/km \qquad \textbf{(3.1)}$$

Note that body mass without powertrain, the total mass of chassis, tires etc., is assumed constant as in Table 2.2. That is, there must be a restriction on the total mass of power train components. The restriction is defined considering some of BEVs in the SUV market. The maximum ratio of gross vehicle weight to body mass without power train, and average difference between gross vehicle weight and unladen weight of the SUV BEVs are used to define maximum allowable energy capacity of the battery. A detailed explanation for the restriction is given in Section 3.4. If it is desired to increase the battery capacity further and exceed the restriction, body mass without power train should also be increased because making some improvements on chassis, tires etc., would be required to carry the greater mass. Moreover, all the calculations regarding vehicle modelling, energy utilization and battery ageing would be needed to recalculate. That is, the optimized point for battery energy capacity

would change too. If the body mass without powertrain is not assumed to be constant and the vehicle body is improved, the physical limitations would be overcome. However, the EV segment would change due to both improvements on the vehicle body and power train components. This would be determining the optimum EV segment, but that is out of the scope of this work.

To sum up, the above assumptions, the objective function and restrictions are used to optimize the battery size in the algorithm given in Figure 3.1.

3.1 BEV Modelling

At the beginning of the optimization algorithm, the block of BEV modelling is used to calculate initial specifications of the components in the vehicle that meet the requirements in Table 2.1 as explained in Chapter 2.

3.2 Utilization and Battery Ageing

Secondly, the BEV with initial components is utilized according to the given assumptions and battery life, i.e., total time passed while SOH is greater than 0.7, is calculated. The block of utilization and battery ageing in the algorithm is explained in detail in Figure 3.2. Using annual distance travelled and distance information in the test procedure (23.15 km for WLTP), how many times the test procedure is conducted in a year and how much time passes between each test procedure are calculated. Initially, SOC is assumed to be 0.5, and the test procedure is performed by the BEV once. Then, SOC decrease is observed, and a projection is made for SOC reduction for the following test procedure. Using this projection of SOC reduction and making the new projections at every step, a few more test procedures are conducted on the BEV until SOC does not exceed the down limit, 0.2. Between test procedure operations, the battery is exposed to calendar ageing at different SOC values. Just after the last operation of the test procedure, it is assumed that the battery is immediately charged until SOC equals 0.5. Then, the calendar ageing is conducted with SOC=0.5 during the time between test procedure operations. Just after this

calendar ageing duration, the battery is assumed to be charged from SOC=0.5 to up limit, SOC=0.8. After this point, the battery is again subjected to test procedures (cycle ageing), rest intervals (calendar ageing) and charging periods keeping SOC in limits (0.2-0.8). The ageing effects on the battery capacity (SOH alterations), temperature alterations and SOC alterations at every step of utilization are reflected to the calculation of battery parameters (current battery capacity, C-rates during discharging, projection of SOC reduction, current battery voltage, current internal resistance and current temperature). During the discharging period, i.e., the BEV is operated in test procedures, battery current is calculated for each time step, 1 second. Considering the current energy capacity of the battery, C-rate is calculated at each time step. Then, ageing of the battery (ΔSOH) is calculated, and current energy capacity is updated using resulting C-rate data. Likewise, using the given C-rate for charging, ΔSOH is calculated and current energy capacity is updated. During rest intervals, ΔSOH is calculated, and current energy capacity is updated, too. That is, all of the related parameters such as C-rate, SOC, SOH, etc., are computed at every appropriate step and battery lifetime, i.e., the time passed while SOH > 0.7 are calculated and recorded. Under these circumstances, the operation is conducted until SOH exceed the EOL=0.7.

Besides, the SOC, status and SOH alterations of the battery are visualized for the first few cycles as in Figure 3.3. The SOC, SOH and temperature alterations of the battery are visualized over the lifespan of the battery as in Figure 3.4. Figures 3.3 and 3.4 shows the data regarding the BEV together with initial power train components. That is, the optimization is not run yet.

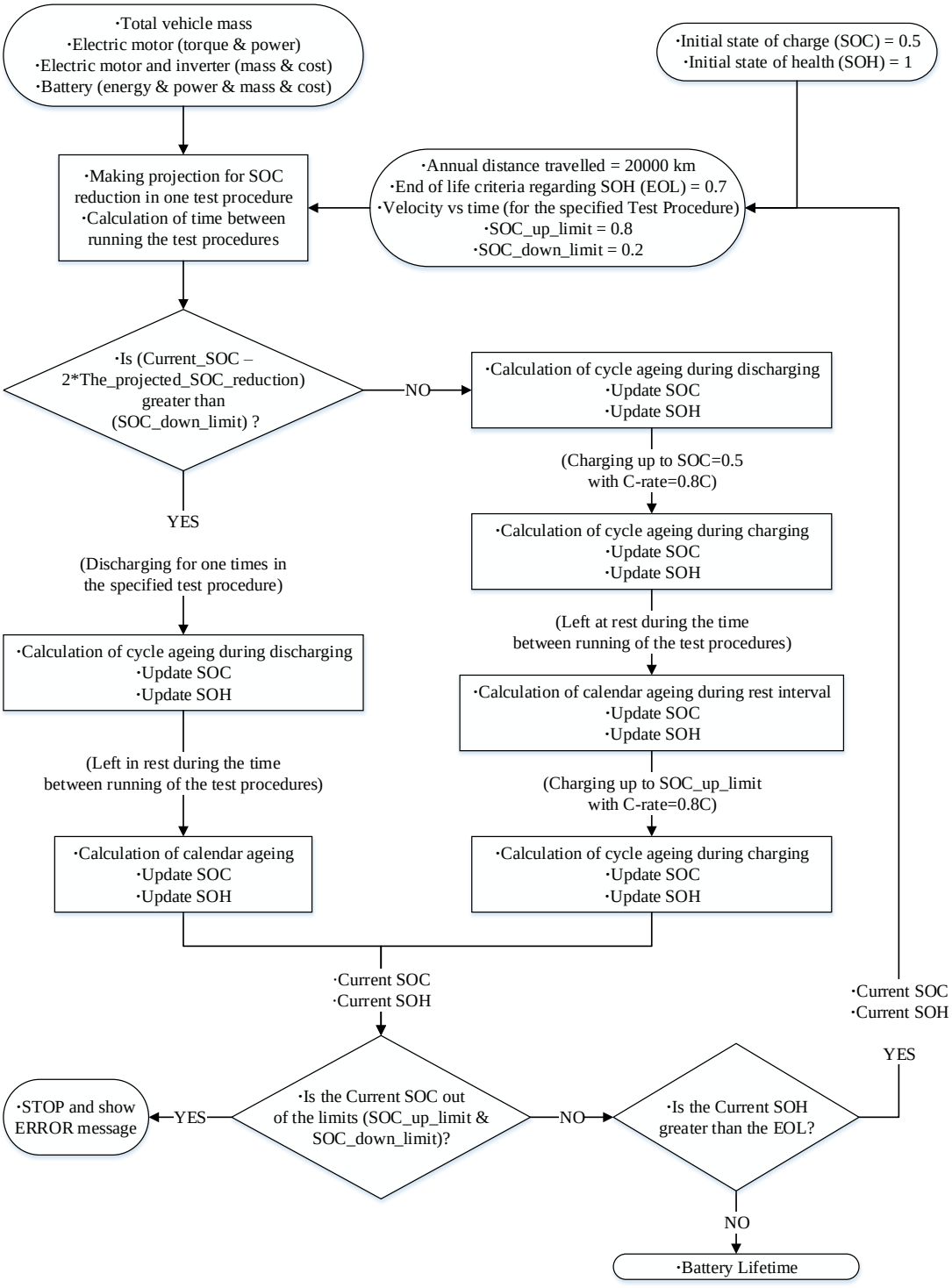

Figure 3.2. Utilization and Battery Ageing

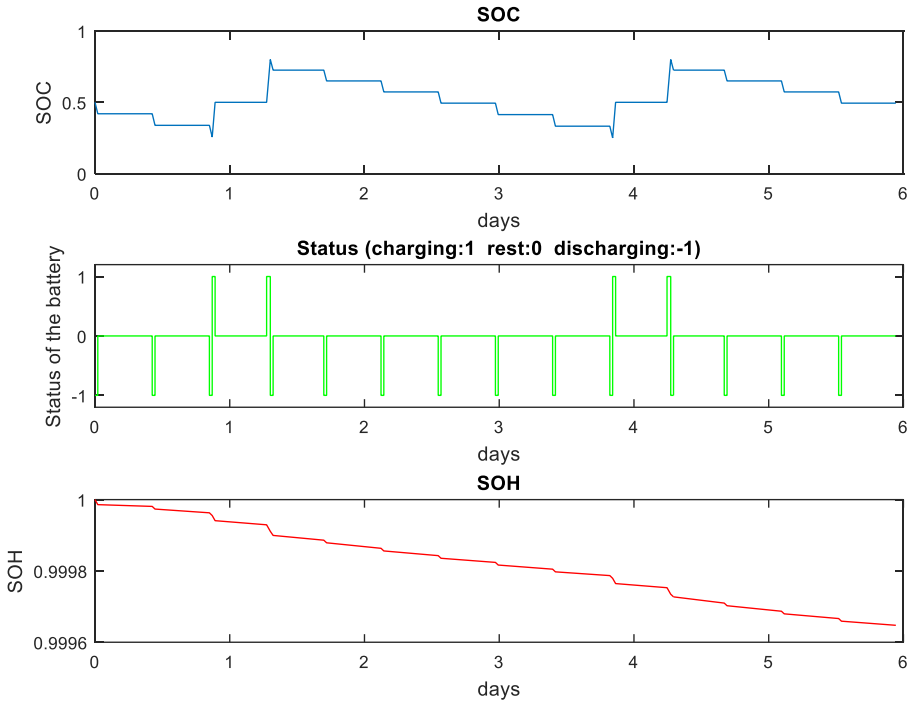

Figure 3.3. SOC, Status and SOH alterations regarding WLTP before the optimization

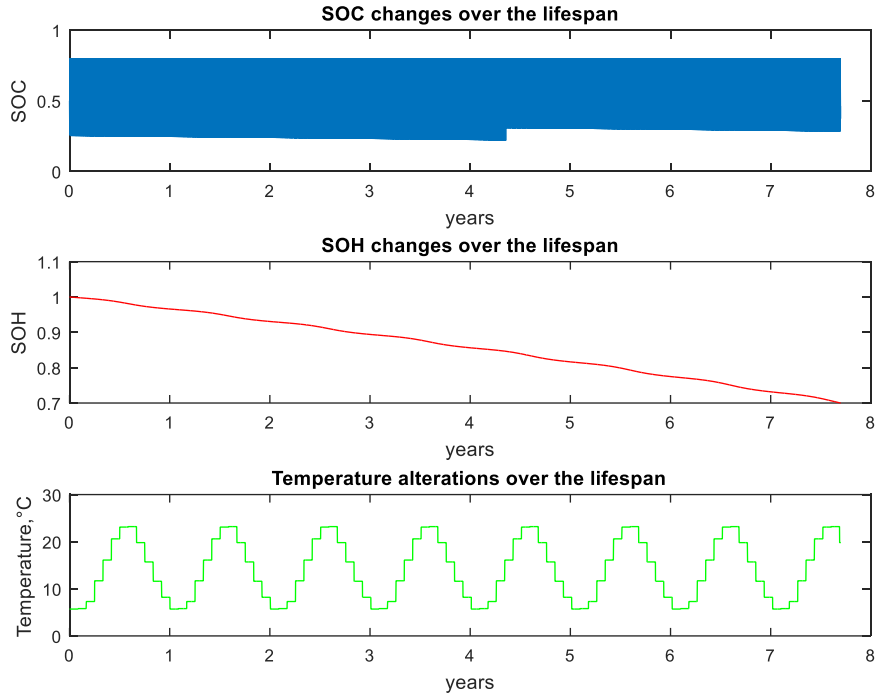

Figure 3.4. SOC, SOH and Temperature alterations over lifespan regarding WLTP before the optimization

3.3 BEV Modelling for variable battery energy capacity

Notice that “BEV modelling” block in Figure 2.2 is used only once at the beginning of the algorithm. The block used for modelling the BEV in the one-dimensional search loop is named as “BEV modelling for variable battery energy capacity”. Although the new block is based on the same logic as the former one given in Figure 2.2, the new one given in Figure 3.5 can accept changing energy capacity of the battery as input while ensuring given requirements are met.

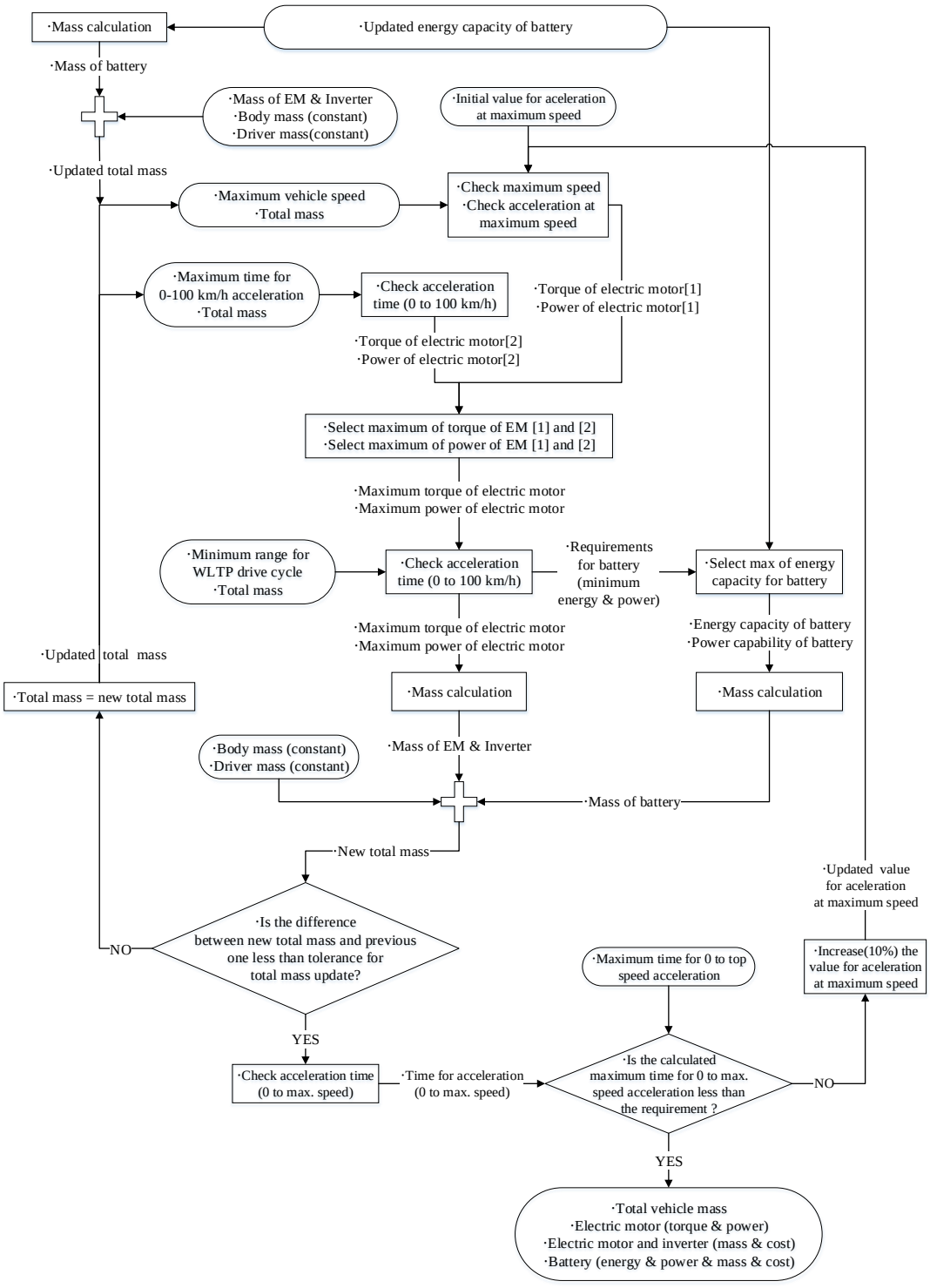

Figure 3.5. BEV modelling for variable battery energy capacity

3.4 Battery Energy Capacity Update Using One Dimensional Search

The energy capacity of the battery for the BEV that meet the requirements in Table 2.1 is given as 48 kWh in Table 2.4. Since slowing the battery ageing down is aimed by decreasing C-rate, the energy capacity of the battery should be increased. To minimize the objective function, a search must be conducted on energy capacity of the battery. That is, using a one-dimensional search method is proper to calculate the energy capacity of the battery that minimizes the objective function. The golden section method [34] is preferred because of its simplicity. The search is conducted in between the initial energy capacity of the battery, 48 kWh, and a maximum allowable energy capacity restricted by the physical limitations of the body of the vehicle. The maximum allowable energy capacity is defined considering some BEVs (Mazda MX-30, Lexus UX 300e, VW ID4, Volvo XC40, Polestar 2, Jaguar I-Pace EV400, BMW iX3, Audi e-tron 50, Mercedes EQC, Audi e-tron 55) in the SUV market. The maximum ratio of gross vehicle weight to body mass without power train and average difference between gross vehicle weight and unladen weight of the investigated SUV BEVs [4] are used to define the maximum allowable energy capacity of the battery. Body mass without powertrain given in Table 2.2 is multiplied with the maximum value of the ratio of gross vehicle weight to body mass without power train for the investigated SUV BEVs, 1.95, and gross vehicle weight is obtained for this study. Then, the average value of the difference between gross vehicle weight and unladen weight for the investigated SUV BEVs, 471 kg, is subtracted from the calculated gross vehicle weight, and the sum of the body mass without power train, mass of EM and inverter, and mass of battery is obtained. Then, maximum allowable energy capacity of the battery is calculated iteratively considering mass of EM and inverter depending on battery mass. The calculated maximum allowable energy capacity of the battery and the initial energy capacity of the battery, 48 kWh, are used as boundaries of the one dimensional search. As can be seen in Figure 3.6, the golden section method finds the minimum of the objective function inside the interval. The one-dimensional search error for convergence is defined as 1 Wh. Then, the energy

capacity of the battery that minimizes the objective function is calculated as 48.61 kWh.

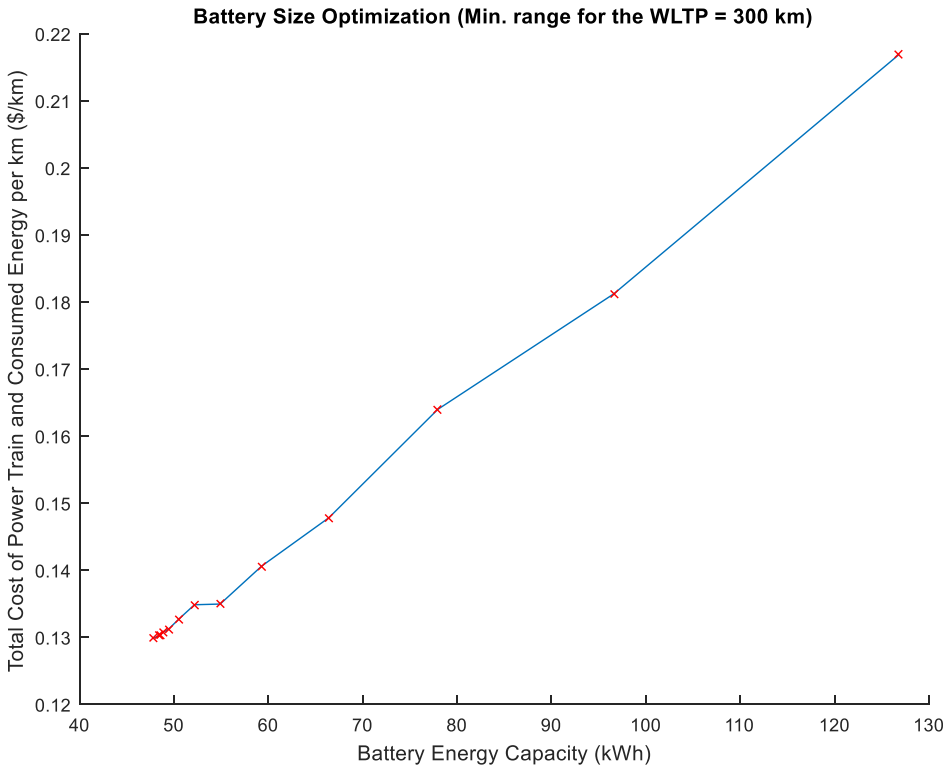

Figure 3.6. Battery Size Optimization (Min. Range for the WLTP = 300 km)

3.5 Determining the Parameters of BEV Assuming the Range Requirement is Waivable

As can be seen in Figure 3.6, the optimization ends up with lowest battery energy capacity for the given interval. Thus, another point that minimizes the objective function may extinct for a different, probably lower, energy capacity value. That is, the minimum range requirement for the WLTP, 300 km, given in Table 2.1 is too high to minimize the objective function. If the requirement is strict for an application, it is impossible to minimize the objective function lower than the case given in Figure 3.6. On the other hand, it is possible to minimize the objective function further than the case given in Figure 3.6 if the requirement is waivable for an application. In this

sense, the requirement of minimum range of 300 km for the WLTP is changed as the minimum range requirement for the WLTP is a shorter distance such that the minimum energy capacity value that meet the requirement of minimum range of 300 km for the WLTP is halved for the low side boundary of the search interval. Then, the optimization is rerun for wider interval of battery energy capacity (including lower values) as can be seen in Figure 3.7. The energy capacity of the battery that minimizes the objective function is calculated as 32.49 kWh. Naming the original case given in Figure 3.6 as Scenario No: 0 and the new case given in Figure 3.7 as scenario no: 1, the resulting BEV parameters are given in Table 3.1. In this table, the BEV's parameters are given regarding not only for scenario no: 1 but also for scenario no: 0. Therefore, improvements can easily be seen.

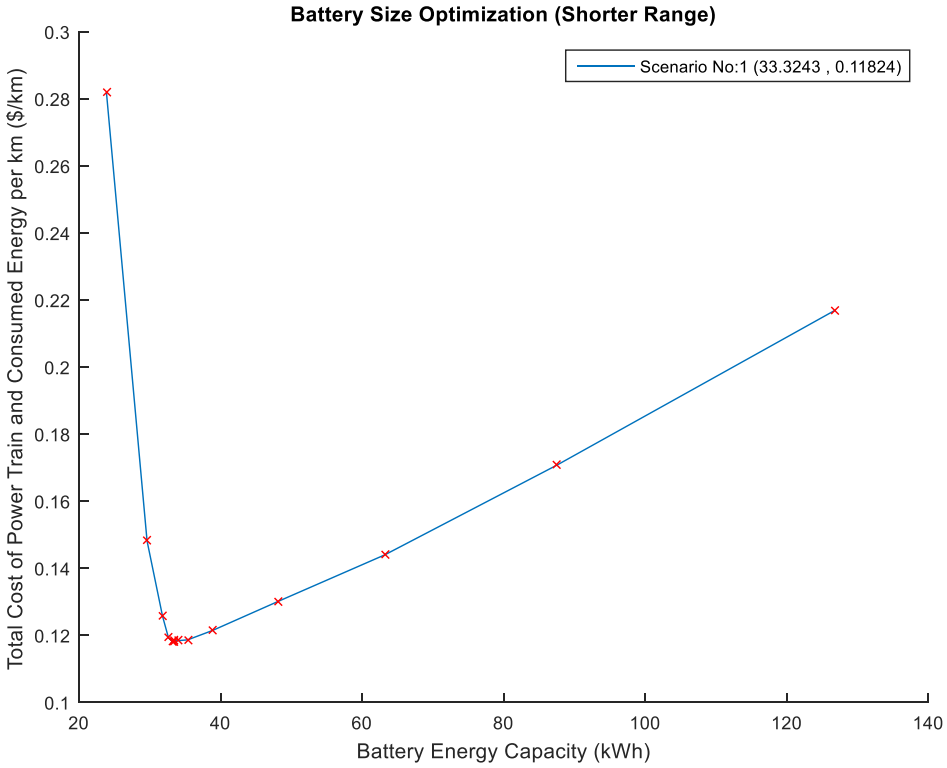

Figure 3.7. Battery Size Optimization (Shorter Range)

Table 3.1. Outputs regarding scenarios no: 0 and 1

		Scenario No	
Parameters	**Unit**	**0**	**1**
Maximum allowable battery energy	kWh	126.8	126.8
Optimum battery energy	kWh	48.6	33.3
Power of battery	kW	193.5	186.3
Mass of battery	kg	378.5	301.9
Initial cost of battery	$	12152	8331
Torque of EM	Nm	402	387
Power of EM	kW	168.4	162.1
Mass of EM	kg	153.1	147.4
Initial cost of EM and Inverter	$	5053	4863
Total mass of BEV	kg	2106.6	2024.2
Battery lifetime	years	7.75	6.66
Total distance traveled in lifetime	km	155097	133216
Range for given test procedure	km	305	212
Time for acceleration from 0 to top speed	sec	24	24.3
Consumed energy in one cycle for given test procedure	kWh	3.71	3.65
Cost of consumed energy per km	$/km	0.0195	0.0192
Initial cost of power train per km	$/km	0.1109	0.099
Objective Function	***$/km***	***0.1304***	***0.1182***

The optimum battery energy appears to be lower when the requirement of minimum range for the WLTP is waivable. Thus, the range for the WLTP is 212km and the lifetime of the battery is 6.66 years in scenario no: 1. Although the range for WLTP is reduced by 30.5% and lifetime of the battery is reduced by 14.1%, the objective function is reduced by 9.3% because initial cost of power train components and consumed energy per km are decreased in scenario no: 1. Optimal battery size is determined by combined consideration of total cost of power train components and consumed energy per km, and physical limitations of the vehicle body.

CHAPTER 4

RESULTS

The algorithm presented in the previous chapter is implemented in MATLAB to obtain the simulation results. In addition, some scenarios for the battery size optimization are run considering possible future improvements in the technology or alterations in user preferences regarding ageing mechanisms, annual distance, price of electricity, specific cost of battery pack, specific mass of battery pack, specific cost of EM and inverter, specific mass of EM and inverter, and test procedures.

4.1 The Parameters that Define Scenarios

"Scaling factor for calendar ageing", "Scaling factor for cycle ageing", "Ageing model in [14]", "Annual distance", "Cost of electricity", "Maximum charging power", "Specific cost of battery pack", "Scaling factor for specific mass of battery pack", "Specific cost of EM and inverter", "Scaling factor for specific mass of EM and inverter" and "Test Procedure" are the parameters that define the scenarios. Each parameter is explained in the following sections.

4.1.1 Scaling Factor for Calendar Ageing

Note that calendar ageing part of the model in [14] is given in Equation 2.7. Then, the parameters in the equation are updated using real data as explained in Section 2.3. Considering possible future improvements in calendar ageing mechanisms, it is desired to investigate the effects of calendar ageing on battery size optimization. Thus, a scaling factor multiplication named as SF_{Cal} is added to Equation 2.7 and Equation 4.1 is obtained. SF_{Cal} equals 1 originally, but SF_{Cal} takes values of 0.8 and 0.6 to slow down the calendar ageing linearly in some scenarios.

$$a_j = SF_{Cal} * a_{v,j} * \left(\boldsymbol{v_{cell}} - a_{0,j}\right) * \exp\left(-\frac{a_{T,j}}{\boldsymbol{T}}\right) \quad \textbf{(4.1)}$$

4.1.2 Scaling Factor for Cycle Ageing

Note that cycle ageing part of the model in [14] is given in Equation 2.8. Then, the parameters in the equation are updated using real data as explained in Section 2.3. Considering possible future improvements in cycle ageing mechanisms, it is desired to investigate the effects of cycle ageing on the battery size optimization. Thus, a scaling factor multiplication named as SF_{Cyc} is added to Equation 2.8 and Equation 4.2 is obtained. SF_{Cyc} equals 1 originally, but SF_{Cyc} takes values of 0.8 and 0.6 to slow down the cycle ageing linearly in some scenarios.

$$\beta_j = SF_{Cyc} * (b_{0,j} + b_{v,j} * \left(\boldsymbol{v_{cyc}} - b_{v0,j}\right)^2 + b_{DOD,j} * \boldsymbol{DOD} + b_{I,j} * \exp\left(b_{exp,j} * \frac{|\boldsymbol{i_{bat}}|}{\boldsymbol{C}}\right)) \quad \textbf{(4.2)}$$

4.1.3 Ageing model in [14]

Note that ageing parameter of the model in [14] is given in Table 2.5. Then, the parameters are updated using real data as explained in Section 2.3. In order to show the effects of the updating the ageing model parameters on the battery size optimization, a parameter named as "Ageing model in [14]" is defined. "Ageing model in [14]" equals 0 originally i.e. the updated parameters are used for battery ageing. On the other hand, "Ageing model in [14]" takes value of 1 in a scenario i.e. the parameters given in Table 2.5 are used for battery ageing.

4.1.4 Annual Distance

As explained in Chapter 3, annual distance travelled is considered as 20000 km. However, some of the users who drive for short ranges does not travel as much as 20000 km annually. Considering user preferences, it is desired to investigate the effects of annual distance travelled on the battery size optimization. Thus, annual distance travelled takes values of 15000 km and 10000 km in some scenarios.

4.1.5 Cost of Electricity

As explained in Chapter 3, cost of electricity is considered as 0.11 $/kWh [32]. Considering possible future improvements such as spreading of renewable energy sources in electricity generation, it is desired to investigate the effects of cost of electricity on the battery size optimization. Thus, cost of electricity takes values of 0.088 $/kWh and 0.066 $/kWh in some scenarios.

4.1.6 Maximum Charging Power

As explained in Chapter 3, an AC standard household charger of 22kW is used and maximum C-rate during charging is limited to 0.7C. However, some of the users who want to charge his/her BEV fast and may use a DC fast charger of up to 100kW. Considering user preferences, it is desired to investigate the effects of maximum charging power on the battery size optimization. Thus, maximum charging power is considered as 100kW in some scenarios. Note that, assuming charger and battery management system is able to communicate and maximum C-rate during charging is limited to 0.7C by the battery. That is, full power may not be drawn from the DC fast charger by the battery if the energy capacity of the battery is not big enough.

4.1.7 Specific Cost of Battery Pack

Note that the battery pack specific cost is given as $250/kWh in Table 2.3. Considering possible future improvements as it is projected that the average battery pack price will be equal to 101$/kWh by 2023 in [35], it is desired to investigate the effects of specific cost of battery pack on the battery size optimization. Thus, specific cost of battery pack takes values of $175/kWh and $100/kWh in some scenarios.

4.1.8 Scaling Factor for Specific Mass of Battery Pack

Note that the battery pack specific mass is given as (200 - 3 x Pbatt/Ebatt) Wh/kg +120 kg in Table 2.3. Considering possible future improvements, it is desired to investigate the effects of specific mass of battery pack on the battery size optimization. Thus, a scaling factor multiplication named as $SF_{MassBat}$ is added to the

expression given in Table 2.3 and the expression, *"$SF_{MassBat}$* x ((200 - 3 x Pbatt/Ebatt) Wh/kg +120 kg)", is obtained. $SF_{MassBat}$ equals 1 originally, but $SF_{MassBat}$ takes values of 0.8 and 0.6 to decrease the battery mass in some scenarios.

4.1.9 Specific Cost of EM and Inverter

Note that the specific cost of EM and inverter is given as $30/kW in Table 2.3. Considering possible future improvements, it is desired to investigate the effects of specific cost of EM and inverter on the battery size optimization. Thus, specific cost of EM and inverter takes values of $24/kW and $18/kW in some scenarios.

4.1.10 Scaling Factor for Specific Mass of EM and Inverter

Note that the specific mass of EM and inverter is given as 1.1 kW/kg in Table 2.3. Considering possible future improvements, it is desired to investigate the effects of specific mass of EM and inverter on the battery size optimization. Thus, a scaling factor multiplication named as $SF_{MassEMI}$ is added to the expression given in Table 2.3 and the expression, *"$SF_{MassEMI}$* x 1.1 kW/kg", is obtained. $SF_{MassEMI}$ equals 1 originally, but $SF_{MassEMI}$ takes values of 0.8 and 0.6 to decrease the EM and inverter mass in some scenarios.

4.1.11 Test procedure

As stated in Section 2.1, the test procedure that used for utilization of the BEV is considered as the WLTP given in Figure 2.1. Note that, the WLTP includes low, medium, high and extra high speed parts to simulate urban, suburban, rural and highway scenarios, respectively. However, some of the users may drive more often in urban areas or highways. To consider user preferences, four more test procedures are formed using the low, medium, high and extra high speed parts of the WLTP: a modified WLTP that includes only the low speed part, a modified WLTP that includes predominantly the low speed part, a modified WLTP that includes only the extra high speed part and a modified WLTP that includes predominantly the extra high speed part as given in Figures 4.1, 4.2, 4.3 and 4.4 respectively. These test

procedures are used to investigate the effects of test procedure on the battery size optimization in some scenarios.

WLTP given in Figure 2.1 range 23.27 km, lead 30 minutes, has 46.5 km/h average speed and 131.3 km/h maximum speed. The modified WLTP given in Figure 4.1 range 3.09 km, lead 9.8 minutes, has 18.9 km/h average speed and 56.5 km/h maximum speed. The modified WLTP given in Figure 4.2 range 29.45 km, lead 49.7 minutes, has 35.6 km/h average speed and 131.3 km/h maximum speed. The modified WLTP given in Figure 4.3 range 8.25 km, lead 5.4 minutes, has 91.4 km/h average speed and 131.3 km/h maximum speed. The modified WLTP given in Figure 4.4 range 39.77 km, lead 40.8 minutes, has 58.4 km/h average speed and 131.3 km/h maximum speed.

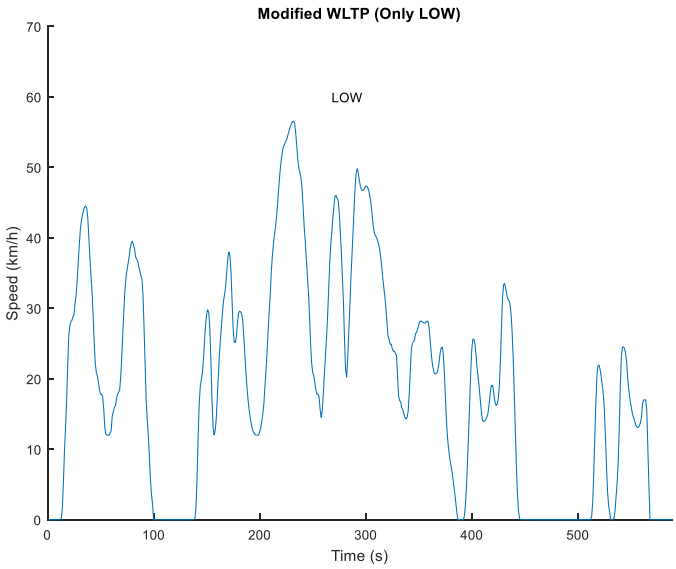

Figure 4.1. A modified WLTP that includes only the low speed part

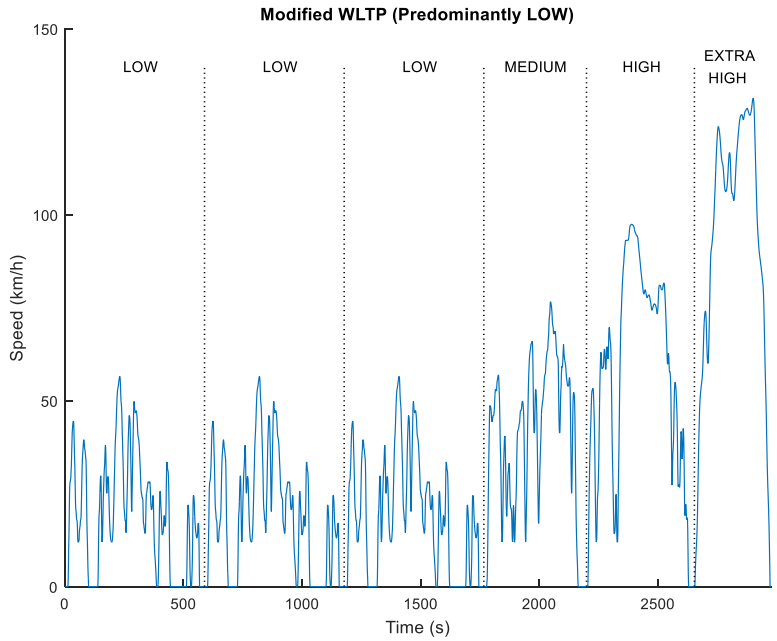

Figure 4.2. A modified WLTP that includes predominantly the low speed part

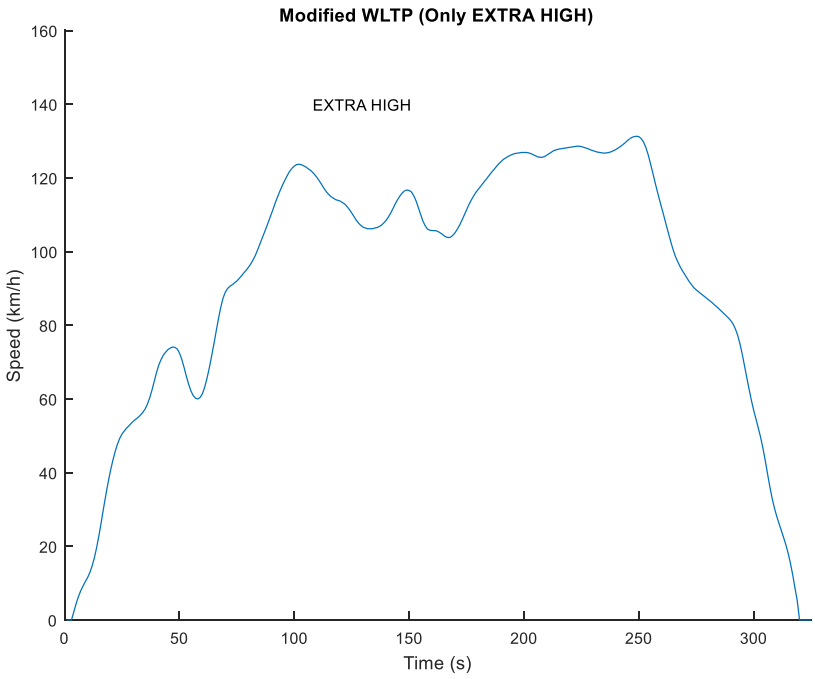

Figure 4.3. A modified WLTP that includes only the extra high speed part

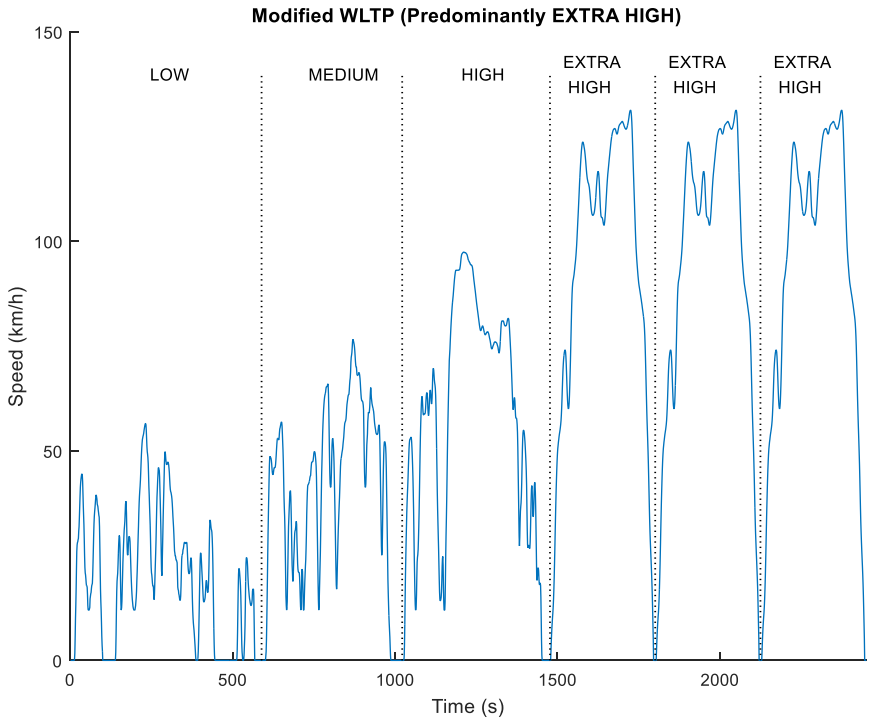

Figure 4.4. A modified WLTP that includes predominantly the extra high speed part

4.1.12 The Original Values in Scenarios No: 0 and 1

In Table 4.1, values of the parameters that define scenarios no: 0 and 1 are given. Changing some of these values, the following scenarios are formed and effects of the parameters on battery size optimization are investigated.

Table 4.1. Values of the parameters regarding scenarios no: 0 and 1

		Scenario No	
Parameters	**Unit**	**0**	**1**
Scaling factor for calendar ageing		1	1
Scaling factor for cycle ageing		1	1
Ageing model in [14]		0	0
Annual distance	km	20000	20000
Cost of electricity	$/kWh	0.11	0.11
Maximum charging power	kW	22	22
Specific cost of battery pack	$/kWh	250	250
Scaling factor for specific mass of battery pack		1	1
Specific cost of EM and inverter	$/kW	30	30
Scaling factor for specific mass of EM and inverter		1	1
Test procedure		WLTP	WLTP

4.2 Investigation of the Effects by the Ageing Mechanisms on Battery Size Optimization

In Table 4.2, values of the parameters that define scenarios no: 1, 2, 3 and 4 are given. The values of "Scaling factor for calendar ageing" and "Scaling factor for cycle ageing" are changed simultaneously in scenarios no: 2 and 3, and the value of "Ageing model in [14]" is changed in scenario no: 4.

Table 4.2. Values of the parameters regarding scenarios no: 1, 2, 3 and 4

		Scenario No			
Parameters	**Unit**	**1**	**2**	**3**	**4**
Scaling factor for calendar ageing		1	**0.8**	**0.6**	**1**
Scaling factor for cycle ageing		1	**0.8**	**0.6**	**1**
Ageing model in [14]		0	**0**	**0**	**1**
Annual distance	km	20000	20000	20000	20000
Cost of electricity	$/kWh	0.11	0.11	0.11	0.11
Maximum charging power	kW	22	22	22	22
Specific cost of battery pack	$/kWh	250	250	250	250
Scaling factor for specific mass of battery pack		1	1	1	1
Specific cost of EM and inverter	$/kW	30	30	30	30
Scaling factor for specific mass of EM and inverter		1	1	1	1
Test procedure		WLTP	WLTP	WLTP	WLTP

In Figures 4.5 and 4.6, the data regarding scenario no: 1 are presented. In Figure 4.5, the SOC, status and SOH alterations of the battery are visualized for the first few cycles. The SOC, SOH and temperature alterations of the battery are visualized over the lifespan of the battery as in Figure 4.6. In Figures 4.7 and 4.8, the data regarding scenario no: 2 are presented. In Figure 4.7, the SOC, status and SOH alterations of the battery are visualized for the first few cycles. The SOC, SOH and temperature alterations of the battery are visualized over the lifespan of the battery as in Figure 4.8. In Figures 4.9 and 4.10, the data regarding scenario no: 3 are presented. In Figure

4.9, the SOC, status and SOH alterations of the battery are visualized for the first few cycles. The SOC, SOH and temperature alterations of the battery are visualized over the lifespan of the battery as in Figure 4.10. In Figures 4.11 and 4.12, the data regarding scenario no: 4 are presented. In Figure 4.11, the SOC, status and SOH alterations of the battery are visualized for the first few cycles. The SOC, SOH and temperature alterations of the battery are visualized over the lifespan of the battery as in Figure 4.12.

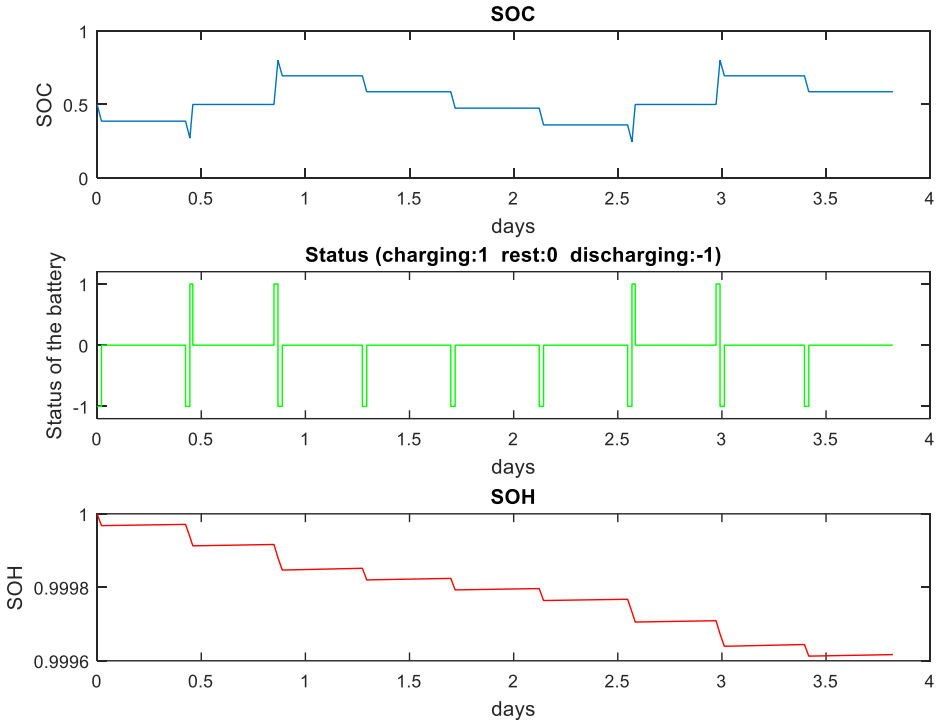

Figure 4.5. SOC, status and SOH alterations regarding scenario no: 1

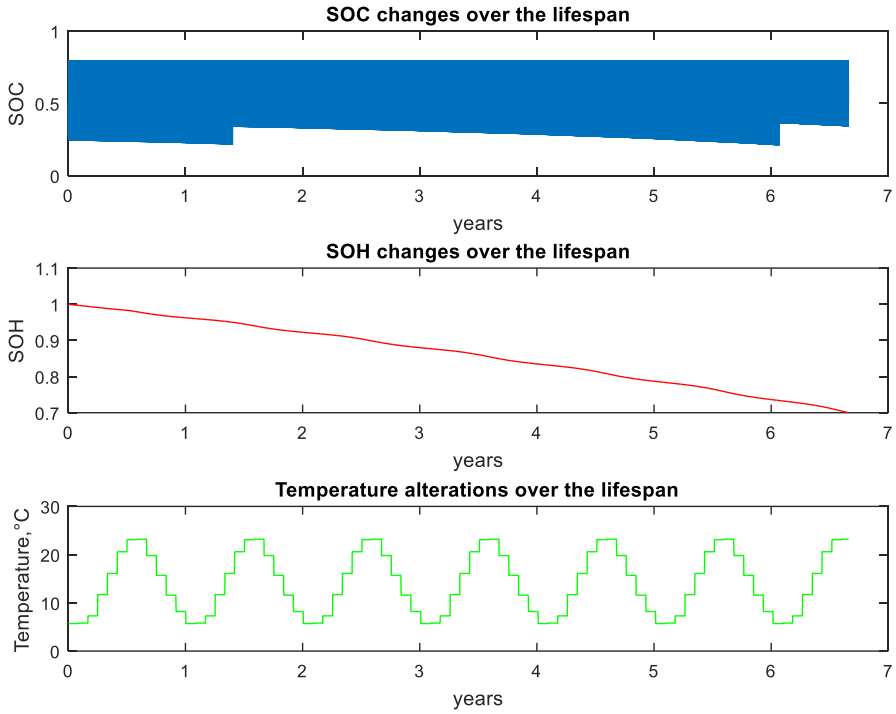

Figure 4.6. SOC, SOH and temperature alterations over lifespan regarding scenario no: 1

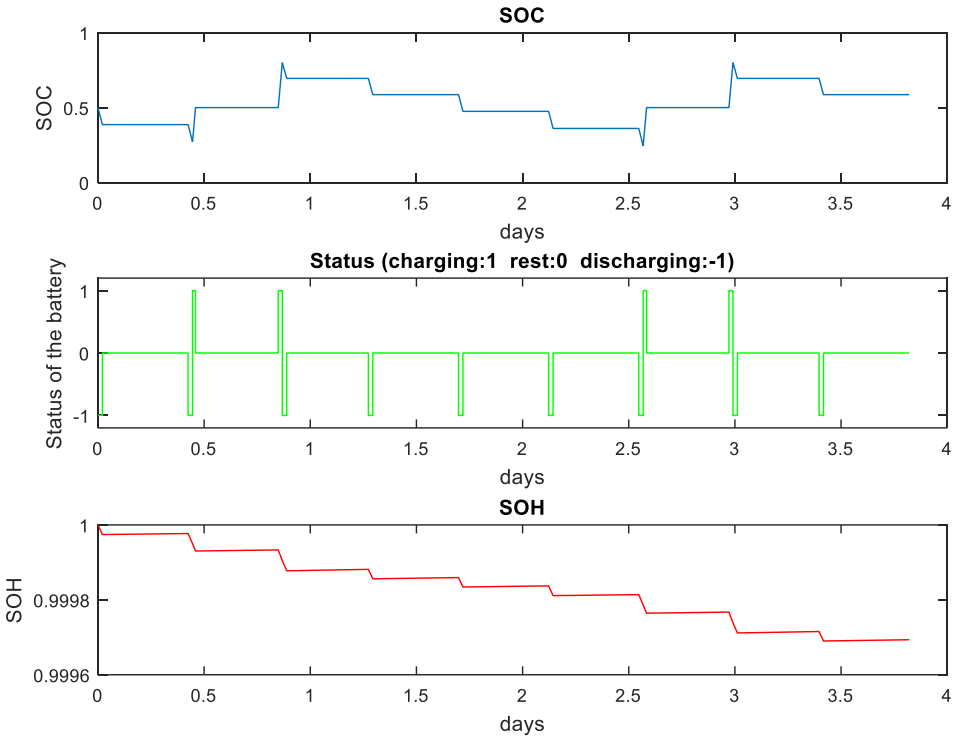

Figure 4.7. SOC, status and SOH alterations regarding scenario no: 2

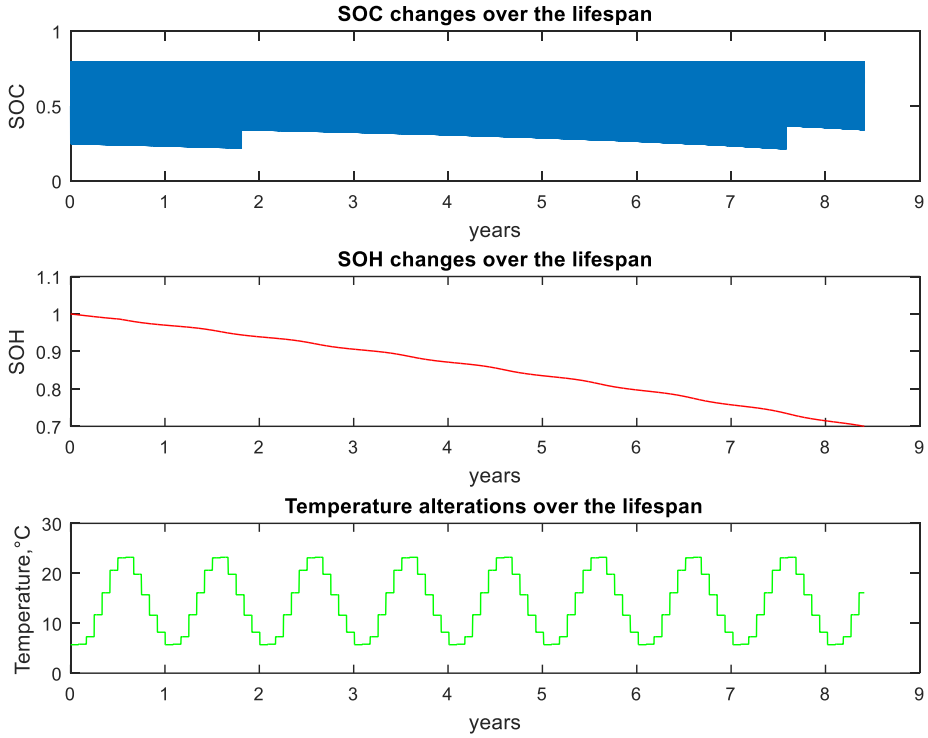

Figure 4.8. SOC, SOH and temperature alterations over lifespan regarding scenario no: 2

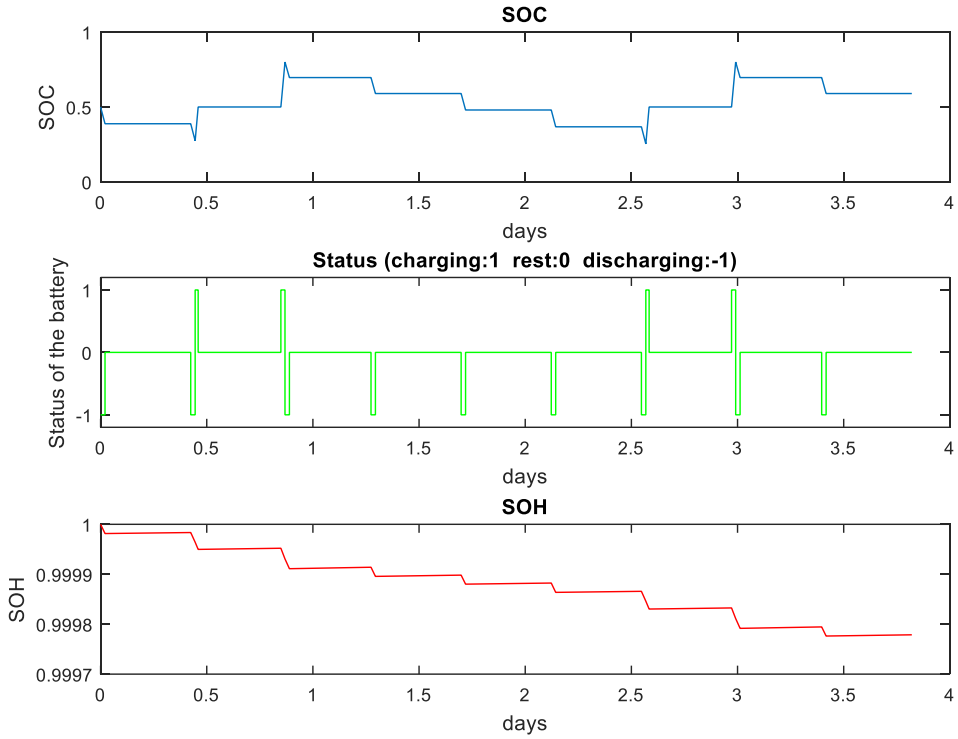

Figure 4.9. SOC, status and SOH alterations regarding scenario no: 3

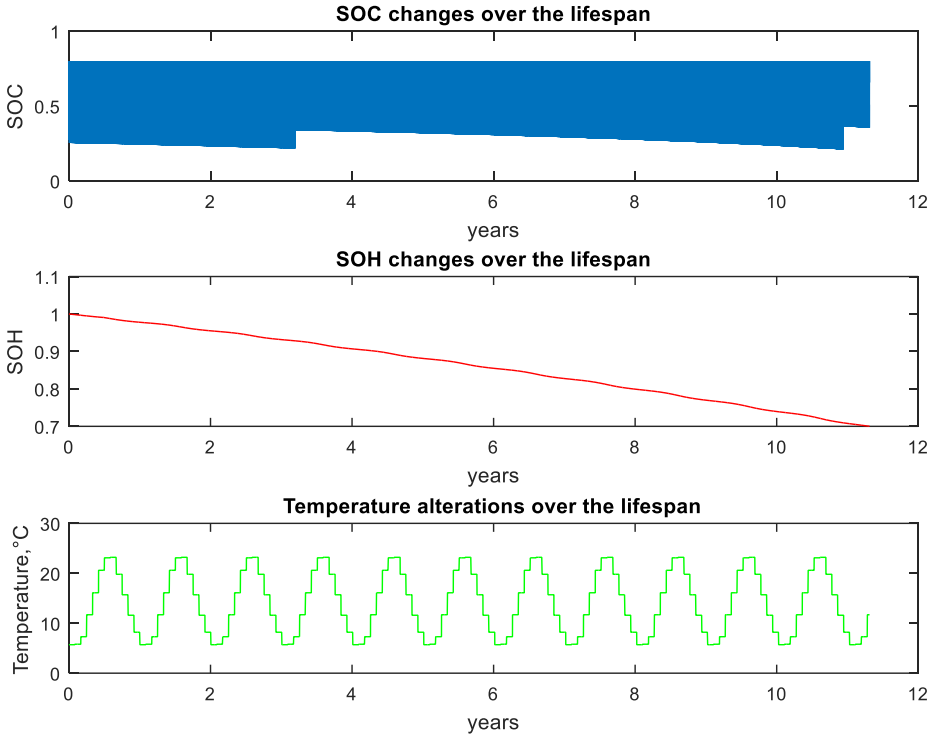

Figure 4.10. SOC, SOH and temperature alterations over lifespan regarding scenario no: 3

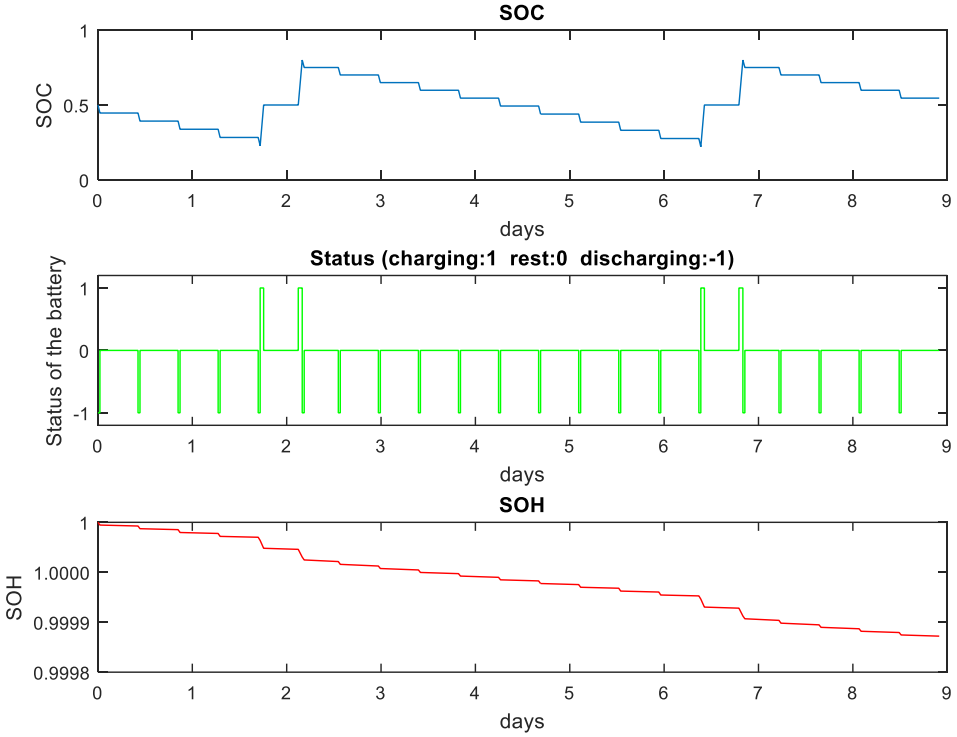

Figure 4.11. SOC, status and SOH alterations regarding scenario no: 4

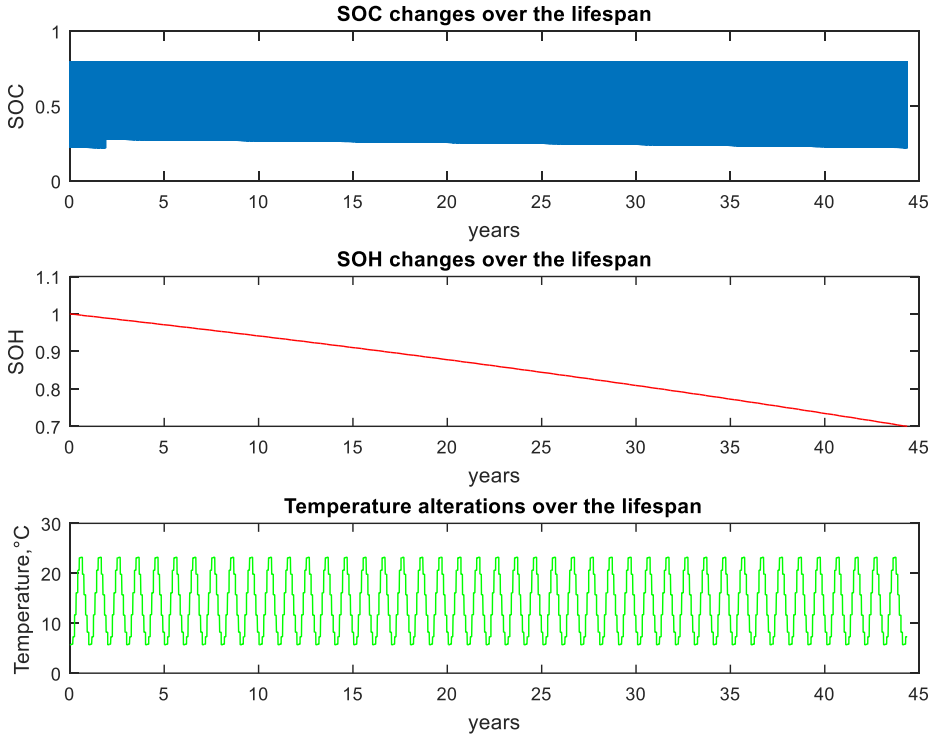

Figure 4.12. SOC, SOH and temperature alterations over lifespan regarding scenario no: 4

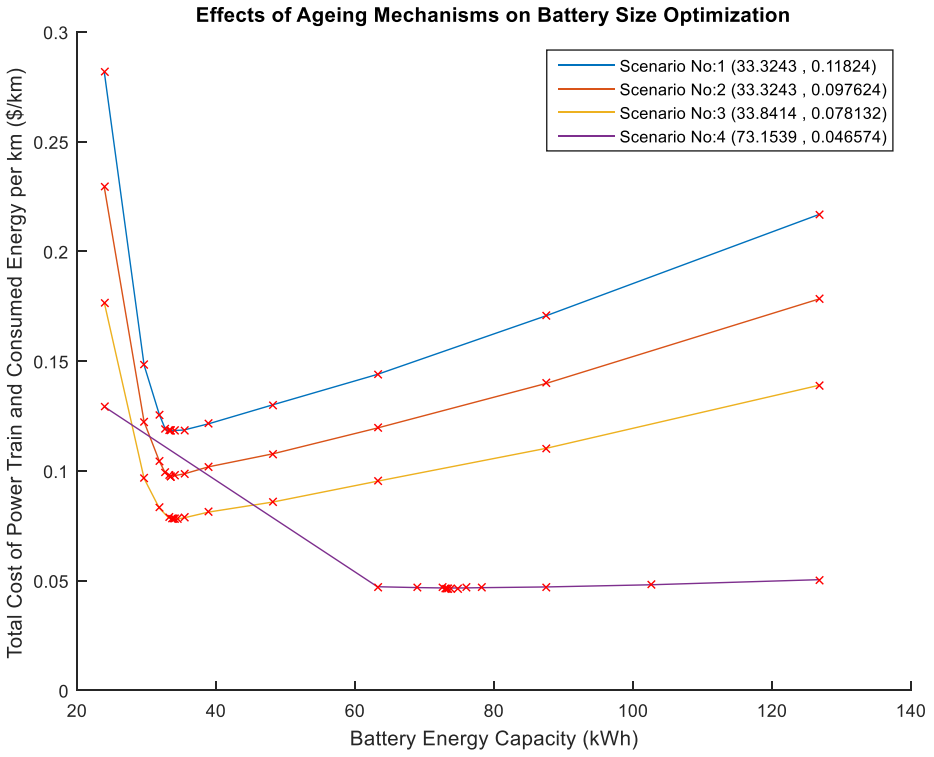

Figure 4.13. Effects of ageing mechanisms

In Figure 4.13 and Table 4.3, the data regarding scenarios no: 1, 2, 3 and 4 are presented. In the figure, how the battery size optimization ends up for each scenario is visualized. Besides, the detailed results regarding the scenarios are given in the table. Considering scenarios no: 2 and 3, the optimum battery energy becomes a bit higher when scaling factors for calendar ageing and cycle ageing are decreased. Since lifetime of the battery is increased, the objective function is reduced significantly in these scenarios. On the other hand, the differences become greater in scenario no: 4. In scenario no: 4, the optimum battery energy becomes more than double compared to scenario no:1. Besides, lifetime of the battery is increased dramatically, and the objective function is reduced by 60.5%.

Table 4.3. Outputs regarding scenarios no: 1, 2, 3 and 4

		Scenario No			
Parameters	**Unit**	**1**	**2**	**3**	**4**
Maximum allowable battery energy	kWh	126.8	126.8	126.8	126.8
Optimum battery energy	kWh	33.3	33.3	33.8	73.2
Power of battery	kW	186.3	186.3	186.6	204.9
Mass of battery	kg	301.9	301.9	304.5	501.8
Initial cost of battery	$	8331	8331	8460	18288
Torque of EM	Nm	387	387	387	427
Power of EM	kW	162.1	162.1	162.4	178.4
Mass of EM	kg	147.4	147.4	147.6	162.2
Initial cost of EM and Inverter	$	4863	4863	4872	5352
Total mass of BEV	kg	2024.2	2024.2	2027.1	2239
Battery lifetime	years	6.66	8.41	11.31	44.37
Total distance traveled in lifetime	km	133216	168229	226242	887379
Range for given test procedure	km	212	212	215	449
Time for acceleration from 0 to top speed	sec	24.3	24.3	24.2	23.7
Consumed energy in one cycle for given test procedure	kWh	3.65	3.65	3.65	3.79
Cost of consumed energy per km	$/km	0.0192	0.0192	0.0192	0.0199
Initial cost of power train per km	$/km	0.099	0.0784	0.0589	0.0266
Objective Function	***$/km***	***0.1182***	***0.0976***	***0.0781***	***0.0466***

4.3 Investigation of Separate Effects by the Calendar and Cycle Ageing Mechanisms on Battery Size Optimization

In Table 4.4, values of the parameters that define scenarios no: 1, 5, 6, 7 and 8 are given. The value of "Scaling factor for calendar ageing" is changed in scenarios no: 5 and 6. On the other hand, the value of "Scaling factor for cycle ageing" is changed in scenarios no: 7 and 8. Notice that the parameters are changing one by one in these scenarios while they are changing simultaneously in scenarios no: 2 and 3.

Table 4.4. Values of the parameters regarding scenarios no: 1, 5, 6, 7 and 8

		Scenario No				
Parameters	**Unit**	**1**	**5**	**6**	**7**	**8**
Scaling factor for calendar ageing		1	**0.8**	**0.6**	**1**	**1**
Scaling factor for cycle ageing		1	**1**	**1**	**0.8**	**0.6**
Ageing model in [14]		0	0	0	0	0
Annual distance	km	20000	20000	20000	20000	20000
Cost of electricity	$/kWh	0.11	0.11	0.11	0.11	0.11
Maximum charging power	kW	22	22	22	22	22
Specific cost of battery pack	$/kWh	250	250	250	250	250
Scaling factor for specific mass of battery pack		1	1	1	1	1
Specific cost of EM and inverter	$/kW	30	30	30	30	30
Scaling factor for specific mass of EM and inverter		1	1	1	1	1
Test procedure		WLTP	WLTP	WLTP	WLTP	WLTP

In Figures 4.14 and 4.15, the data regarding scenario no: 5 are presented. In Figure 4.14, the SOC, status and SOH alterations of the battery are visualized for the first few cycles. The SOC, SOH and temperature alterations of the battery are visualized over the lifespan of the battery as in Figure 4.15. In Figures 4.16 and 4.17, the data

regarding scenario no: 6 are presented. In Figure 4.16, the SOC, status and SOH alterations of the battery are visualized for the first few cycles. The SOC, SOH and temperature alterations of the battery are visualized over the lifespan of the battery as in Figure 4.17. In Figures 4.18 and 4.19, the data regarding scenario no: 7 are presented. In Figure 4.18, the SOC, status and SOH alterations of the battery are visualized for the first few cycles. The SOC, SOH and temperature alterations of the battery are visualized over the lifespan of the battery as in Figure 4.19. In Figures 4.20 and 4.21, the data regarding scenario no: 8 are presented. In Figure 4.20, the SOC, status and SOH alterations of the battery are visualized for the first few cycles. The SOC, SOH and temperature alterations of the battery are visualized over the lifespan of the battery as in Figure 4.21.

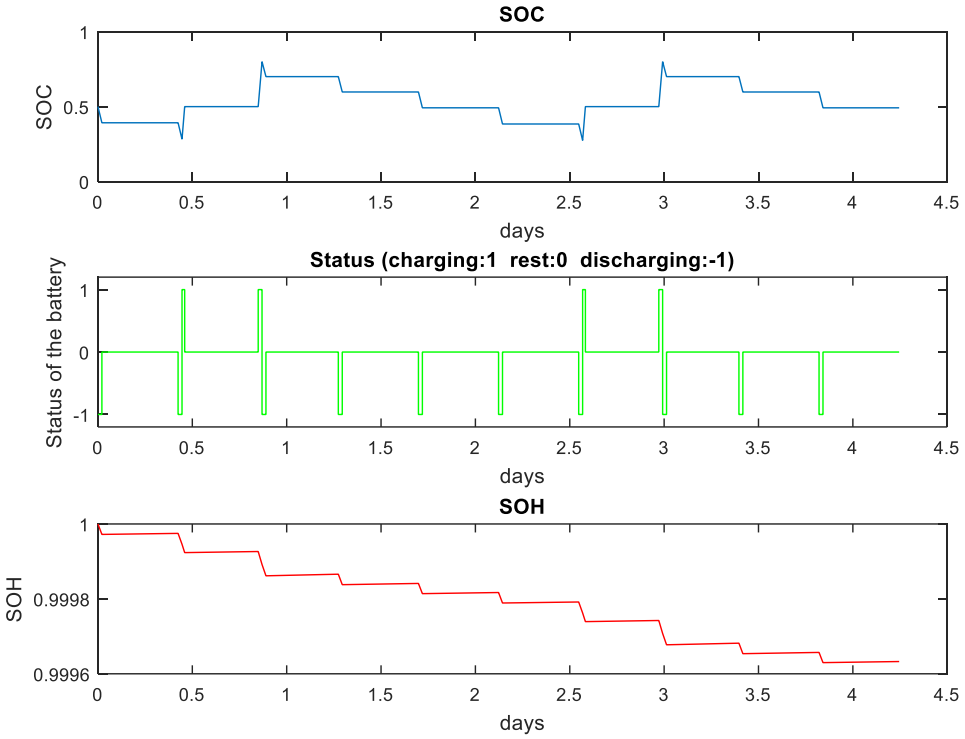

Figure 4.14. SOC, status and SOH alterations regarding scenario no: 5

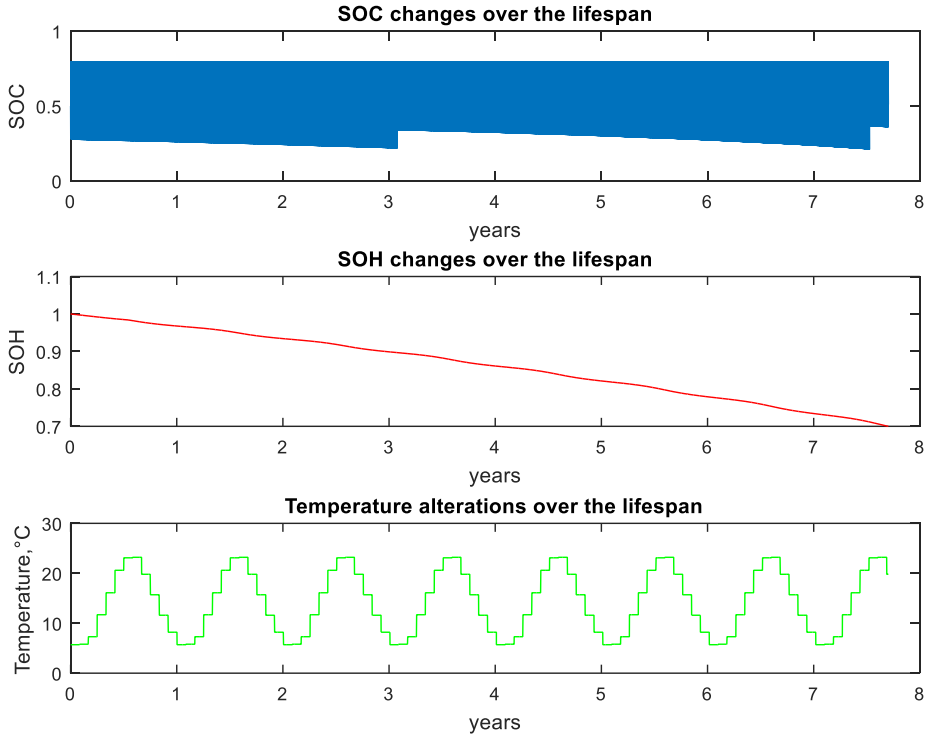

Figure 4.15. SOC, SOH and temperature alterations over lifespan regarding scenario no: 5

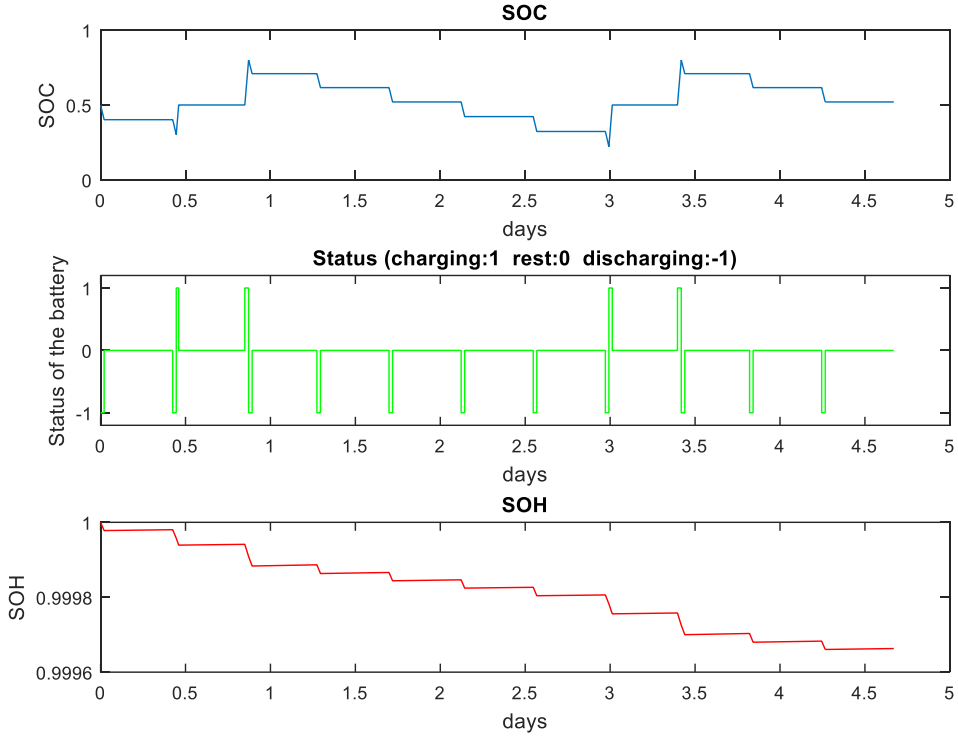

Figure 4.16. SOC, status and SOH alterations regarding scenario no: 6

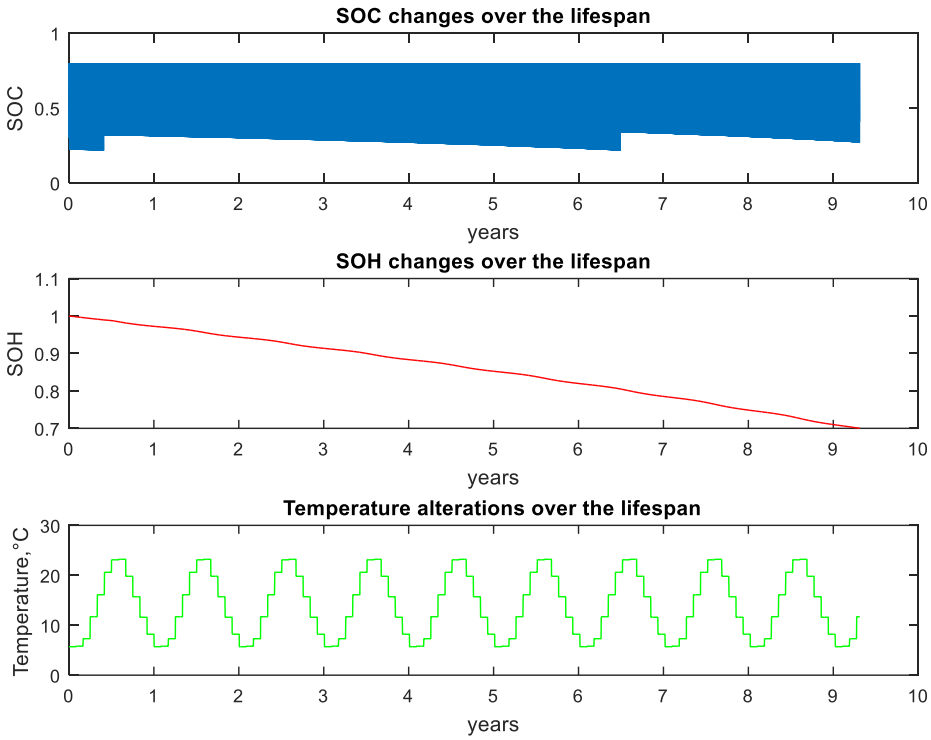

Figure 4.17. SOC, SOH and temperature alterations over lifespan regarding scenario no: 6

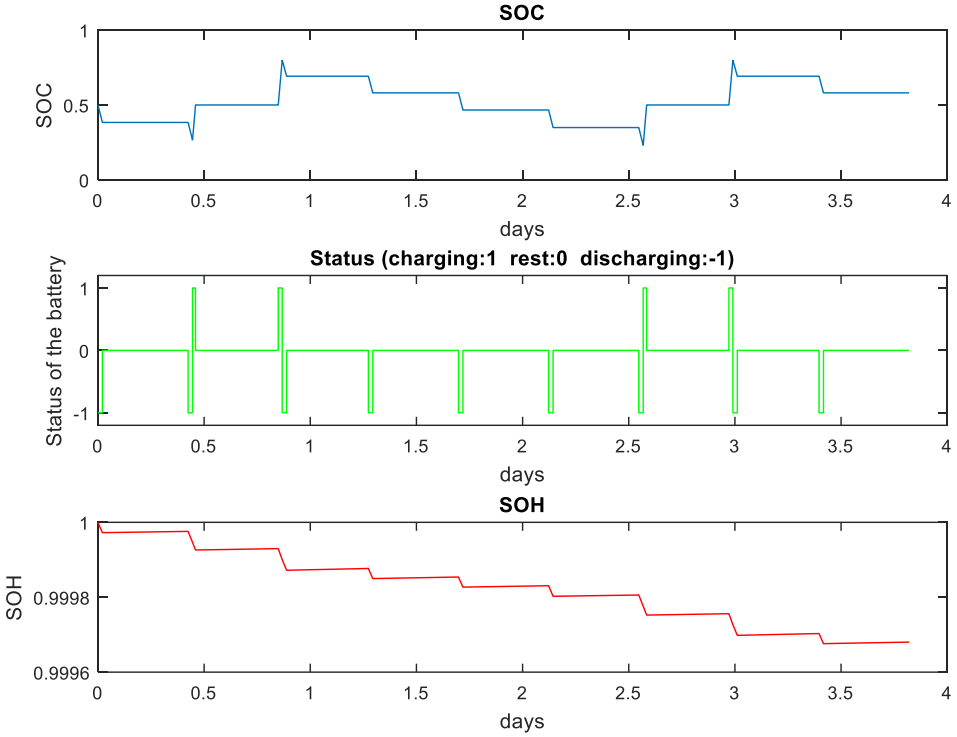

Figure 4.18. SOC, status and SOH alterations regarding scenario no: 7

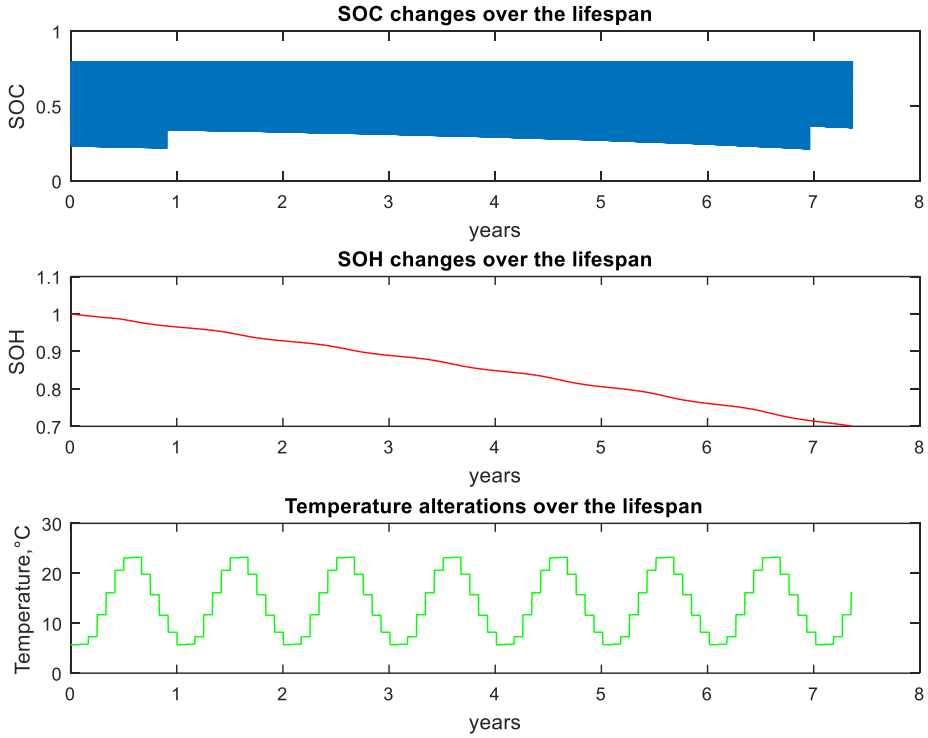

Figure 4.19. SOC, SOH and temperature alterations over lifespan regarding scenario no: 7

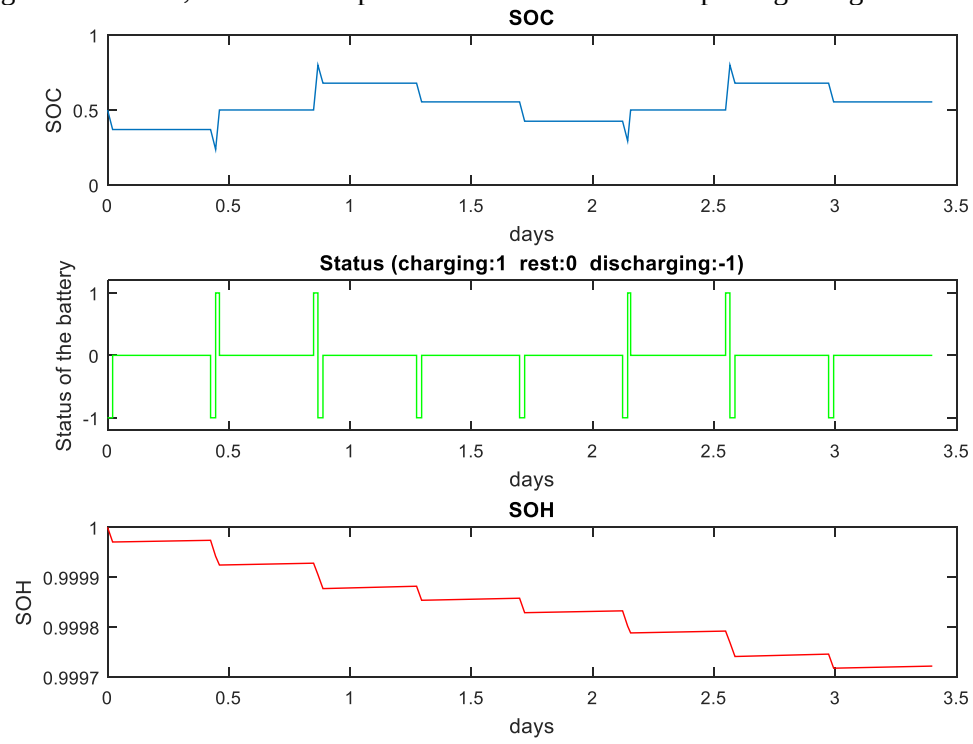

Figure 4.20. SOC, status and SOH alterations regarding scenario no: 8

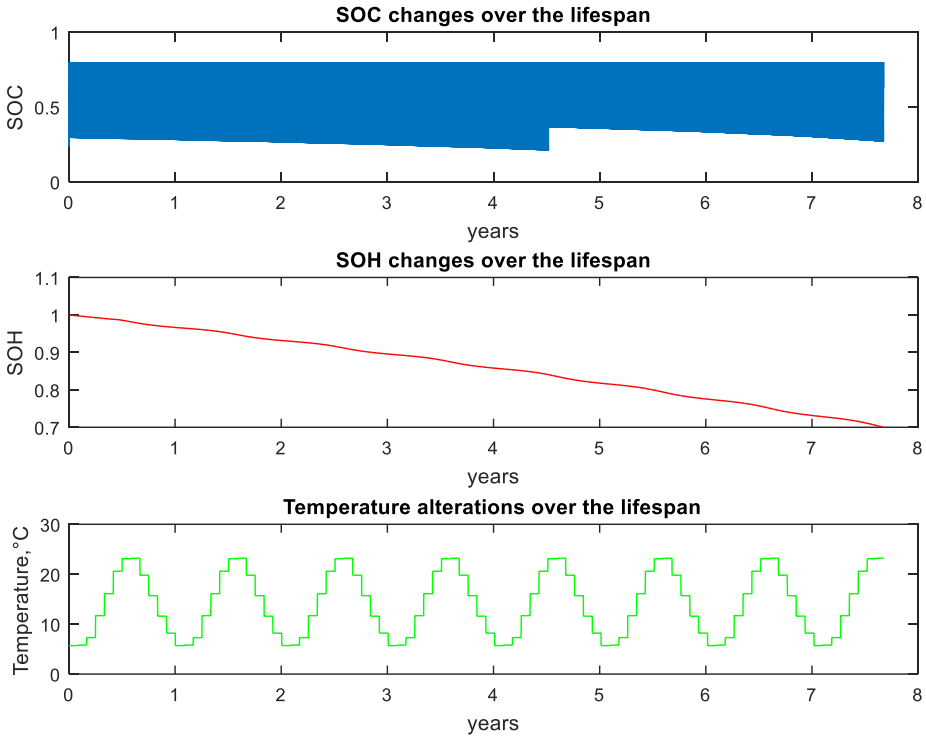

Figure 4.21. SOC, SOH and temperature alterations over lifespan regarding scenario no: 8

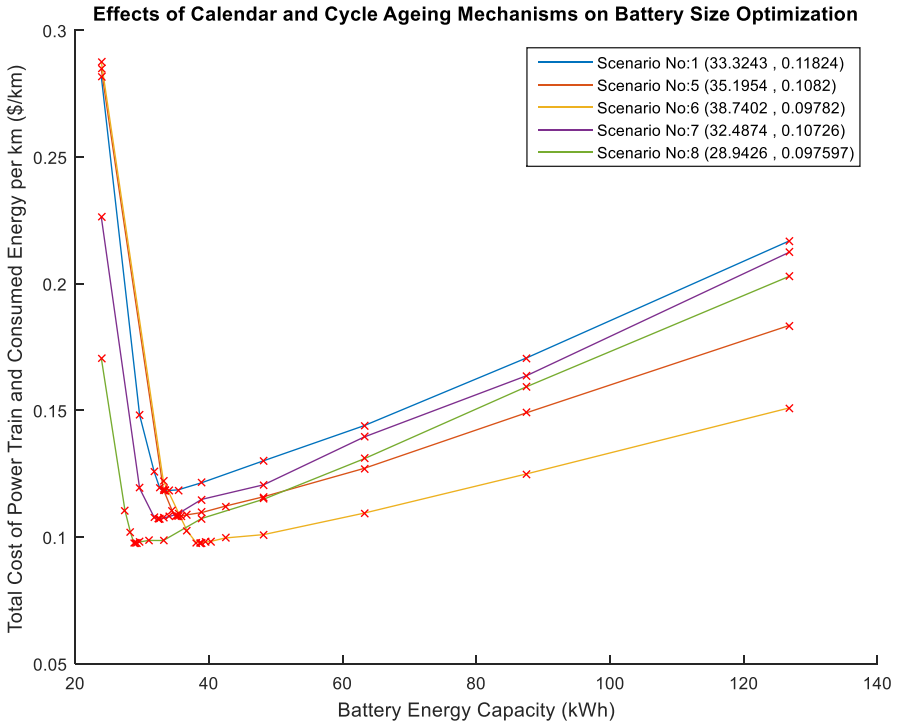

Figure 4.22. Separate effects of the calendar and cycle ageing mechanisms

In Figure 4.22 and Table 4.5, the data regarding scenarios no: 1, 5, 6, 7 and 8 are presented. In the figure, how the battery size optimization ends up for each scenario is visualized. Besides, the detailed results regarding the scenarios are given in the table. Considering scenarios no: 5 and 6, the optimum battery energy becomes greater when scaling factors for calendar ageing are decreased. On the other hand, the optimum battery energy becomes lower when scaling factors for cycle ageing are decreased considering scenarios no: 7 and 8. Since lifetime of the battery is increased for all of the scenarios no: 5, 6, 7 and 8, the objective function is reduced significantly compared to scenario no: 1.

Table 4.5. Outputs regarding scenarios no: 1, 5, 6, 7 and 8

		Scenario No				
Parameters	**Unit**	**1**	**5**	**6**	**7**	**8**
Maximum allowable battery energy	kWh	126.8	126.8	126.8	126.8	126.8
Optimum battery energy	kWh	33.3	35.2	38.7	32.5	28.9
Power of battery	kW	186.3	187.9	189.1	185.9	184.3
Mass of battery	kg	301.9	311.3	329	297.7	280
Initial cost of battery	$	8331	8799	9685	8122	7236
Torque of EM	Nm	387	389	393	386	382
Power of EM	kW	162.1	163.5	164.6	161.8	160.4
Mass of EM	kg	147.4	148.7	149.6	147.1	145.8
Initial cost of EM and Inverter	$	4863	4906	4937	4853	4813
Total mass of BEV	kg	2024.2	2035	2053.6	2019.8	2000.8
Battery lifetime	years	6.66	7.7	9.31	7.37	7.68
Total distance traveled in lifetime	km	133216	154070	186237	147306	153510
Range for given test procedure	km	212	224	245	207	185
Time for acceleration from 0 to top speed	sec	24.3	24.1	24.1	24.3	24.3
Consumed energy in one cycle for given test procedure	kWh	3.65	3.66	3.67	3.65	3.64
Cost of consumed energy per km	$/km	0.0192	0.0192	0.0193	0.0192	0.0191
Initial cost of power train per km	$/km	0.099	0.089	0.0785	0.0881	0.0785
Objective Function	***$/km***	***0.1182***	***0.1082***	***0.0978***	***0.1073***	***0.0976***

4.4 Investigation of Effects by Annual Distance on Battery Size Optimization

In Table 4.6, values of the parameters that define scenarios no: 1, 9 and 10 are given. The value of "Annual distance" is changed in scenarios no: 9 and 10.

Table 4.6. Values of the parameters regarding scenarios no: 1, 9 and 10

		Scenario No		
Parameters	**Unit**	**1**	**9**	**10**
Scaling factor for calendar ageing		1	1	1
Scaling factor for cycle ageing		1	1	1
Ageing model in [14]		0	0	0
Annual distance	km	20000	**15000**	**10000**
Cost of electricity	$/kWh	0.11	0.11	0.11
Maximum charging power	kW	22	22	22
Specific cost of battery pack	$/kWh	250	250	250
Scaling factor for specific mass of battery pack		1	1	1
Specific cost of EM and inverter	$/kW	30	30	30
Scaling factor for specific mass of EM and inverter		1	1	1
Test procedure		WLTP	WLTP	WLTP

In Figures 4.23 and 4.24, the data regarding scenario no: 9 are presented. In Figure 4.23, the SOC, status and SOH alterations of the battery are visualized for the first few cycles. The SOC, SOH and temperature alterations of the battery are visualized over the lifespan of the battery as in Figure 4.24. In Figures 4.25 and 4.26, the data regarding scenario no: 10 are presented. In Figure 4.25, the SOC, status and SOH alterations of the battery are visualized for the first few cycles. The SOC, SOH and temperature alterations of the battery are visualized over the lifespan of the battery as in Figure 4.26.

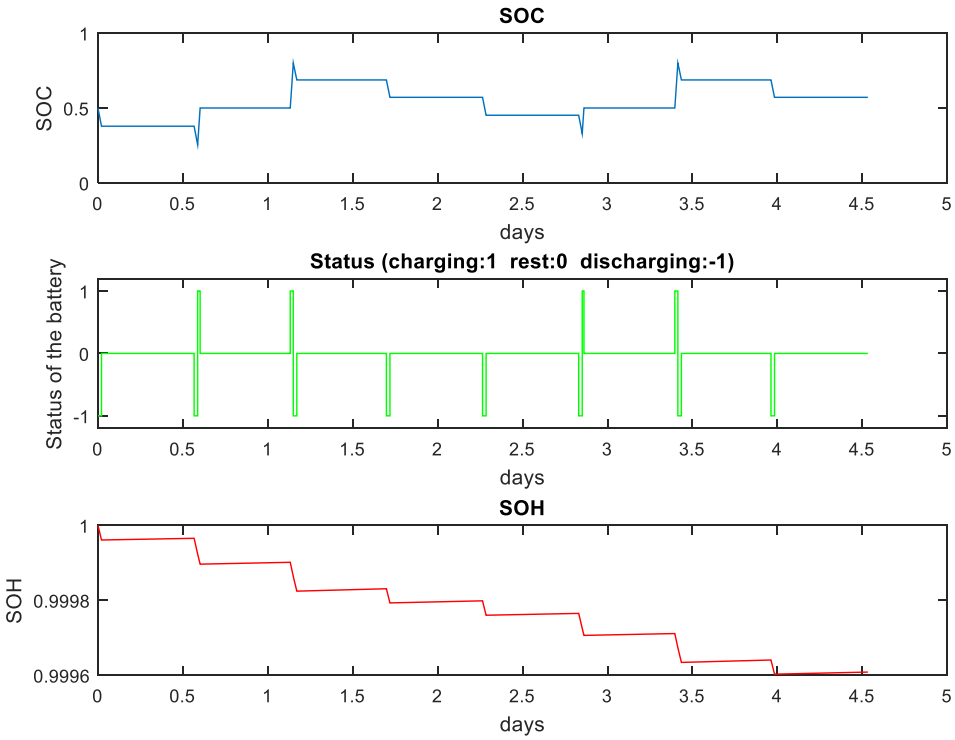

Figure 4.23. SOC, status and SOH alterations regarding scenario no: 9

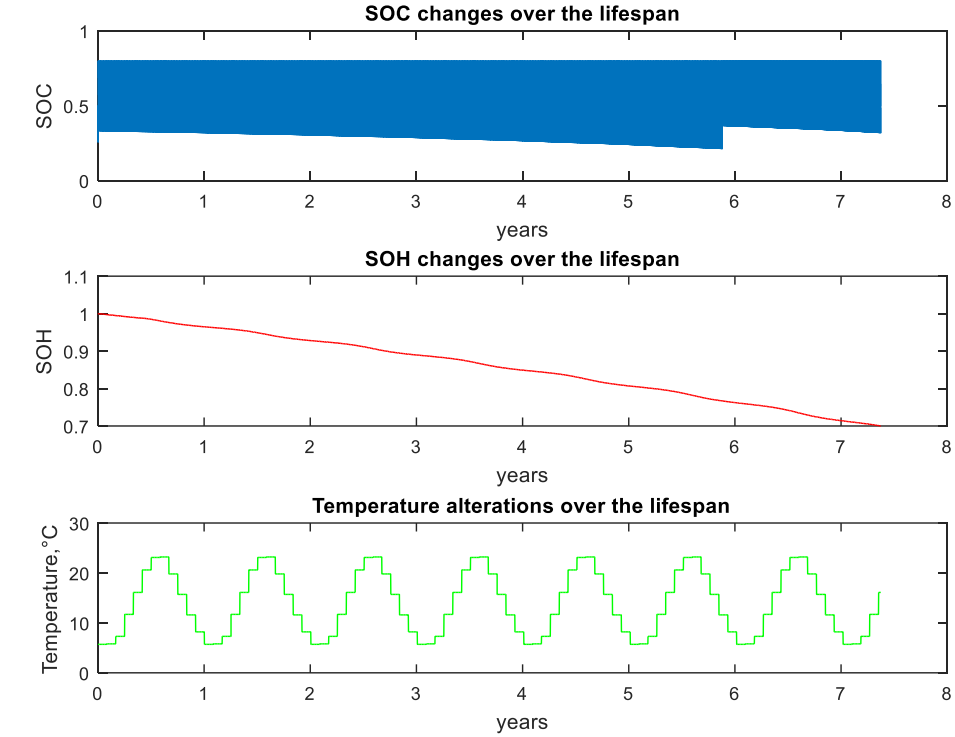

Figure 4.24. SOC, SOH and temperature alterations over lifespan regarding scenario no: 9

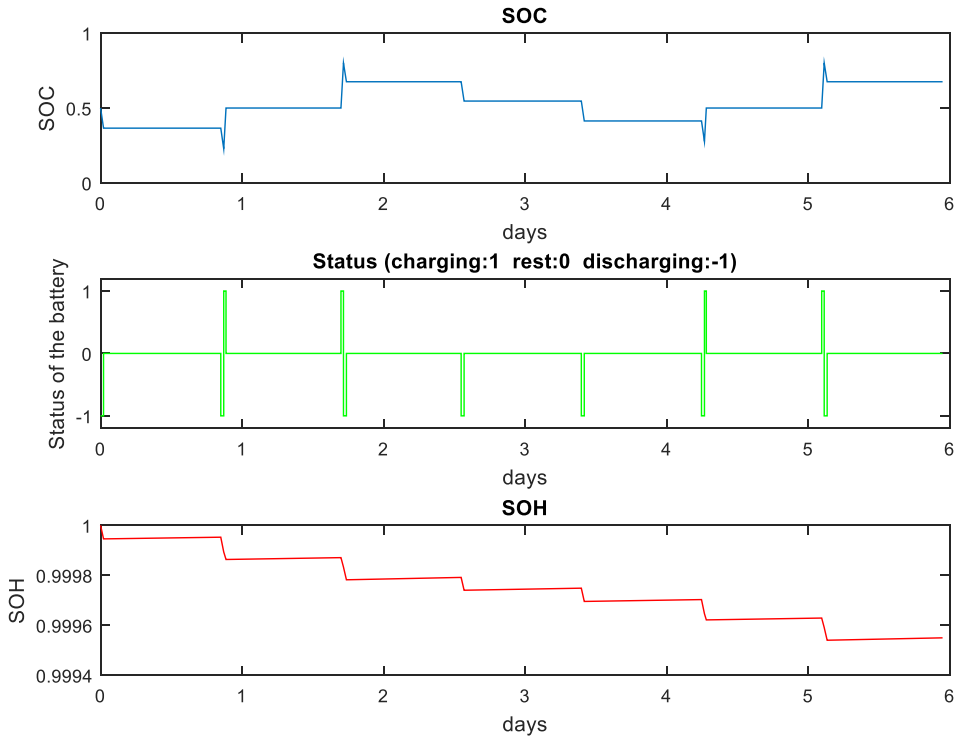

Figure 4.25. SOC, status and SOH alterations regarding scenario no: 10

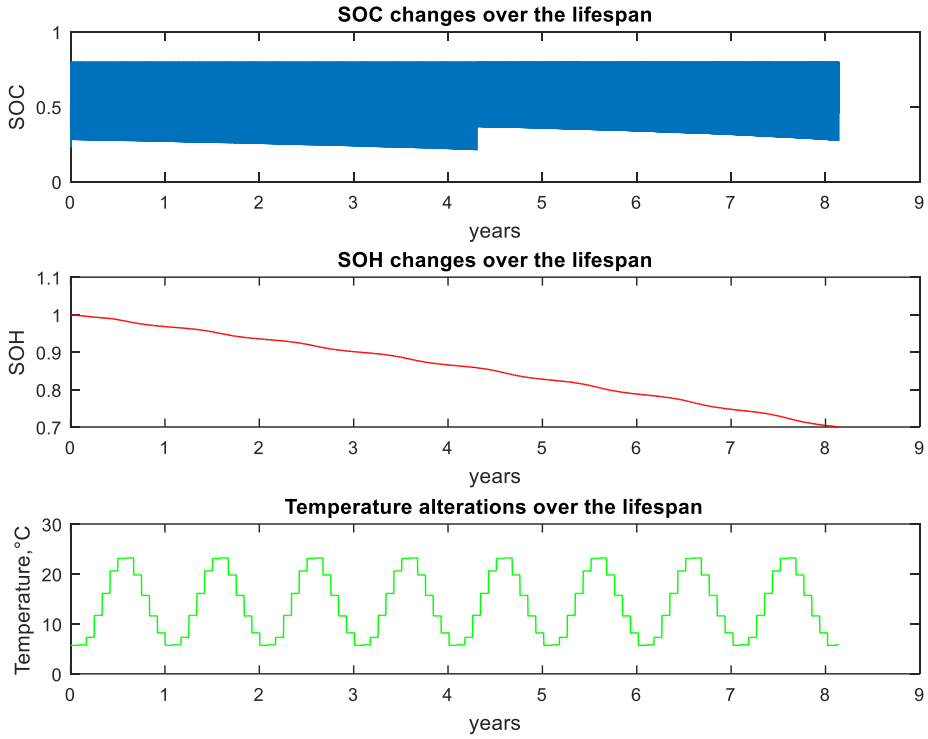

Figure 4.26. SOC, SOH and temperature alterations over lifespan regarding scenario no: 10

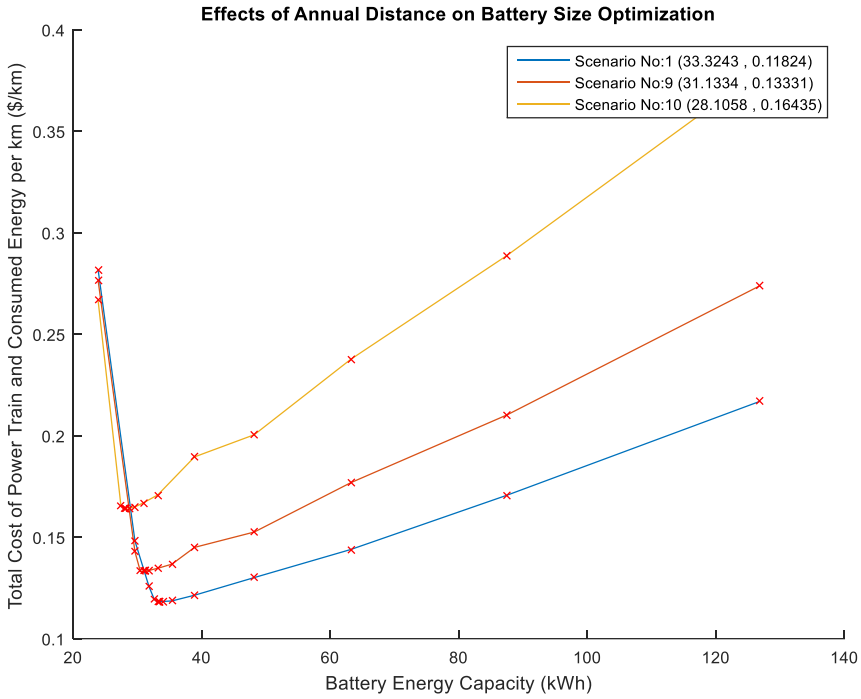

Figure 4.27. Effects of annual distance travelled

In Figure 4.27 and Table 4.7, the data regarding scenarios no: 1, 9 and 10 are presented. In the figure, how the battery size optimization ends up for each scenario is visualized. Besides, the detailed results regarding the scenarios are given in the table. The optimum battery energy becomes lower when the annual distance is decreased. Although the lifetime of the battery is increased due to utilization of the BEV less frequently, the objective function is increased significantly compared to scenario no: 1.

Table 4.7. Outputs regarding scenarios no: 1, 9 and 10

		Scenario No		
Parameters	**Unit**	**1**	**9**	**10**
Maximum allowable battery energy	kWh	126.8	126.8	126.8
Optimum battery energy	kWh	33.3	31.1	28.1
Power of battery	kW	186.3	185.5	184.1
Mass of battery	kg	301.9	290.9	275.8
Initial cost of battery	$	8331	7783	7026
Torque of EM	Nm	387	384	381
Power of EM	kW	162.1	161.5	160.2
Mass of EM	kg	147.4	146.8	145.6
Initial cost of EM and Inverter	$	4863	4844	4806
Total mass of BEV	kg	2024.2	2012.7	1996.5
Battery lifetime	years	6.66	7.37	8.15
Total distance traveled in lifetime	km	133216	110613	81455
Range for given test procedure	km	212	199	180
Time for acceleration from 0 to top speed	sec	24.3	24.2	24.3
Consumed energy in one cycle for given test procedure	kWh	3.65	3.65	3.63
Cost of consumed energy per km	$/km	0.0192	0.0192	0.0191
Initial cost of power train per km	$/km	0.099	0.1142	0.1453
Objective Function	***$/km***	***0.1182***	***0.1333***	***0.1644***

4.5 Investigation of Effects by Price of Electricity on Battery Size Optimization

In Table 4.8, values of the parameters that define scenarios no: 1, 11, 12, 13, 14 and 15 are given. The values of "Cost of electricity" and "Maximum charging power" are changed in scenarios no: 11, 12, 13, 14 and 15. Maximum charging power is constant for scenarios no: 1, 11 and 12, and only reduction of cost of electricity is investigated in these scenarios. Likely, maximum charging power is constant for scenarios no: 13, 14 and 15, and only reduction of cost of electricity is investigated in these scenarios. In addition, the effect of maximum charging power is investigated comparing scenarios no: 1, 11 and 12, and scenarios no: 13, 14 and 15.

Table 4.8. Values of the parameters regarding scenarios no: 1, 11, 12, 13, 14 and 15

		Scenario No					
Parameters	**Unit**	**1**	**11**	**12**	**13**	**14**	**15**
Scaling factor for calendar ageing		1	1	1	1	1	1
Scaling factor for cycle ageing		1	1	1	1	1	1
Ageing model in [14]		0	0	0	0	0	0
Annual distance	km	20000	20000	20000	20000	20000	20000
Cost of electricity	$/kWh	0.11	**0.088**	**0.066**	**0.5**	**0.4**	**0.3**
Maximum charging power	kW	22	**22**	**22**	**100**	**100**	**100**
Specific cost of battery pack	$/kWh	250	250	250	250	250	250
Scaling factor for specific mass of battery pack		1	1	1	1	1	1
Specific cost of EM and inverter	$/kW	30	30	30	30	30	30
Scaling factor for specific mass of EM and inverter		1	1	1	1	1	1
Test procedure		WLTP	WLTP	WLTP	WLTP	WLTP	WLTP

In Figures 4.28 and 4.29, the data regarding scenario no: 11 are presented. In Figure 4.28, the SOC, status and SOH alterations of the battery are visualized for the first few cycles. The SOC, SOH and temperature alterations of the battery are visualized over the lifespan of the battery as in Figure 4.29. In Figures 4.30 and 4.31, the data regarding scenario no: 12 are presented. In Figure 4.30, the SOC, status and SOH alterations of the battery are visualized for the first few cycles. The SOC, SOH and temperature alterations of the battery are visualized over the lifespan of the battery as in Figure 4.31. In Figures 4.32 and 4.33, the data regarding scenario no: 13 are presented. In Figure 4.32, the SOC, status and SOH alterations of the battery are visualized for the first few cycles. The SOC, SOH and temperature alterations of the battery are visualized over the lifespan of the battery as in Figure 4.33. In Figures 4.34 and 4.35, the data regarding scenario no: 14 are presented. In Figure 4.34, the SOC, status and SOH alterations of the battery are visualized for the first few cycles. The SOC, SOH and temperature alterations of the battery are visualized over the lifespan of the battery as in Figure 4.35. In Figures 4.36 and 4.37, the data regarding scenario no: 15 are presented. In Figure 4.36, the SOC, status and SOH alterations of the battery are visualized for the first few cycles. The SOC, SOH and temperature alterations of the battery are visualized over the lifespan of the battery as in Figure 4.37.

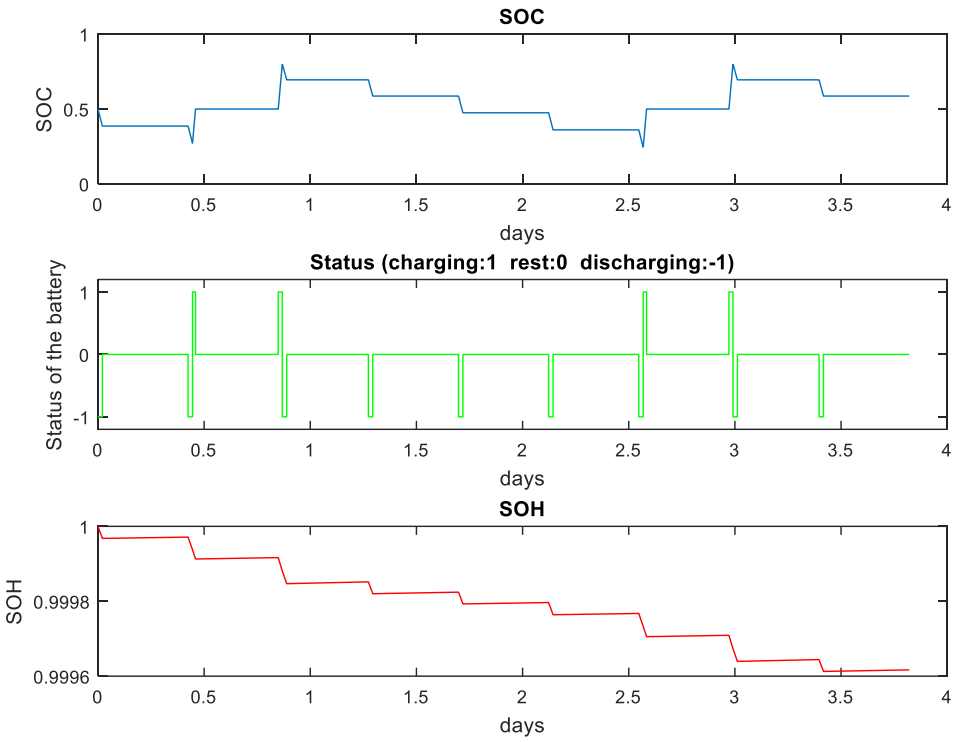

Figure 4.28. SOC, status and SOH alterations regarding scenario no: 11

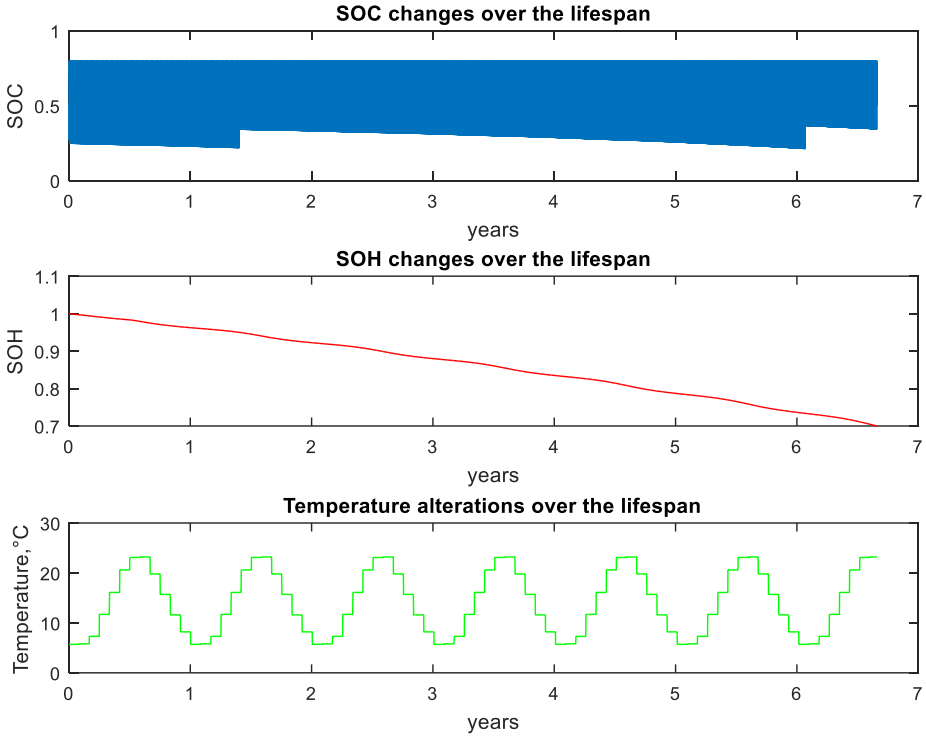

Figure 4.29. SOC, SOH and temperature alterations over lifespan regarding scenario no: 11

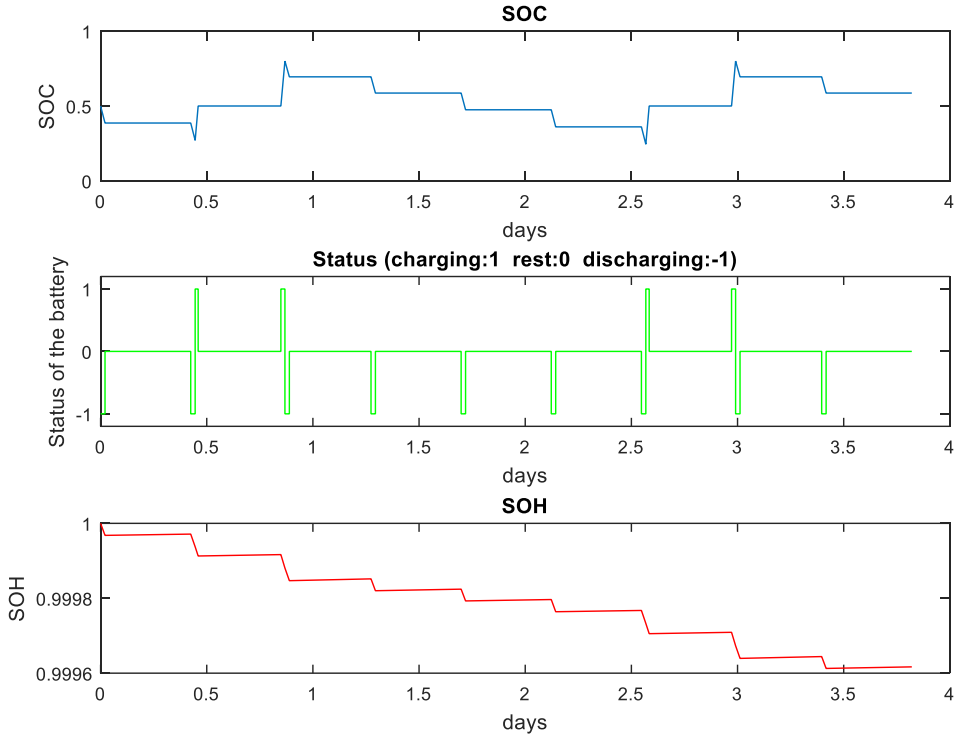

Figure 4.30. SOC, status and SOH alterations regarding scenario no: 12

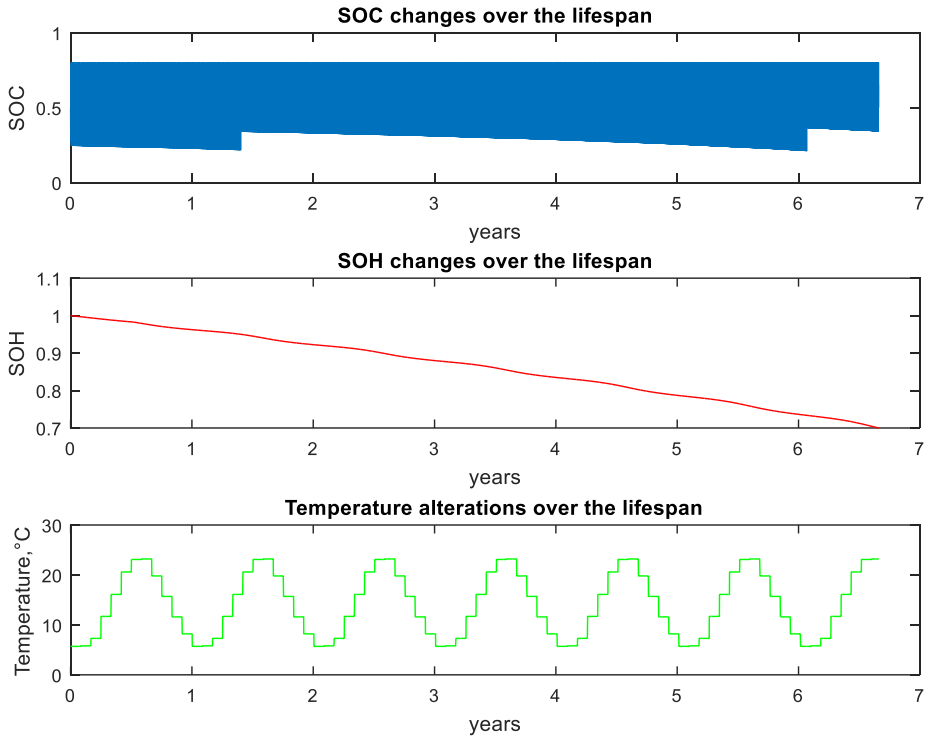

Figure 4.31. SOC, SOH and temperature alterations over lifespan regarding scenario no: 12

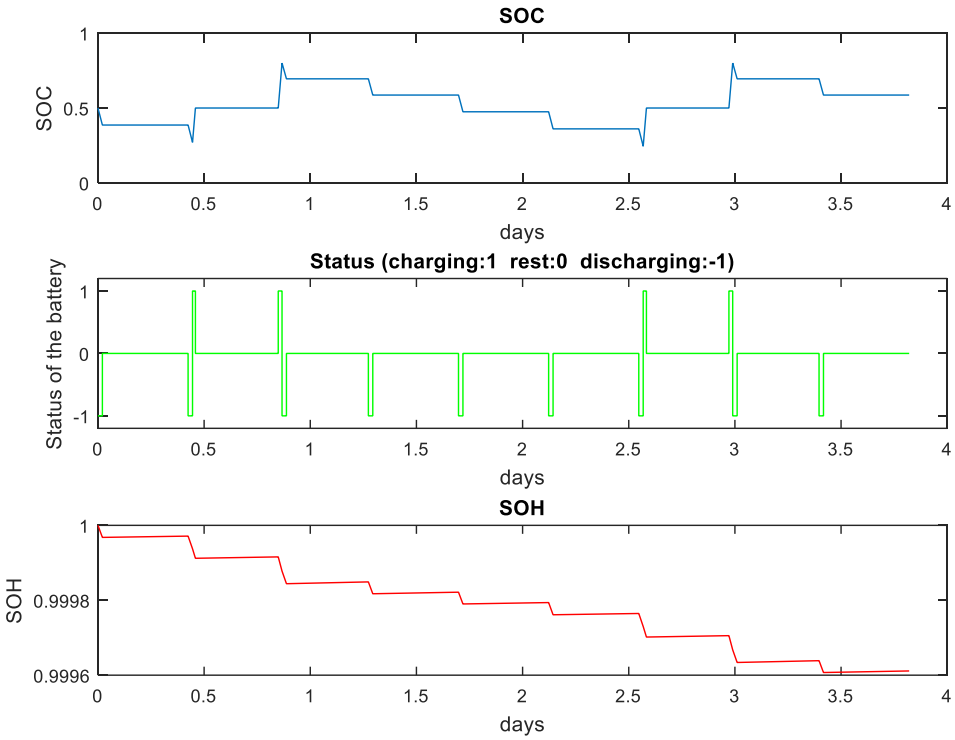

Figure 4.32. SOC, status and SOH alterations regarding scenario no: 13

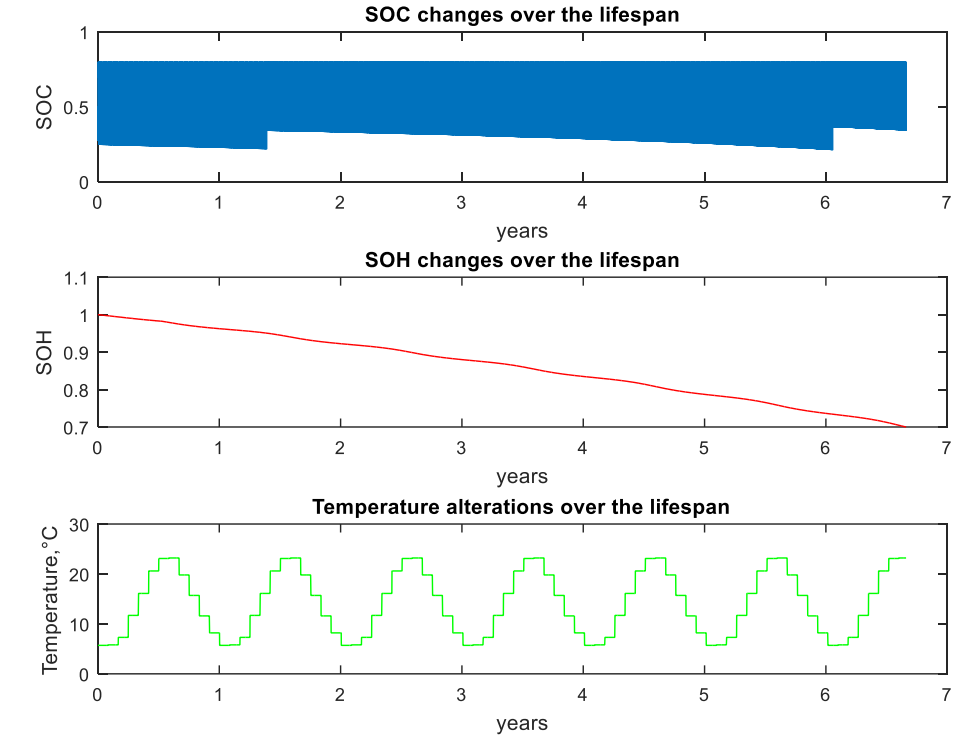

Figure 4.33. SOC, SOH and temperature alterations over lifespan regarding scenario no: 13

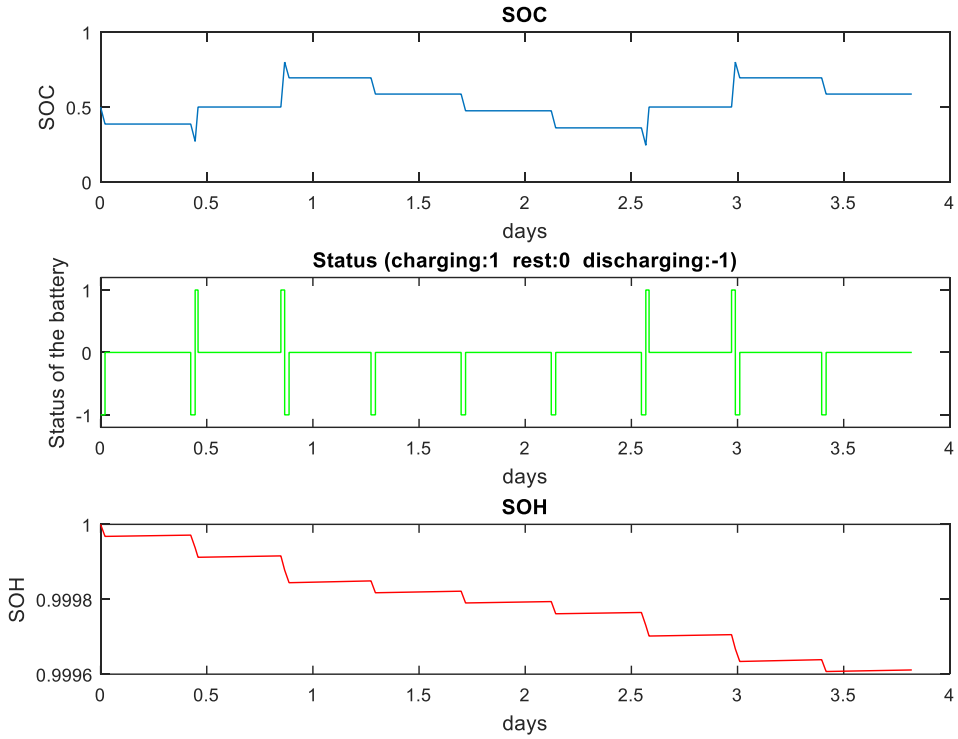

Figure 4.34. SOC, status and SOH alterations regarding scenario no: 14

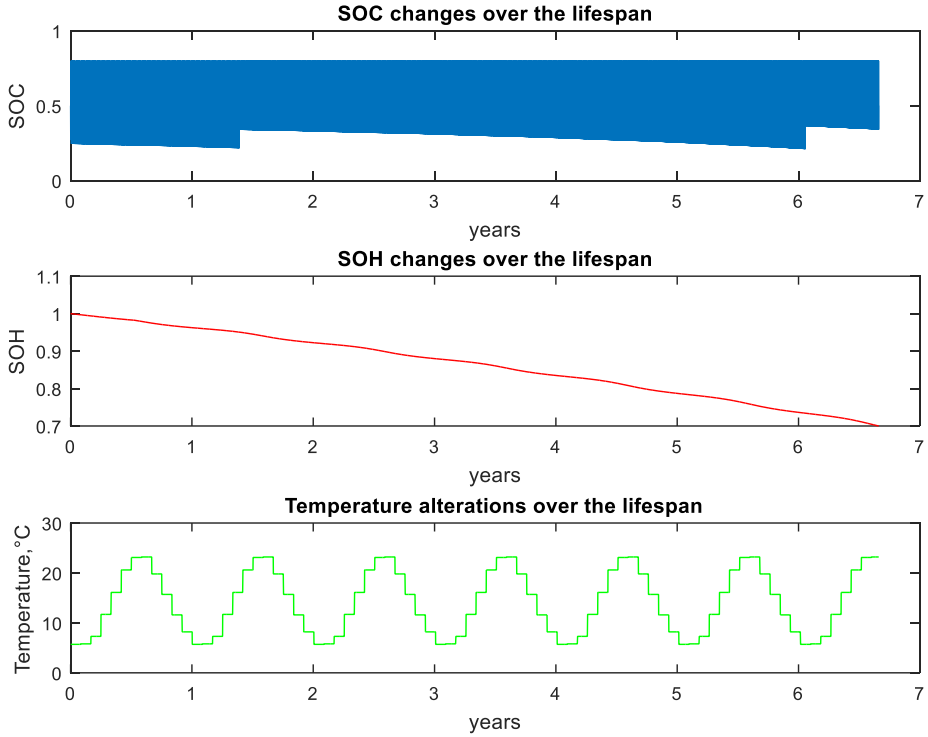

Figure 4.35. SOC, SOH and temperature alterations over lifespan regarding scenario no: 14

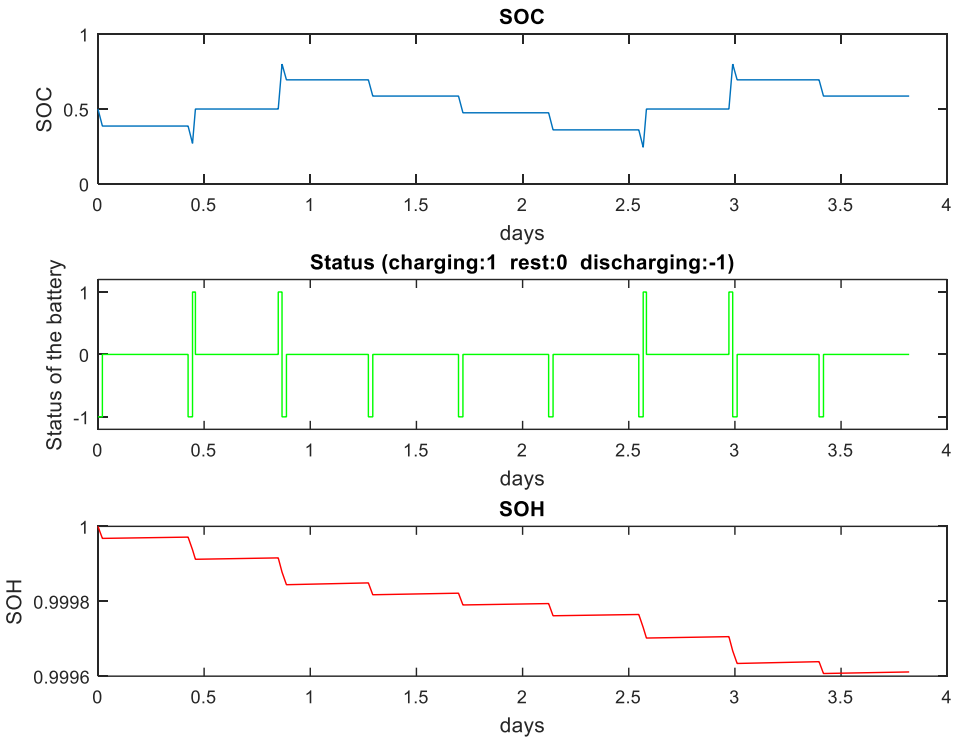

Figure 4.36. SOC, status and SOH alterations regarding scenario no: 15

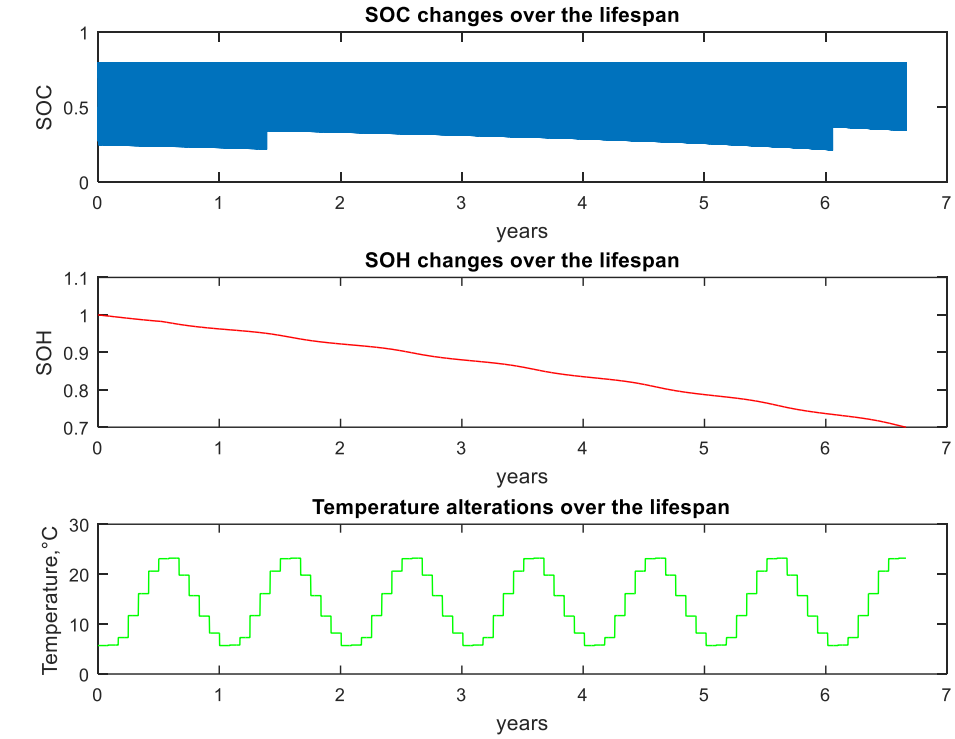

Figure 4.37. SOC, SOH and temperature alterations over lifespan regarding scenario no: 15

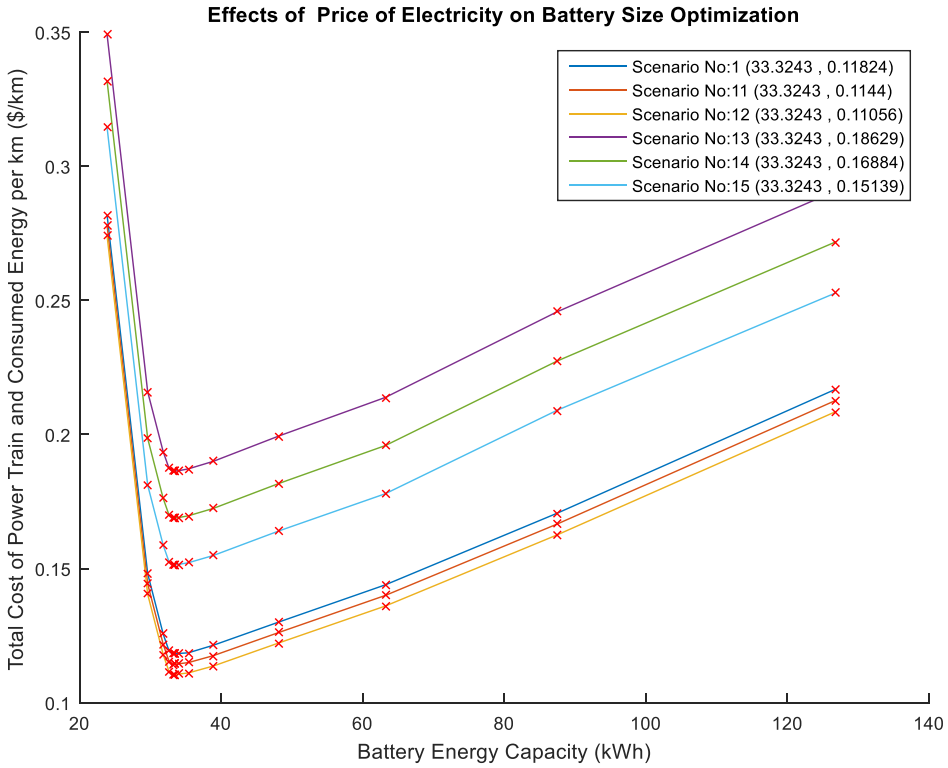

Figure 4.38. Effects of the price of electricity

In Figure 4.38 and Table 4.9, the data regarding scenarios no: 1, 11, 12, 13, 14 and 15 are presented. In the figure, how the battery size optimization ends up for each scenario is visualized. Besides, the detailed results regarding the scenarios are given in the table. The optimum battery energy stays constant when the cost of electricity is decreased and maximum charging power is increased. Meanwhile, objective function is increased compared to scenario no: 1 since the cost of electricity is increased.

Table 4.9. Outputs regarding scenarios no: 1, 11, 12, 13, 14 and 15

		Scenario No					
Parameters	**Unit**	**1**	**11**	**12**	**13**	**14**	**15**
Maximum allowable battery energy	kWh	126.8	126.8	126.8	126.8	126.8	126.8
Optimum battery energy	kWh	33.3	33.3	33.3	33.3	33.3	33.3
Power of battery	kW	186.3	186.3	186.3	186.3	186.3	186.3
Mass of battery	kg	301.9	301.9	301.9	301.9	301.9	301.9
Initial cost of battery	$	8331	8331	8331	8331	8331	8331
Torque of EM	Nm	387	387	387	387	387	387
Power of EM	kW	162.1	162.1	162.1	162.1	162.1	162.1
Mass of EM	kg	147.4	147.4	147.4	147.4	147.4	147.4
Initial cost of EM and Inverter	$	4863	4863	4863	4863	4863	4863
Total mass of BEV	kg	2024.2	2024.2	2024.2	2024.2	2024.2	2024.2
Battery lifetime	years	6.66	6.66	6.66	6.66	6.66	6.66
Total distance traveled in lifetime	km	133216	133216	133216	133216	133216	133216
Range for given test procedure	km	212	212	212	212	212	212
Time for acceleration from 0 to top speed	sec	24.3	24.3	24.3	24.3	24.3	24.3
Consumed energy in one cycle for given test procedure	kWh	3.65	3.65	3.65	3.65	3.65	3.65
Cost of consumed energy per km	$/km	0.0192	0.0154	0.0115	0.0872	0.0698	0.0523
Initial cost of power train per km	$/km	0.099	0.099	0.099	0.099	0.099	0.099
Objective Function	***$/km***	***0.1182***	***0.1144***	***0.1106***	***0.1863***	***0.1688***	***0.1514***

4.6 Investigation of Effects by Specific Cost of Battery Pack on Battery Size Optimization

In Table 4.10, values of the parameters that define scenarios no: 1, 16 and 17 are given. The value of "Specific cost of battery pack" is changed in scenarios no: 16 and 17.

Table 4.10. Values of the parameters regarding scenarios no: 1, 16 and 17

		Scenario No		
Parameters	**Unit**	**1**	**16**	**17**
Scaling factor for calendar ageing		1	1	1
Scaling factor for cycle ageing		1	1	1
Ageing model in [14]		0	0	0
Annual distance	km	20000	20000	20000
Cost of electricity	$/kWh	0.11	0.11	0.11
Maximum charging power	kW	22	22	22
Specific cost of battery pack	$/kWh	250	**175**	**100**
Scaling factor for specific mass of battery pack		1	1	1
Specific cost of EM and inverter	$/kW	30	30	30
Scaling factor for specific mass of EM and inverter		1	1	1
Test procedure		WLTP	WLTP	WLTP

In Figures 4.39 and 4.40, the data regarding scenario no: 16 are presented. In Figure 4.39, the SOC, status and SOH alterations of the battery are visualized for the first few cycles. The SOC, SOH and temperature alterations of the battery are visualized over the lifespan of the battery as in Figure 4.40. In Figures 4.41 and 4.42, the data regarding scenario no: 17 are presented. In Figure 4.41, the SOC, status and SOH alterations of the battery are visualized for the first few cycles. The SOC, SOH and temperature alterations of the battery are visualized over the lifespan of the battery as in Figure 4.42.

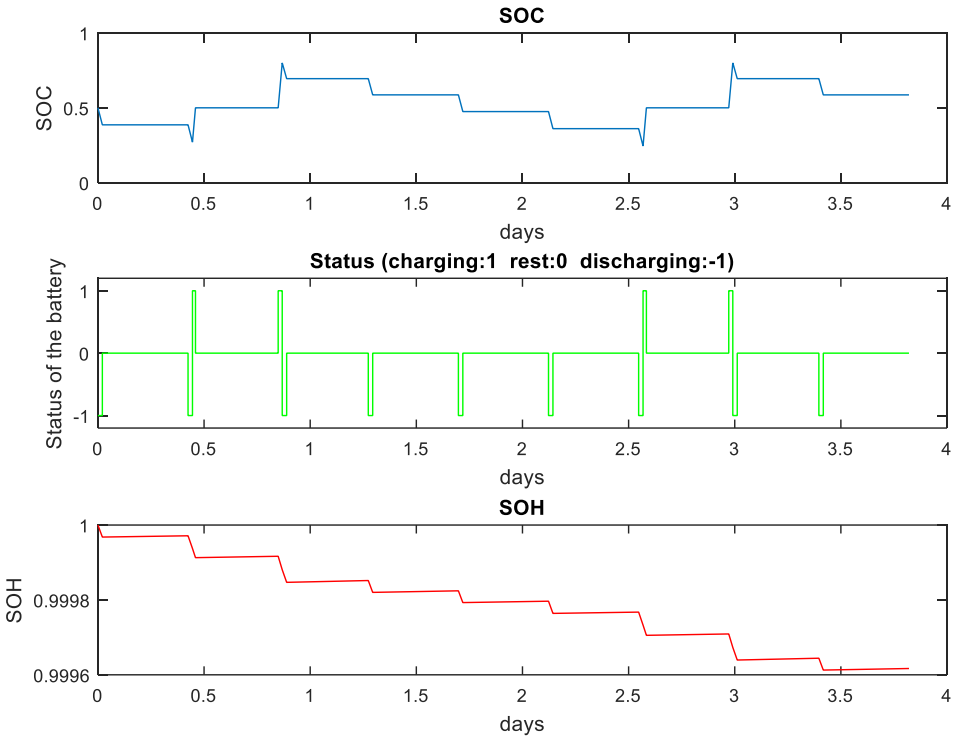

Figure 4.39. SOC, status and SOH alterations regarding scenario no: 16

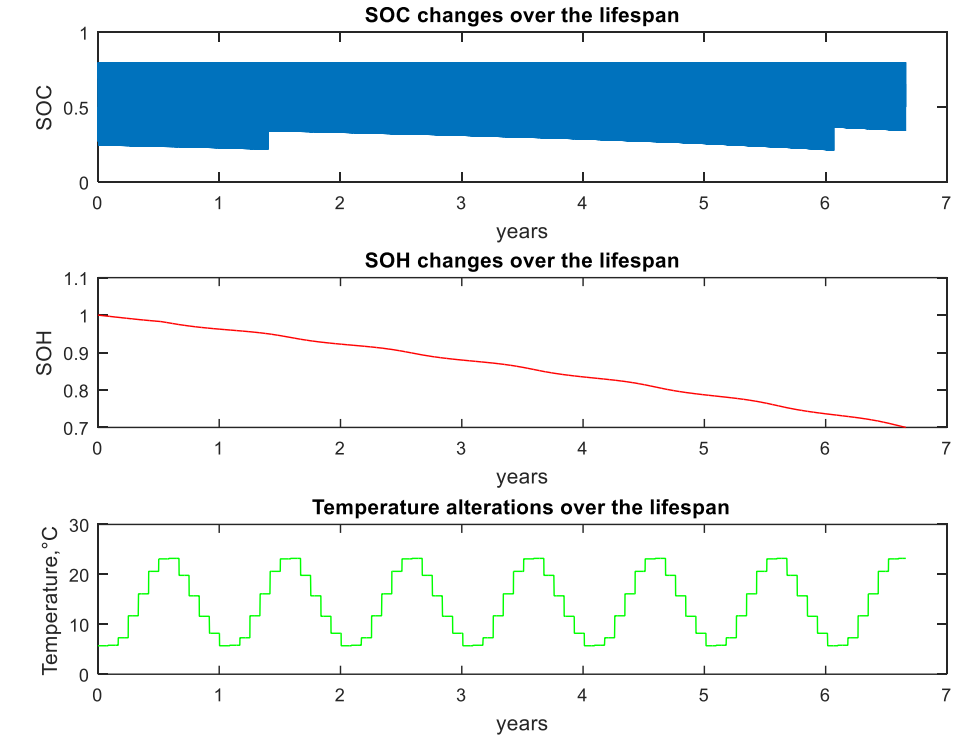

Figure 4.40. SOC, SOH and temperature alterations over lifespan regarding scenario no: 16

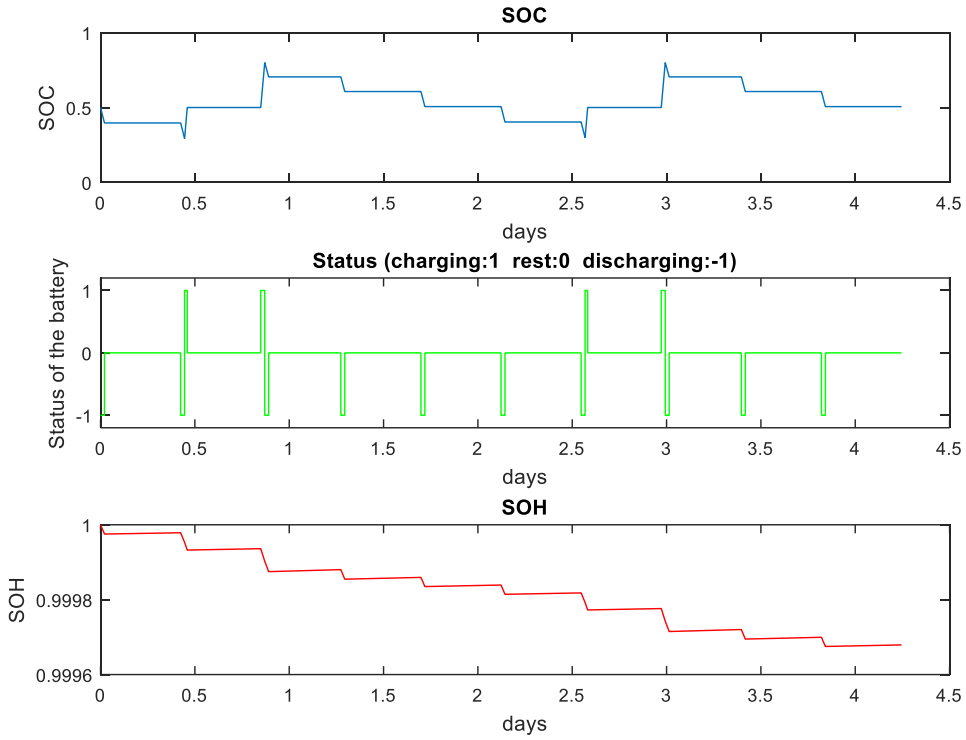

Figure 4.41. SOC, status and SOH alterations regarding scenario no: 17

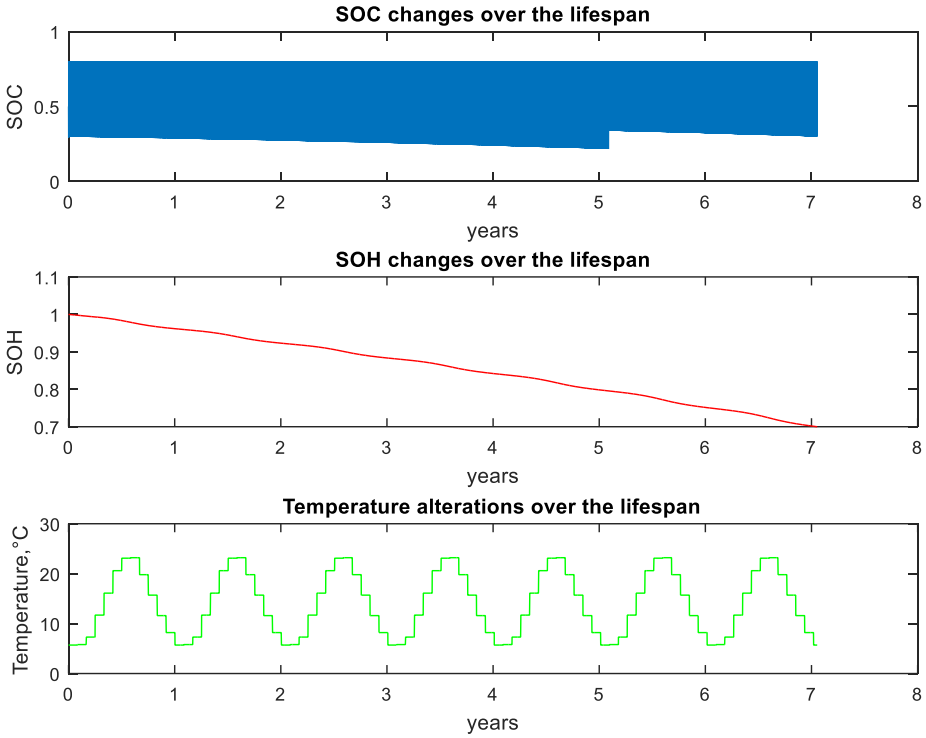

Figure 4.42. SOC, SOH and temperature alterations over lifespan regarding scenario no: 17

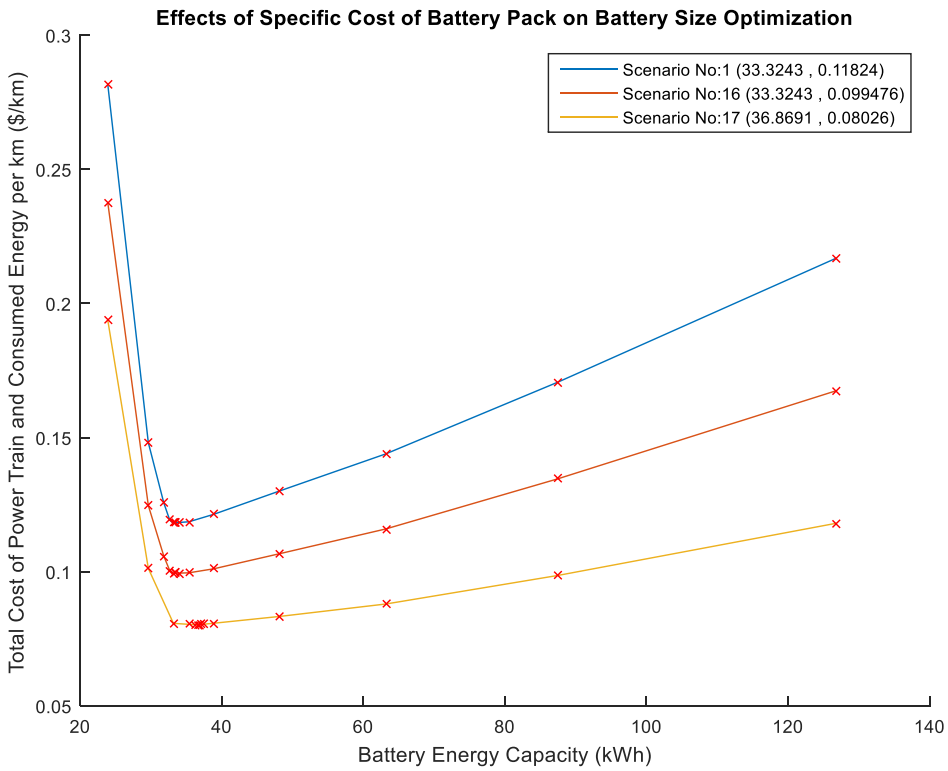

Figure 4.43. Effects of specific cost of battery pack

In Figure 4.43 and Table 4.11, the data regarding scenarios no: 1, 16 and 17 are presented. In the figure, how the battery size optimization ends up for each scenario is visualized. Besides, the detailed results regarding the scenarios are given in the table. The optimum battery energy becomes a bit higher when specific cost of battery pack is decreased. Since initial cost of the battery is decreased, the objective function is reduced significantly compared to scenario no: 1.

Table 4.11. Outputs regarding scenarios no: 1, 16 and 17

		Scenario No		
Parameters	**Unit**	**1**	**16**	**17**
Maximum allowable battery energy	kWh	126.8	126.8	126.8
Optimum battery energy	kWh	33.3	33.3	36.9
Power of battery	kW	186.3	186.3	188.3
Mass of battery	kg	301.9	301.9	319.6
Initial cost of battery	$	8331	5832	3687
Torque of EM	Nm	387	387	391
Power of EM	kW	162.1	162.1	163.9
Mass of EM	kg	147.4	147.4	149
Initial cost of EM and Inverter	$	4863	4863	4917
Total mass of BEV	kg	2024.2	2024.2	2043.6
Battery lifetime	years	6.66	6.66	7.05
Total distance traveled in lifetime	km	133216	133216	141077
Range for given test procedure	km	212	212	234
Time for acceleration from 0 to top speed	sec	24.3	24.3	24.1
Consumed energy in one cycle for given test procedure	kWh	3.65	3.65	3.67
Cost of consumed energy per km	$/km	0.0192	0.0192	0.0193
Initial cost of power train per km	$/km	0.099	0.0803	0.061
Objective Function	***$/km***	***0.1182***	***0.0995***	***0.0803***

4.7 Investigation of Effects by Specific Mass of Battery Pack on Battery Size Optimization

In Table 4.12, values of the parameters that define scenarios no: 1, 18 and 19 are given. The value of "Scaling factor for specific mass of battery pack" is changed in scenarios no: 18 and 19.

Table 4.12. Values of the parameters regarding scenarios no: 1, 18 and 19

		Scenario No		
Parameters	**Unit**	**1**	**18**	**19**
Scaling factor for calendar ageing		1	1	1
Scaling factor for cycle ageing		1	1	1
Ageing model in [14]		0	0	0
Annual distance	km	20000	20000	20000
Cost of electricity	$/kWh	0.11	0.11	0.11
Maximum charging power	kW	22	22	22
Specific cost of battery pack	$/kWh	250	250	250
Scaling factor for specific mass of battery pack		1	**0.8**	**0.6**
Specific cost of EM and inverter	$/kW	30	30	30
Scaling factor for specific mass of EM and inverter		1	1	1
Test procedure		WLTP	WLTP	WLTP

In Figures 4.44 and 4.45, the data regarding scenario no: 18 are presented. In Figure 4.44, the SOC, status and SOH alterations of the battery are visualized for the first few cycles. The SOC, SOH and temperature alterations of the battery are visualized over the lifespan of the battery as in Figure 4.45. In Figures 4.46 and 4.47, the data regarding scenario no: 19 are presented. In Figure 4.46, the SOC, status and SOH alterations of the battery are visualized for the first few cycles. The SOC, SOH and temperature alterations of the battery are visualized over the lifespan of the battery as in Figure 4.47.

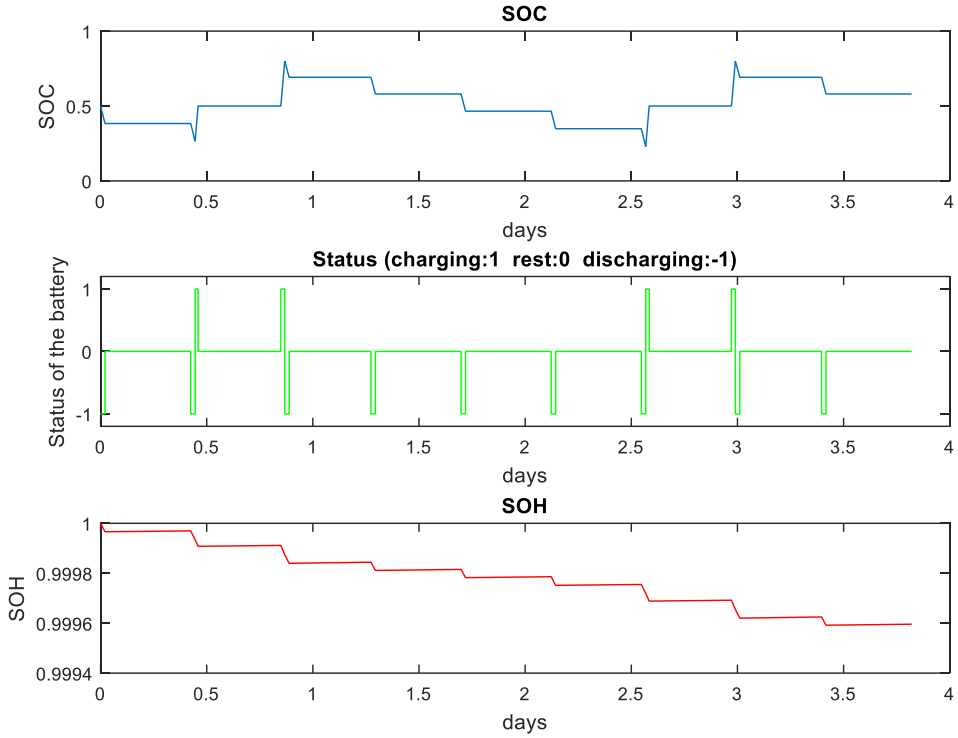

Figure 4.44. SOC, status and SOH alterations regarding scenario no: 18

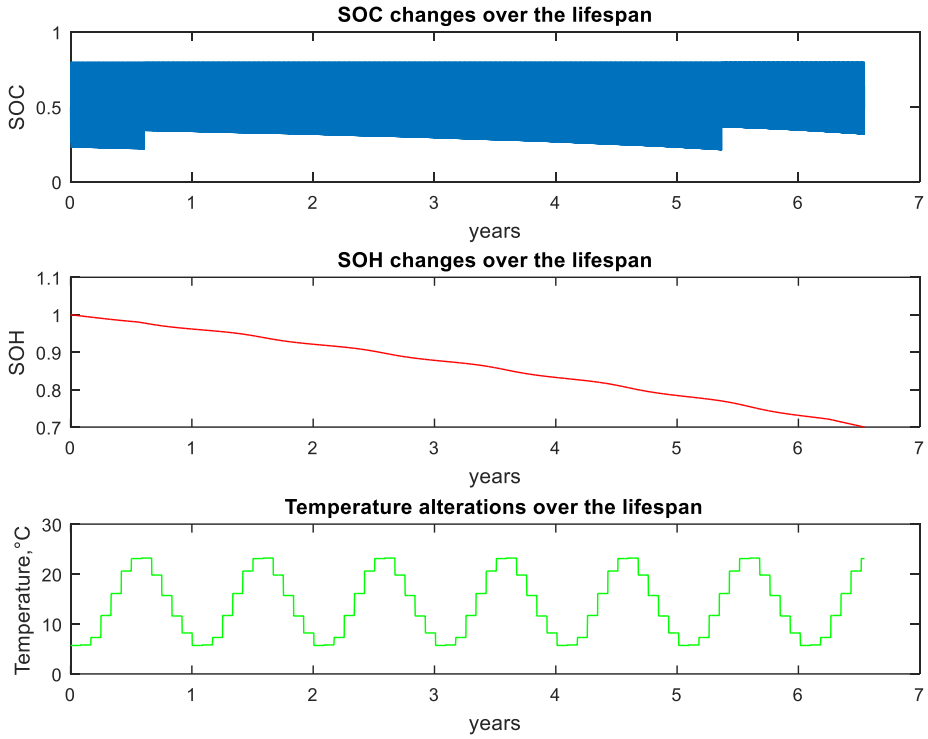

Figure 4.45. SOC, SOH and temperature alterations over lifespan regarding scenario no: 18

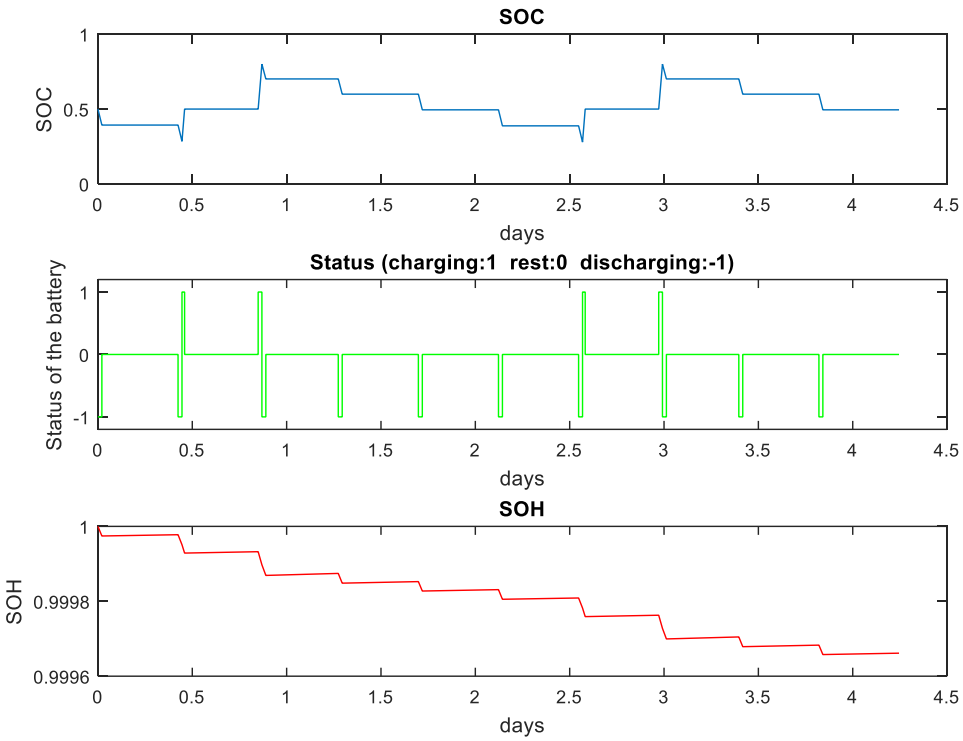

Figure 4.46. SOC, status and SOH alterations regarding scenario no: 19

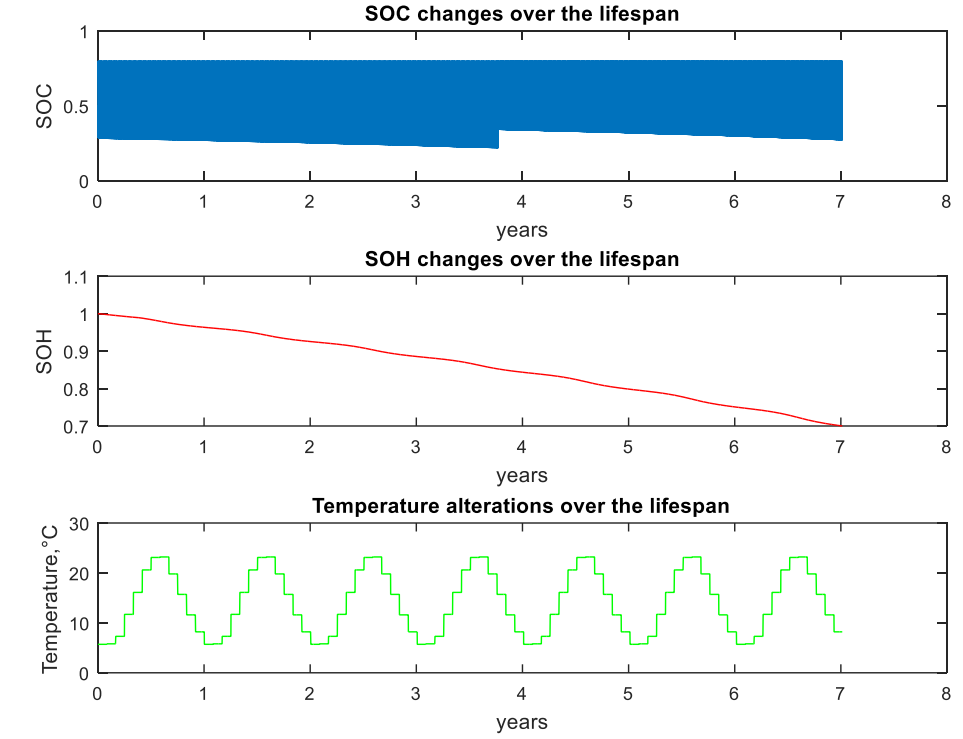

Figure 4.47. SOC, SOH and temperature alterations over lifespan regarding scenario no: 19

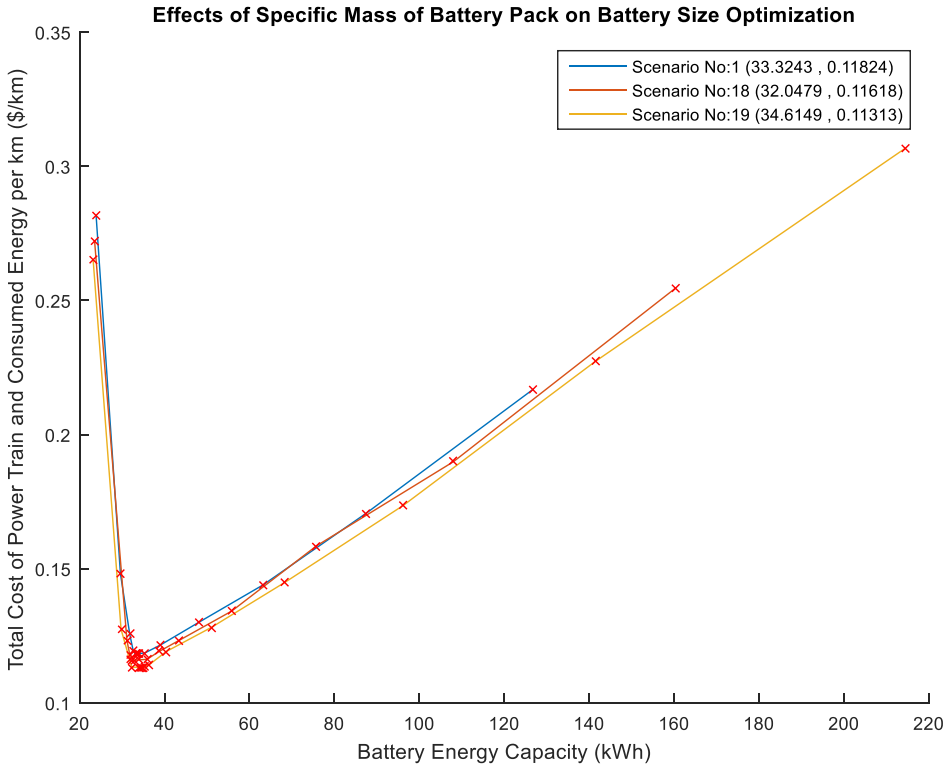

Figure 4.48. Effects of specific mass of battery pack

In Figure 4.48 and Table 4.13, the data regarding scenarios no: 1, 18 and 19 are presented. In the figure, how the battery size optimization ends up for each scenario is visualized. Besides, the detailed results regarding the scenarios are given in the table. The optimum battery energy becomes a bit lower when scaling factor for specific mass of battery pack is decreased by 20%. The optimum battery energy becomes a bit higher when scaling factor for specific mass of battery pack is decreased by 40%. Since mass of the battery pack is decreased, total mass of the BEV and cost of consumed energy per km is reduced. Thus, the objective function is reduced slightly compared to scenario no: 1.

Table 4.13. Outputs regarding scenarios no: 1, 18 and 19

		Scenario No		
Parameters	**Unit**	**1**	**18**	**19**
Maximum allowable battery energy	kWh	126.8	160.3	214.5
Optimum battery energy	kWh	33.3	32	34.6
Power of battery	kW	186.3	180.6	175.6
Mass of battery	kg	301.9	236	184.4
Initial cost of battery	$	8331	8012	8654
Torque of EM	Nm	387	374	363
Power of EM	kW	162.1	157.1	152.7
Mass of EM	kg	147.4	142.9	138.9
Initial cost of EM and Inverter	$	4863	4714	4582
Total mass of BEV	kg	2024.2	1953.9	1898.3
Battery lifetime	years	6.66	6.55	7.01
Total distance traveled in lifetime	km	133216	130907	140261
Range for given test procedure	km	212	207	225
Time for acceleration from 0 to top speed	sec	24.3	24.4	24.6
Consumed energy in one cycle for given test procedure	kWh	3.65	3.61	3.57
Cost of consumed energy per km	$/km	0.0192	0.019	0.0188
Initial cost of power train per km	$/km	0.099	0.0972	0.0944
Objective Function	***$/km***	***0.1182***	***0.1162***	***0.1131***

4.8 Investigation of Effects by Specific Cost of EM and Inverter on Battery Size Optimization

In Table 4.14, values of the parameters that define scenarios no: 1, 20 and 21 are given. The value of "Specific cost of EM and inverter" is changed in scenarios no: 20 and 21.

Table 4.14. Values of the parameters regarding scenarios no: 1, 20 and 21

		Scenario No		
Parameters	**Unit**	**1**	**20**	**21**
Scaling factor for calendar ageing		1	1	1
Scaling factor for cycle ageing		1	1	1
Ageing model in [14]		0	0	0
Annual distance	km	20000	20000	20000
Cost of electricity	$/kWh	0.11	0.11	0.11
Maximum charging power	kW	22	22	22
Specific cost of battery pack	$/kWh	250	250	250
Scaling factor for specific mass of battery pack		1	1	1
Specific cost of EM and inverter	$/kW	30	**24**	**18**
Scaling factor for specific mass of EM and inverter		1	1	1
Test procedure		WLTP	WLTP	WLTP

In Figures 4.49 and 4.50, the data regarding scenario no: 20 are presented. In Figure 4.49, the SOC, status and SOH alterations of the battery are visualized for the first few cycles. The SOC, SOH and temperature alterations of the battery are visualized over the lifespan of the battery as in Figure 4.50. In Figures 4.51 and 4.52, the data regarding scenario no: 21 are presented. In Figure 4.51, the SOC, status and SOH alterations of the battery are visualized for the first few cycles. The SOC, SOH and temperature alterations of the battery are visualized over the lifespan of the battery as in Figure 4.52.

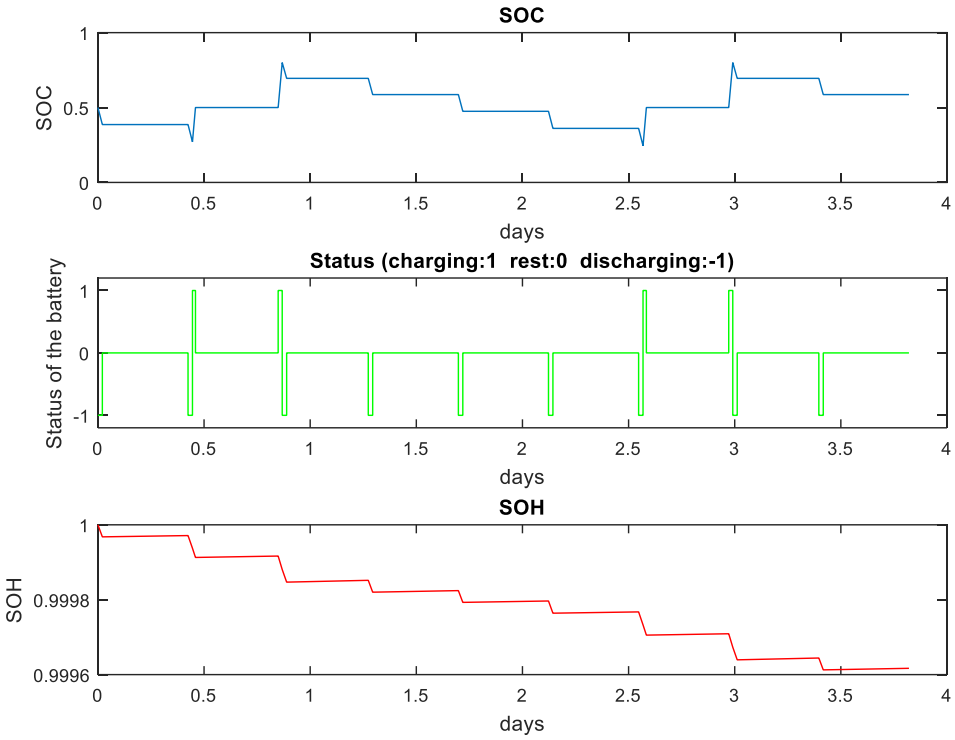

Figure 4.49. SOC, status and SOH alterations regarding scenario no: 20

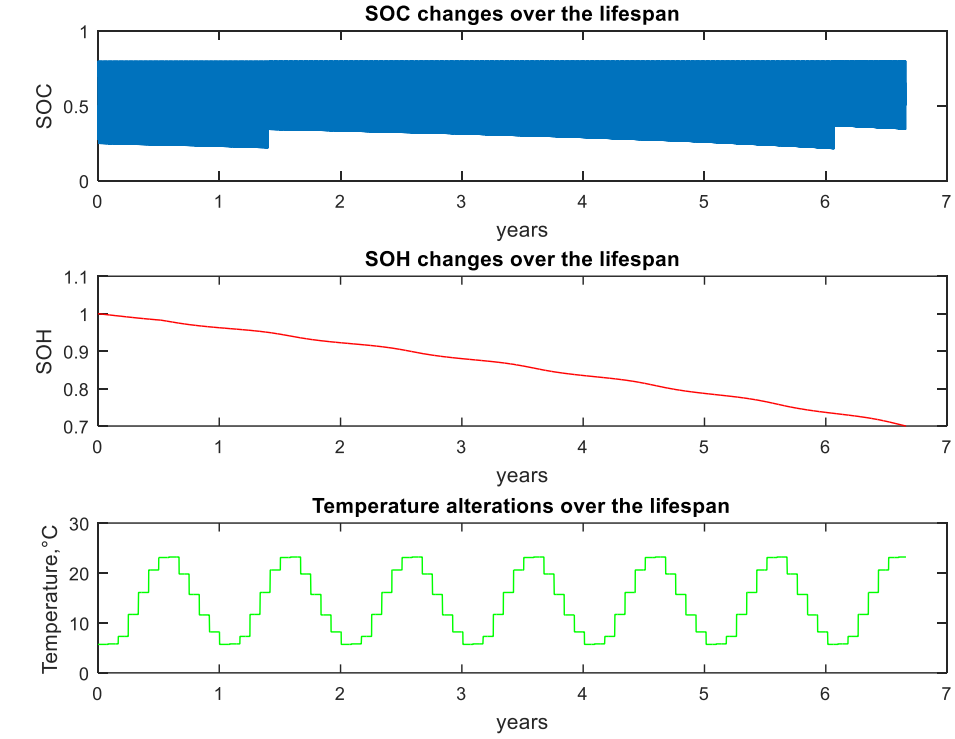

Figure 4.50. SOC, SOH and temperature alterations over lifespan regarding scenario no: 20

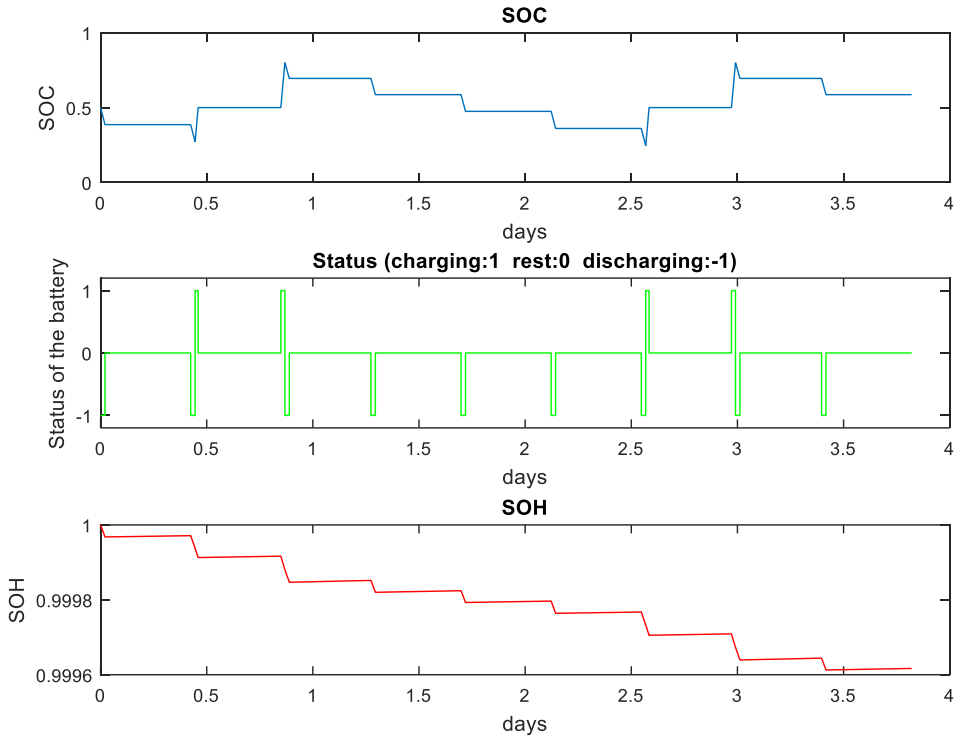

Figure 4.51. SOC, status and SOH alterations regarding scenario no: 21

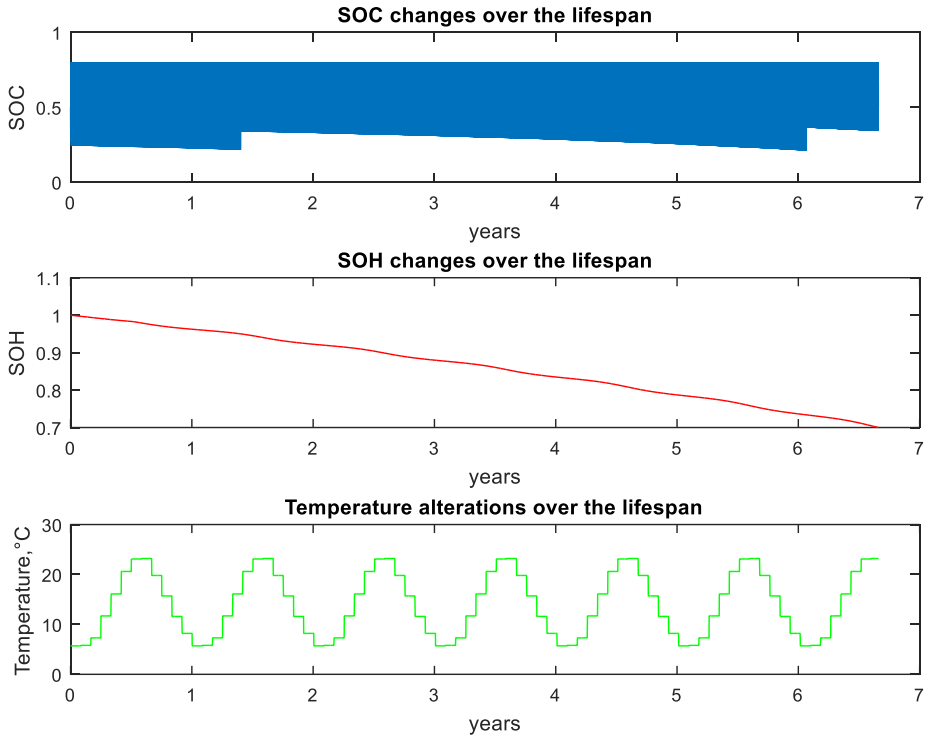

Figure 4.52. SOC, SOH and temperature alterations over lifespan regarding scenario no: 21

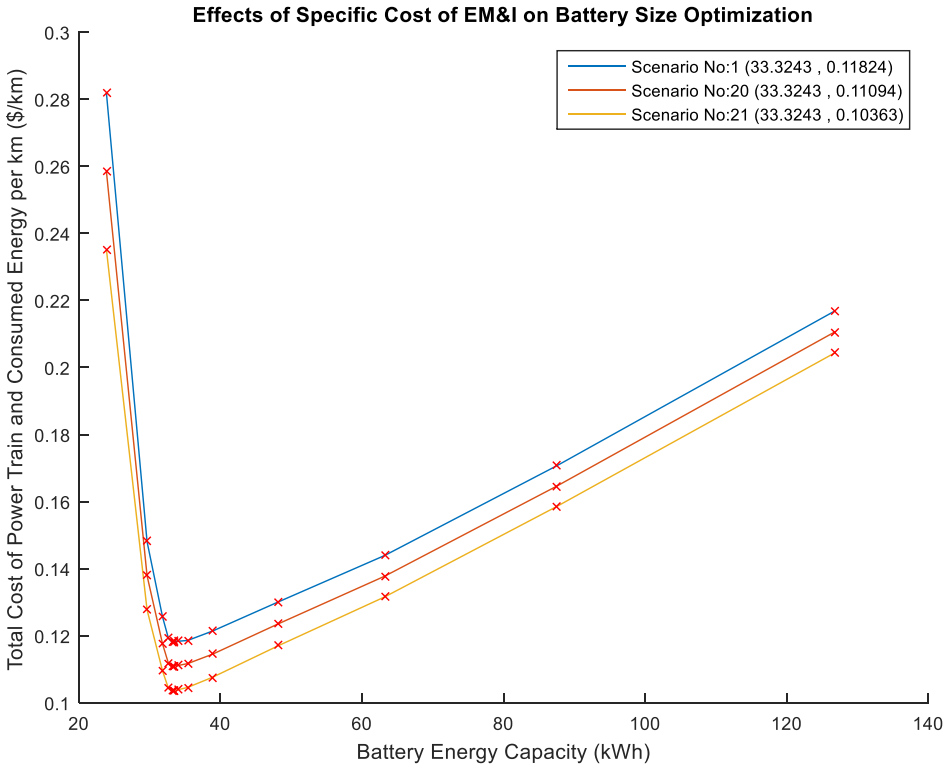

Figure 4.53. Effects of specific cost of EM and inverter

In Figure 4.53 and Table 4.15, the data regarding scenarios no: 1, 20 and 21 are presented. In the figure, how the battery size optimization ends up for each scenario is visualized. Besides, the detailed results regarding the scenarios are given in the table. The optimum battery energy stays constant when specific cost of EM and inverter is decreased. Since initial cost of the EM and inverter is decreased, the objective function is reduced significantly compared to scenario no: 1.

Table 4.15. Outputs regarding scenarios no: 1, 20 and 21

		Scenario No		
Parameters	**Unit**	**1**	**20**	**21**
Maximum allowable battery energy	kWh	126.8	126.8	126.8
Optimum battery energy	kWh	33.3	33.3	33.3
Power of battery	kW	186.3	186.3	186.3
Mass of battery	kg	301.9	301.9	301.9
Initial cost of battery	$	8331	8331	8331
Torque of EM	Nm	387	387	387
Power of EM	kW	162.1	162.1	162.1
Mass of EM	kg	147.4	147.4	147.4
Initial cost of EM and Inverter	$	4863	3891	2918
Total mass of BEV	kg	2024.2	2024.2	2024.2
Battery lifetime	years	6.66	6.66	6.66
Total distance traveled in lifetime	km	133216	133216	133216
Range for given test procedure	km	212	212	212
Time for acceleration from 0 to top speed	sec	24.3	24.3	24.3
Consumed energy in one cycle for given test procedure	kWh	3.65	3.65	3.65
Cost of consumed energy per km	$/km	0.0192	0.0192	0.0192
Initial cost of power train per km	$/km	0.099	0.0917	0.0844
Objective Function	***$/km***	***0.1182***	***0.1109***	***0.1036***

4.9 Investigation of Effects by Specific Mass of EM and Inverter on Battery Size Optimization

In Table 4.16, values of the parameters that define scenarios no: 1, 22 and 23 are given. The value of "Scaling factor for specific mass of EM and inverter" is changed in scenarios no: 22 and 23.

Table 4.16. Values of the parameters regarding scenarios no: 1, 22 and 23

		Scenario No		
Parameters	**Unit**	**1**	**22**	**23**
Scaling factor for calendar ageing		1	1	1
Scaling factor for cycle ageing		1	1	1
Ageing model in [14]		0	0	0
Annual distance	km	20000	20000	20000
Cost of electricity	$/kWh	0.11	0.11	0.11
Maximum charging power	kW	22	22	22
Specific cost of battery pack	$/kWh	250	250	250
Scaling factor for specific mass of battery pack		1	1	1
Specific cost of EM and inverter	$/kW	30	30	30
Scaling factor for specific mass of EM and inverter		1	**0.8**	**0.6**
Test procedure		WLTP	WLTP	WLTP

In Figures 4.54 and 4.55, the data regarding scenario no: 22 are presented. In Figure 4.54, the SOC, status and SOH alterations of the battery are visualized for the first few cycles. The SOC, SOH and temperature alterations of the battery are visualized over the lifespan of the battery as in Figure 4.55. In Figures 4.56 and 4.57, the data regarding scenario no: 23 are presented. In Figure 4.56, the SOC, status and SOH alterations of the battery are visualized for the first few cycles. The SOC, SOH and temperature alterations of the battery are visualized over the lifespan of the battery as in Figure 4.57.

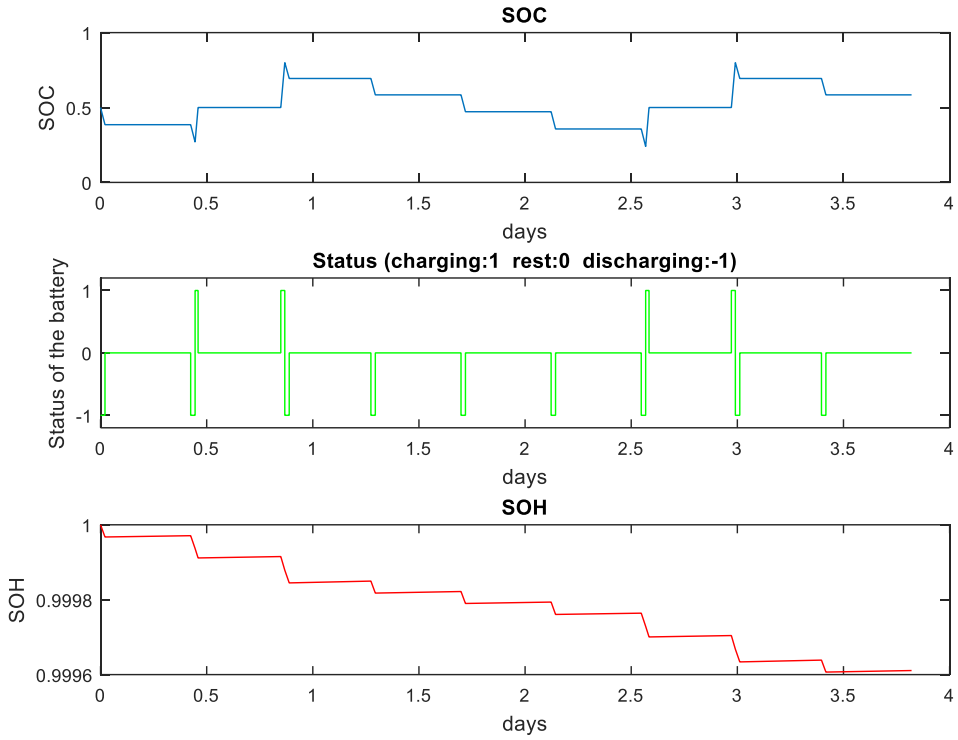

Figure 4.54. SOC, status and SOH alterations regarding scenario no: 22

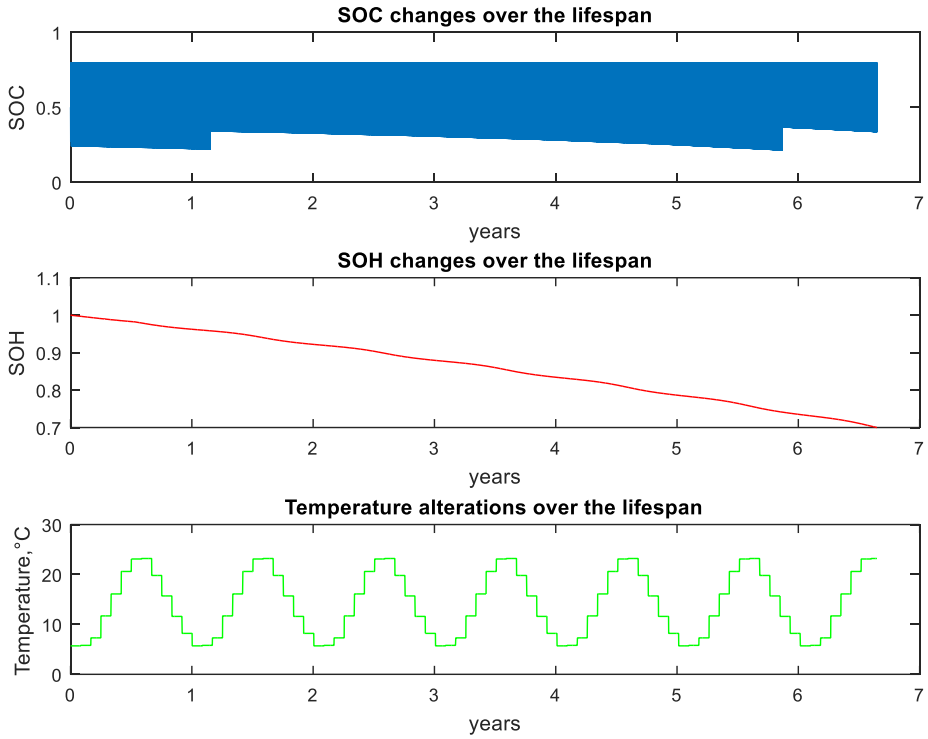

Figure 4.55. SOC, SOH and temperature alterations over lifespan regarding scenario no: 22

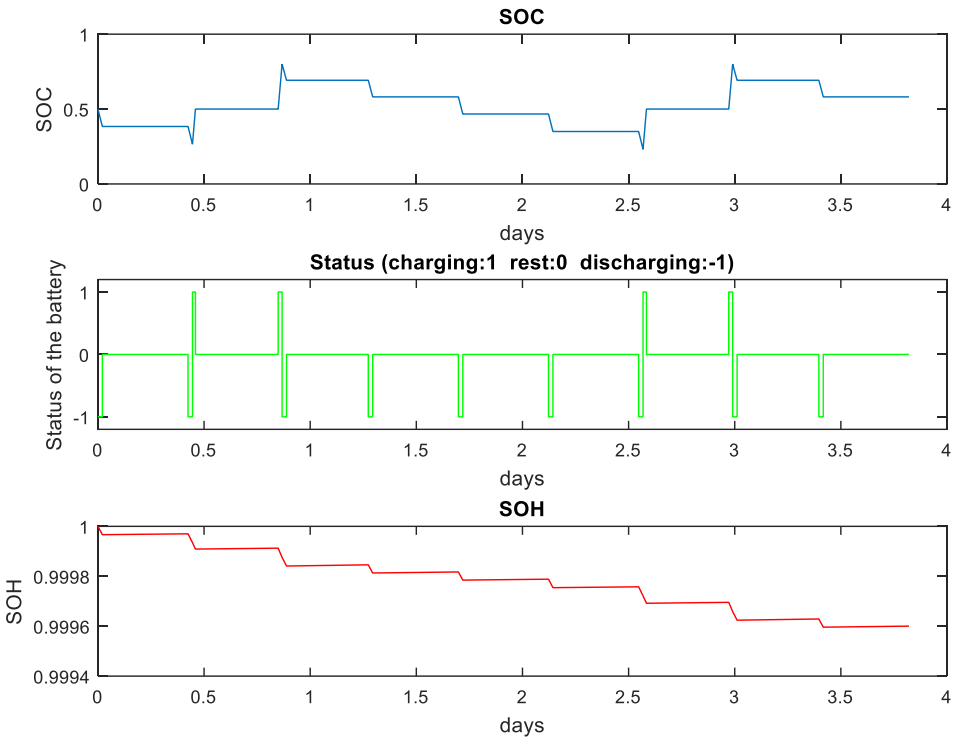

Figure 4.56. SOC, status and SOH alterations regarding scenario no: 23

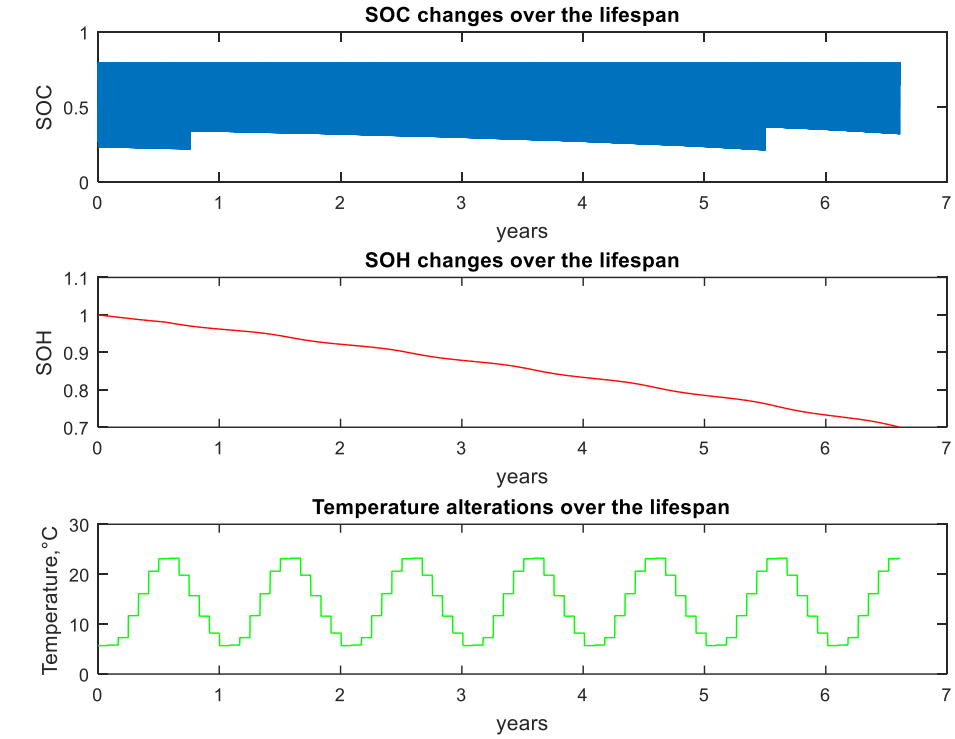

Figure 4.57. SOC, SOH and temperature alterations over lifespan regarding scenario no: 23

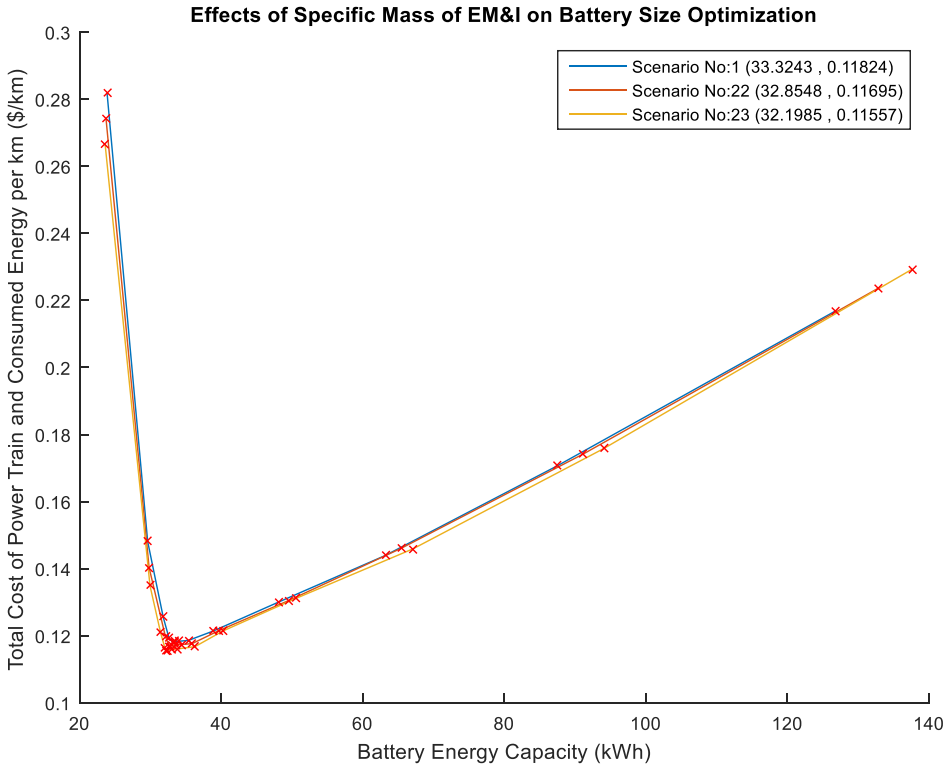

Figure 4.58. Effects of specific mass of EM and inverter

In Figure 4.58 and Table 4.17, the data regarding scenarios no: 1, 22 and 23 are presented. In the figure, how the battery size optimization ends up for each scenario is visualized. Besides, the detailed results regarding the scenarios are given in the table. The optimum battery energy becomes a bit lower when scaling factor for specific mass of EM and inverter is decreased. Since mass of the EM and inverter is decreased, total mass of the BEV and cost of consumed energy per km is reduced. Thus, the objective function is reduced slightly compared to scenario no: 1.

Table 4.17. Outputs regarding scenario no: 1, 22 and 23

		Scenario No		
Parameters	**Unit**	**1**	**22**	**23**
Maximum allowable battery energy	kWh	126.8	132.8	137.6
Optimum battery energy	kWh	33.3	32.9	32.2
Power of battery	kW	186.3	183.8	180.9
Mass of battery	kg	301.9	299.3	295.8
Initial cost of battery	$	8331	8214	8050
Torque of EM	Nm	387	381	374
Power of EM	kW	162.1	159.9	157.4
Mass of EM	kg	147.4	116.3	85.9
Initial cost of EM and Inverter	$	4863	4798	4722
Total mass of BEV	kg	2024.2	1990.6	1956.7
Battery lifetime	years	6.66	6.65	6.61
Total distance traveled in lifetime	km	133216	132960	132213
Range for given test procedure	km	212	210	207
Time for acceleration from 0 to top speed	sec	24.3	24.3	24.4
Consumed energy in one cycle for given test procedure	kWh	3.65	3.63	3.61
Cost of consumed energy per km	$/km	0.0192	0.0191	0.019
Initial cost of power train per km	$/km	0.099	0.0979	0.0966
Objective Function	***$/km***	***0.1182***	***0.117***	***0.1156***

4.10 Investigation of Effects by Test procedure on Battery Size Optimization

In Table 4.18, values of the parameters that define scenarios no: 1, 24, 25, 26 and 27 are given. The "Test procedure" is changed in scenarios no: 24, 25, 26 and 27.

Table 4.18. Values of the parameters regarding scenarios no: 1, 24, 25, 26 and 27

		Scenario No				
Parameters	**Unit**	**1**	**24**	**25**	**26**	**27**
Scaling factor for calendar ageing		1	1	1	1	1
Scaling factor for cycle ageing		1	1	1	1	1
Ageing model in [14]		0	0	0	0	0
Annual distance	km	20000	20000	20000	20000	20000
Cost of electricity	$/kWh	0.11	0.11	0.11	0.11	0.11
Maximum charging power	kW	22	22	22	22	22
Specific cost of battery pack	$/kWh	250	250	250	250	250
Scaling factor for specific mass of battery pack		1	1	1	1	1
Specific cost of EM and inverter	$/kW	30	30	30	30	30
Scaling factor for specific mass of EM and inverter		1	1	1	1	1
Test procedure		WLTP	**Modified WLTP (Only LOW)**	**Modified WLTP (Predominantly LOW)**	**Modified WLTP (Only EXTRA HIGH)**	**Modified WLTP (Predominantly EXTRA HIGH)**

In Figures 4.59 and 4.60, the data regarding scenario no: 24 are presented. In Figure 4.59, the SOC, status and SOH alterations of the battery are visualized for the first few cycles. The SOC, SOH and temperature alterations of the battery are visualized over the lifespan of the battery as in Figure 4.60. In Figures 4.61 and 4.62, the data regarding scenario no: 25 are presented. In Figure 4.61, the SOC, status and SOH alterations of the battery are visualized for the first few cycles. The SOC, SOH and

temperature alterations of the battery are visualized over the lifespan of the battery as in Figure 4.62. In Figures 4.63 and 4.64, the data regarding scenario no: 26 are presented. In Figure 4.63, the SOC, status and SOH alterations of the battery are visualized for the first few cycles. The SOC, SOH and temperature alterations of the battery are visualized over the lifespan of the battery as in Figure 4.64. In Figures 4.65 and 4.66, the data regarding scenario no: 27 are presented. In Figure 4.65, the SOC, status and SOH alterations of the battery are visualized for the first few cycles. The SOC, SOH and temperature alterations of the battery are visualized over the lifespan of the battery as in Figure 4.66.

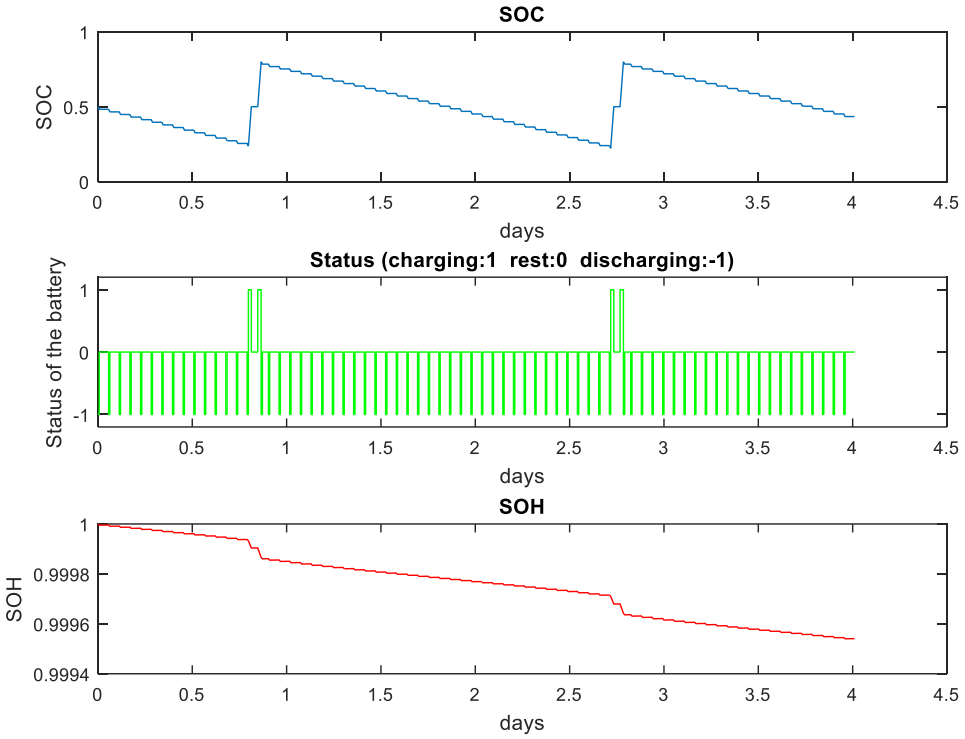

Figure 4.59. SOC, status and SOH alterations regarding scenario no: 24

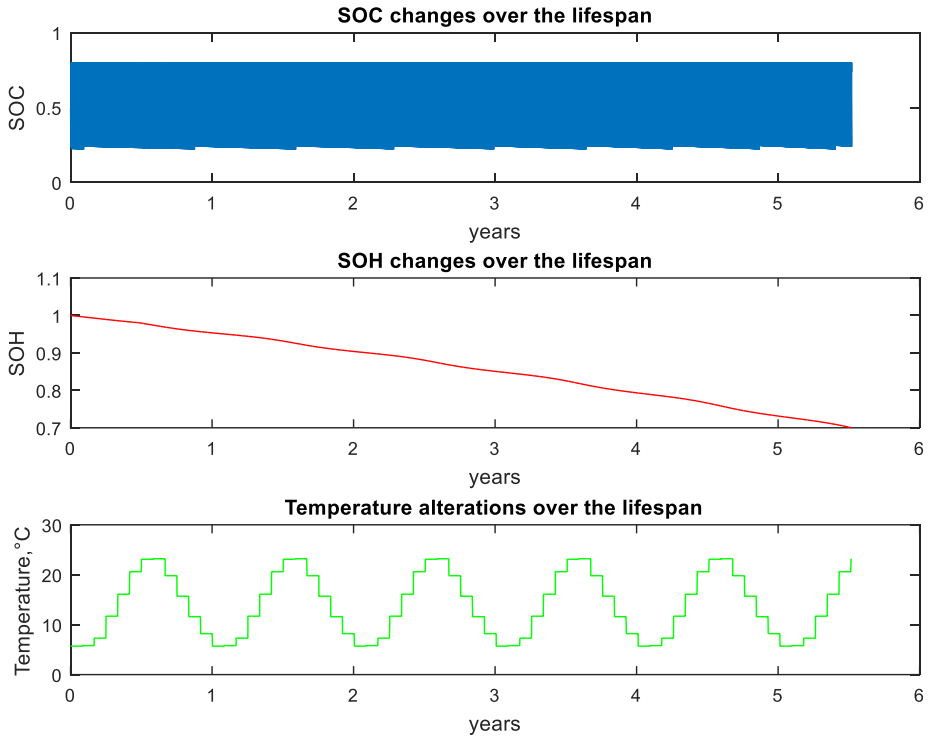

Figure 4.60. SOC, SOH and temperature alterations over lifespan regarding scenario no: 24

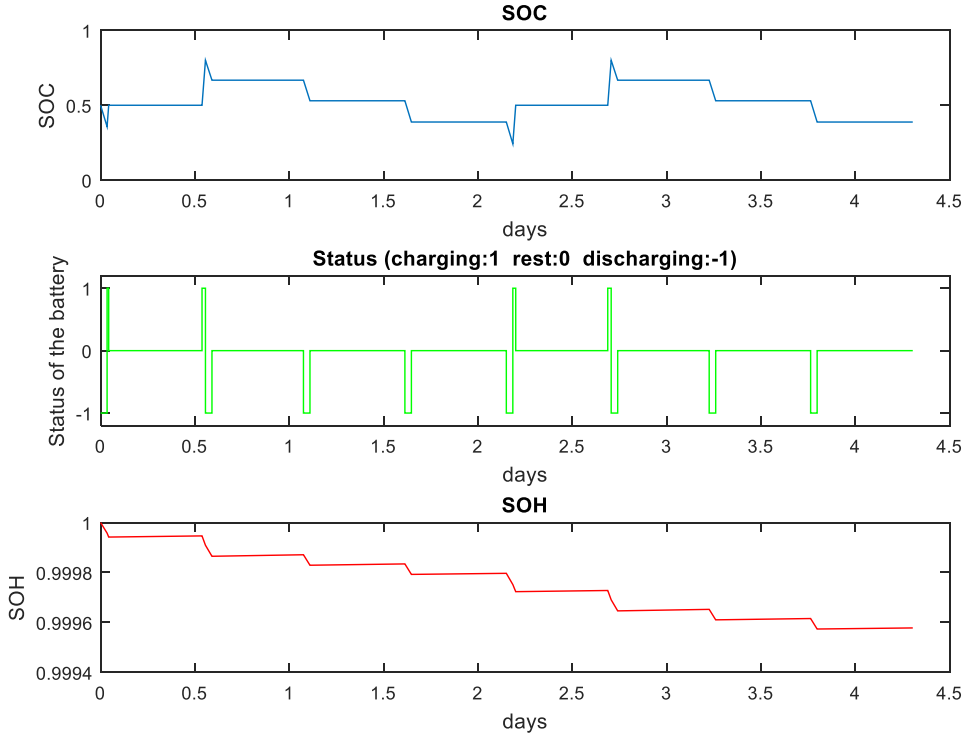

Figure 4.61. SOC, status and SOH alterations regarding scenario no: 25

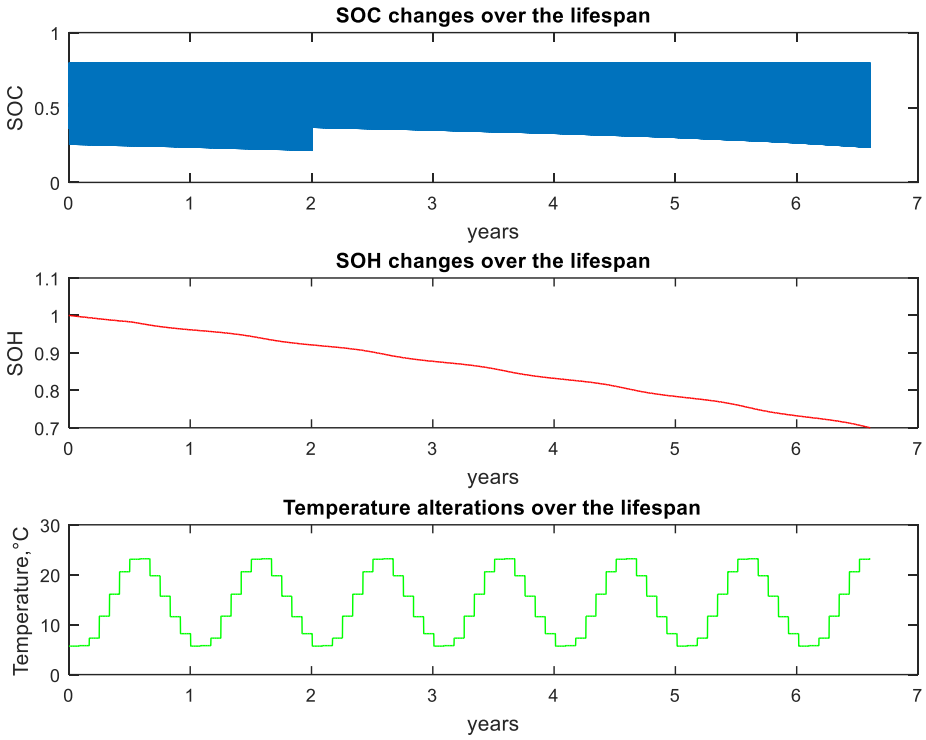

Figure 4.62. SOC, SOH and temperature alterations over lifespan regarding scenario no: 25

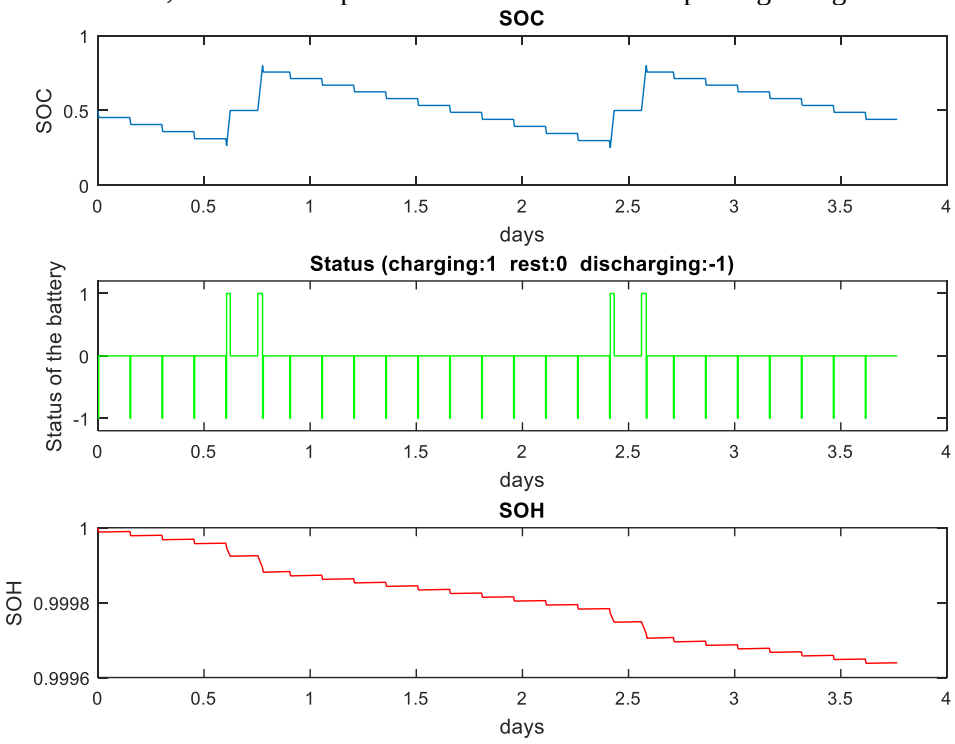

Figure 4.63. SOC, status and SOH alterations regarding scenario no: 26

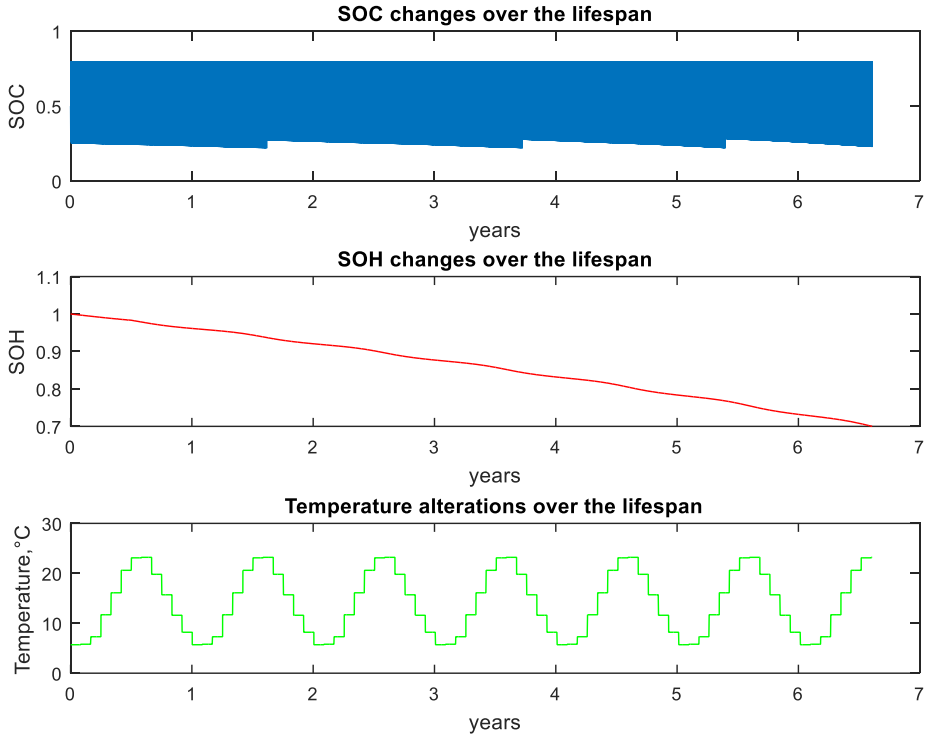

Figure 4.64. SOC, SOH and temperature alterations over lifespan regarding scenario no: 26

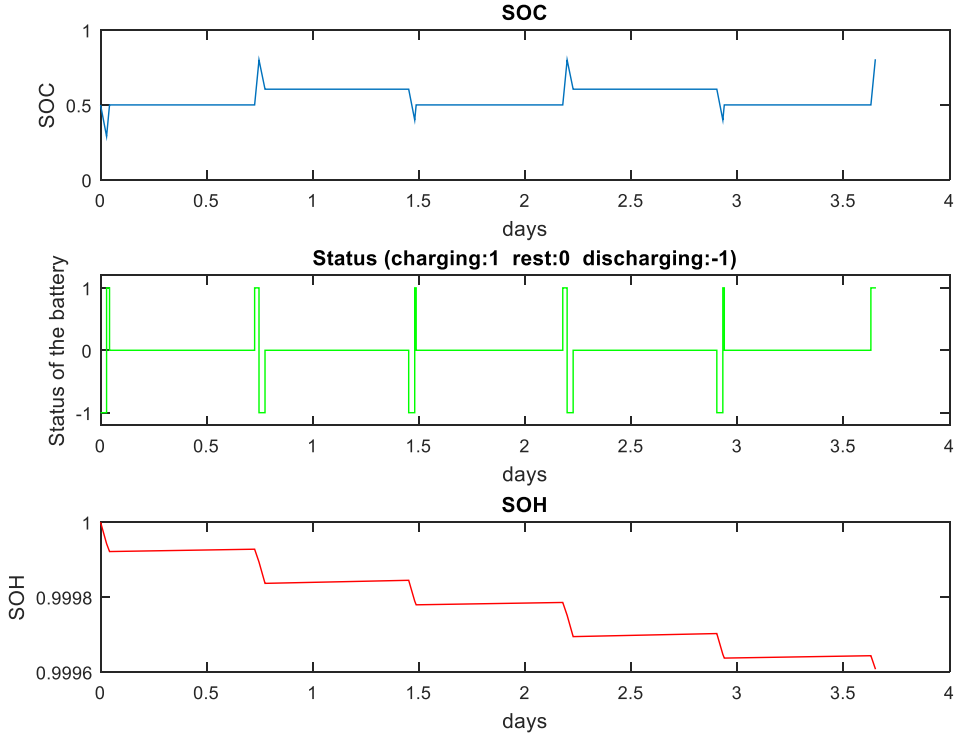

Figure 4.65. SOC, status and SOH alterations regarding scenario no: 27

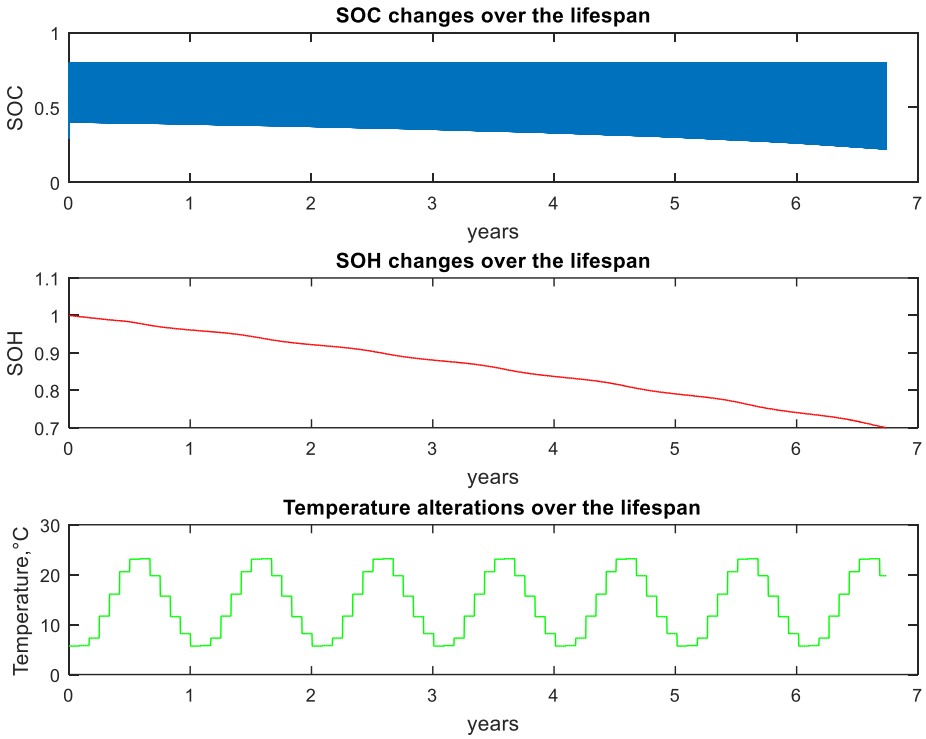

Figure 4.66. SOC, SOH and temperature alterations over lifespan regarding scenario no: 27

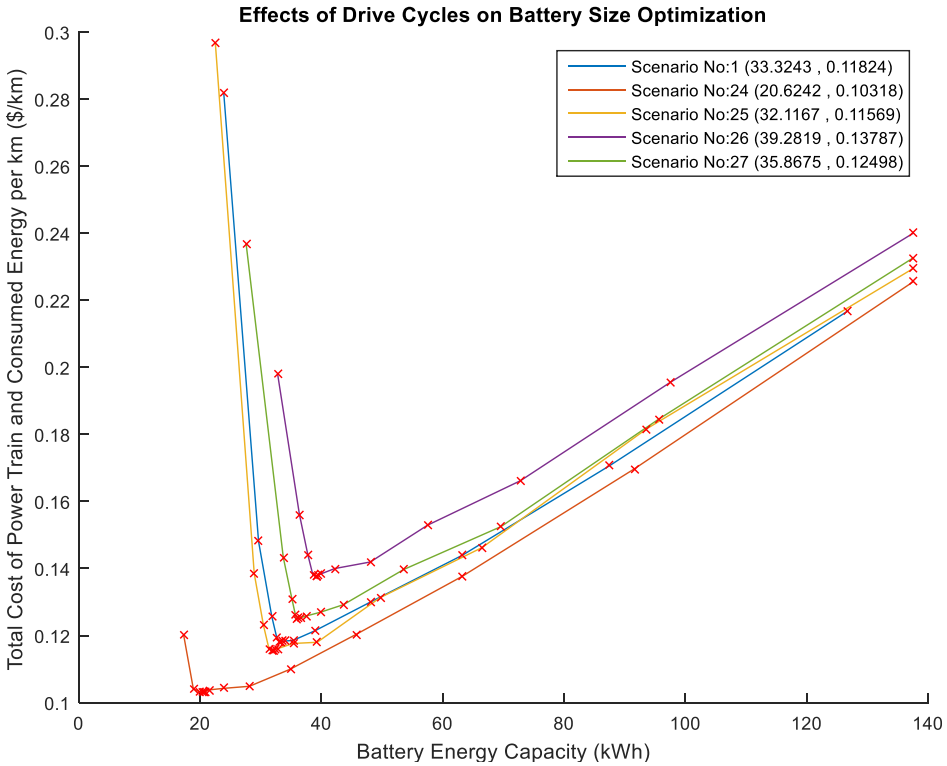

Figure 4.67. Effects of test procedures

In Figure 4.67 and Table 4.19, the data regarding scenarios no: 1, 24, 25, 26 and 27 are presented. In the figure, how the battery size optimization ends up for each scenario is visualized. Besides, the detailed results regarding the scenarios are given in the table. The optimum battery energy increases as average speed of the test procedure is increased, going from the modified WLTP that includes only low speed part to the modified WLTP that includes only extra high speed part. Since mass of the battery pack increases as battery energy is increased, total mass of the BEV and cost of consumed energy per km increase. Thus, the objective function increases in the order of scenarios no: 24, 25, 1, 27 and 26.

Table 4.19. Outputs regarding scenarios no: 1, 24, 25, 26, and 27

		Scenario No				
Parameters	**Unit**	**1**	**24**	**25**	**26**	**27**
Maximum allowable battery energy	kWh	126,8	137,6	137,6	137,6	137,6
Optimum battery energy	kWh	33,3	20,6	32,1	39,3	35,9
Power of battery	kW	186,3	180,4	186,3	189,1	187,6
Mass of battery	kg	301,9	238,7	295,9	331,7	314,6
Initial cost of battery	$	8331	5156	8029	9820	8967
Torque of EM	Nm	387	374	386	393	389
Power of EM	kW	162,1	157	162,2	164,6	163,3
Mass of EM	kg	147,4	142,7	147,4	149,6	148,5
Initial cost of EM and Inverter	$	4863	4710	4865	4937	4899
Total mass of BEV	kg	2024,2	1956,4	2018,3	2056,3	2038,1
Battery lifetime	years	6,66	5,52	6,61	6,61	6,74
Total distance traveled in lifetime	km	133216	110403	132128	132164	134794
Range for given test procedure	km	212	182	217	183	198
Time for acceleration from 0 to top speed	sec	24,3	24,4	24,2	24,2	24,2
Consumed energy in one cycle for given test procedure	kWh	3,65	0,35	4,36	1,77	7,19
Cost of consumed energy per km	$/km	0,0192	0,0138	0,0181	0,0262	0,0221
Initial cost of power train per km	$/km	0,099	0,0894	0,0976	0,1117	0,1029
Objective Function	***$/km***	***0,1182***	***0,1032***	***0,1157***	***0,1379***	***0,125***

4.11 Discussion of Simulation Results

Considering scenarios no: 0 and 1, the effect of minimum range requirement for the WLTP can be seen. If the requirement is strict as given in scenario no: 0, the optimization would not end up with a reduction in the objective function. Thus, it is important to consider the optimization while determining the requirements for an

application. Note that the minimum range requirement for given test procedure is assumed to be waivable in all the scenarios except scenario no: 0 in this study.

Considering scenarios no: 2 and 3, it can be seen that simultaneous improvements on calendar and cycle ageing do not significantly affect the optimal point that the energy capacity converges by the battery size optimization. However, simultaneous improvements can decrease the objective function significantly.

Considering scenario no: 4, the effect of ageing model can be seen. Notice that the biggest differences compared to scenario no:1 regarding the optimized battery energy capacity and resulting objective function in all scenarios occurs in this case. That is, ageing model is the most important parameter for the battery size optimization.

Considering scenarios no: 5, 6, 7 and 8, the effect of C-rate can be seen. As cycle ageing dominates the ageing of the battery, battery size optimization converge to higher values for battery energy capacity. Similarly, C-rate affects the optimization in scenarios no: 9 and 10. As calendar ageing dominates the ageing of the battery due to utilization, battery size optimization converge to lower values for battery energy capacity.

Considering scenarios no: 11, 12, 13, 14 and 15, it can be seen that the reduction in electricity price does not affect the optimal point that the energy capacity converges by the battery size optimization. However, the reduction in electricity price can decrease the objective function significantly. In addition, the change of maximum charging power limit from 22kW to 100kW does not affect the optimal point that the energy capacity converges by the battery size optimization. However, it may be expected that the change of maximum charging power limit would affect the converged point due to effect of C-rate similar to previous scenarios. It is important to note that the maximum C-rate during charging is limited to 0.7C in this work since the cell producer restricts it. Thus, it can be understood that change of maximum charging power limit does not affect the optimization because 22kW already results a C-rate which is pretty close to 0.7C in these scenarios.

Considering scenarios no: 16 and 17, it can be seen that reduction of specific cost of the battery pack slightly affects the optimal point that the energy capacity converges

by the battery size optimization. However, the reduction of specific cost of the battery pack can decrease the objective function significantly.

Considering scenarios no: 18 and 19, it can be seen that reduction of specific mass of the battery pack does not significantly affect the optimal point that the energy capacity converges by the battery size optimization. In addition, the reduction of specific mass of the battery pack decreases the objective function slightly. However, maximum allowable energy capacity is increased by reduction of specific mass of the battery pack.

Considering scenarios no: 20 and 21, it can be seen that reduction of specific cost of the EM and inverter does not affect the optimal point that the energy capacity converges by the battery size optimization. However, the reduction of specific cost of the EM and inverter can decrease the objective function.

Considering scenarios no: 22 and 23, it can be seen that reduction of specific mass of the EM and inverter does not significantly affect the optimal point that the energy capacity converges by the battery size optimization. In addition, the reduction of specific mass of the battery pack decreases the objective function slightly.

Considering scenarios no: 24, 25, 26 and 27, the effect of test procedure can be seen. As average speed of the test procedure is increased, the effect of the cycle ageing dominates the ageing of the battery due to higher C-rate. Thus, battery size optimization converge to higher values for battery energy capacity.

CHAPTER 5

CONCLUSION

In this thesis, batteries are focused on in order to investigate the effects of battery sizing on the feasibility of BEVs. Battery size is optimized under the objective of minimizing the total cost of power train components and consumed energy per km considering battery ageing. Then, the effects of possible future improvements in the technology and alterations in user preferences on battery size optimization are investigated under different scenarios.

Unlike the previous researches in literature, this work draws a more general and bigger picture by investigating the effect of parameters on battery size optimization rather than focusing on a specific case. Firstly, the vehicle dynamic and battery ageing models inspired by the literature are revealed. As explained in Chapter 2, the battery ageing model given in the literature is modified using real ageing data. The models are validated considering a BEV in the market. Using these validated models, the optimization algorithm is developed, as discussed in Chapter 3. Then, assuming that the minimum range requirement for the WLTP is waivable, 9.3% improvement on the objective function by the battery size optimization is presented. Lastly, the effects of possible future improvements in the technology and alterations in user preferences regarding ageing mechanisms, annual distance, price of electricity, specific cost of battery pack, specific mass of battery pack, specific cost of EM and inverter, specific mass of EM and inverter, and test procedures on the battery size optimization are investigated in Chapter 4.

In this study, the major effects on the optimal point that the energy capacity converges by the battery size optimization are observed in the scenarios regarding the test procedures and the battery ageing model. The optimal point that the energy capacity converges by the battery size optimization algorithm takes values from 20.6 kWh

regarding drive only in urban areas to 39.3 kWh regarding drive only in highways. As can be seen, the greatest value for optimal energy capacity is 39.3 kWh for the scenarios regarding the test procedures in this study. On the other hand, some of the BEVs' battery energy capacity in the market may reach up to 100 kWh. Assuming there are sufficient charging facilities so that the long-range vehicles are not needed, this study proposes that BEVs should not have that much battery energy capacity. It is important to notice that this proposition bases on the updated battery ageing model. There exists a huge difference between the optimal value, 73.2 kWh, of the scenario that uses the original ageing model given in the literature and the optimal value, 33.3 kWh, of the scenario that uses the ageing model modified by the real ageing data. The original battery ageing model in the literature results in higher battery energy capacities as the optimal point. That would make the BEVs with high battery energy capacity in the market feasible and nullify the proposition of this work. Note that the battery ageing model is updated using real ageing data, but the data set is very limited. Although the updated battery ageing model is quite consistent, forming a new model using a larger data set and optimizing the battery size will be a good practice for future works.

It is observed that the other possible future improvements in the technology or the alterations in user preferences regarding ageing mechanisms, annual distance, price of electricity, specific cost of battery pack, specific mass of battery pack, specific cost of EM and inverter, and specific mass of EM and inverter do not affect the optimal point significantly. The simultaneous improvements on calendar and cycle ageings do not significantly affect the optimal point that the energy capacity converges by the battery size optimization. However, separate improvements on calendar and cycle ageing mechanisms slightly affect the optimal point. As cycle ageing dominates the ageing of battery, the battery size optimization algorithm converges to higher battery energy capacity values, because the higher battery energy capacity reduces the C-rate which in turn slows down the ageing. The reduction in electricity price does not affect the optimal point significantly as long as the C-rate remains constant. The reduction

of specific cost of the battery pack slightly affects the optimal point. The reduction of specific mass of the battery pack and the reduction of specific mass of the EM and inverter do not affect the optimal point significantly. The reduction of specific cost of the EM and inverter does not affect the optimal point. The maximum allowable energy capacity is increased by reduction of specific mass of the battery pack.

The main motivation for this work is to enable EV manufacturers and OEMs to incorporate the battery size optimization into their strategy for developing and evaluating EVs and components. Since EV producers and OEMs are at the beginning of the value chain, their decisions will shape the potentials of EVs on the market. This study shows what kinds of achievements can be obtained if, taking the battery ageing mechanism into account, the battery size is optimized when designing EVs.

APPENDICES

A. Li-ion Batteries and Their Main Ageing Mechanisms

In battery terminology [36], “cell” that provides ~3V in the case of Li-ion refers the essential element of a battery, “Block” that also provides ~3V in the case of Li-ion refers the parallel-connected multiple cells, “Battery” that provides higher voltage refers the series-connected cells or blocks forming single module, “(Battery) Pack” refers the parallel and/or series-connected batteries.

Basically, a Li-ion cell structure is shown in Figure A.1. As can be seen, it is formed by the combination of the current collector at the anode (negative electrode), anode material, separator, electrolyte, cathode material and the current collector at the cathode (positive electrode).

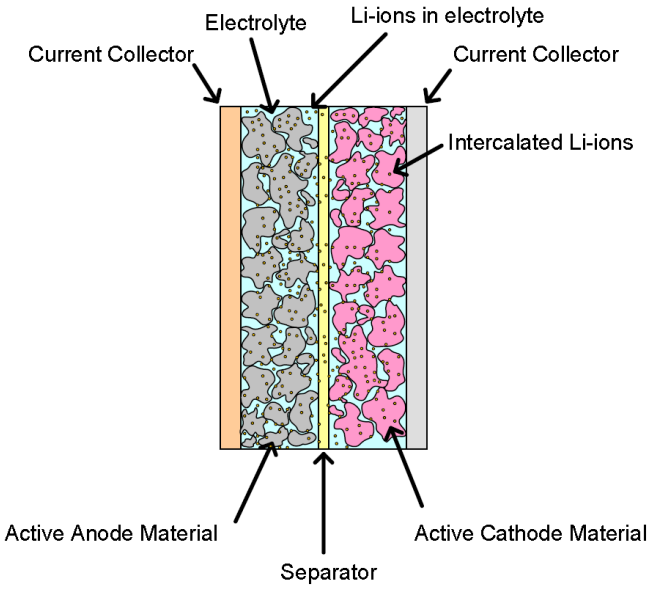

Figure A.1. Schematic illustration of a Li-ion battery [37]

In Figure A.2, common anode and cathode materials used in Li-ion batteries are presented.

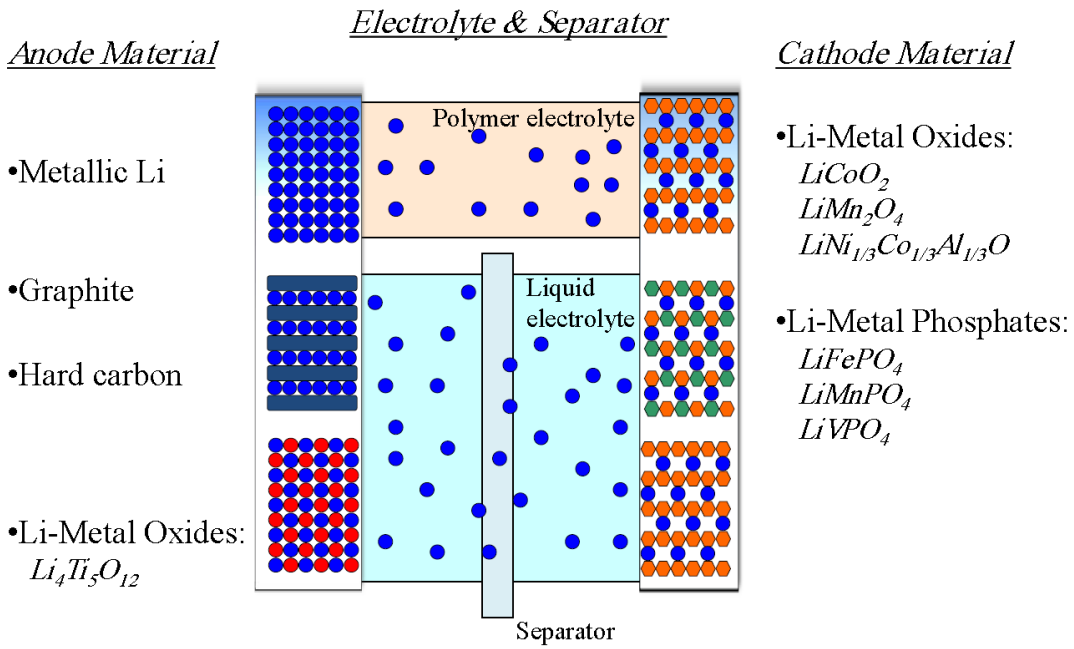

Figure A.2. Overview of the mostly commercialized Li-ion battery concepts [37]

Li-ion cells can be packaged in four main formats, i.e., cylindrical, prismatic, coin and pouch. Depending on the thermal and physical limitations, any type can be preferred. In EVs, cylindrical, prismatic and pouch formats are used widely. In a battery pack in EVs, it is required to provide an overall enclosure whatever the form is. However, the structure highly depends on the format type. Due to chemical reactions, an expansion of cell may be observed. For example, cylindrical cells retain their shape intrinsically against these reactions and need of enclosure is simplified in the case of cylindrical format. In Figure A.3, an illustration of these formats is given:

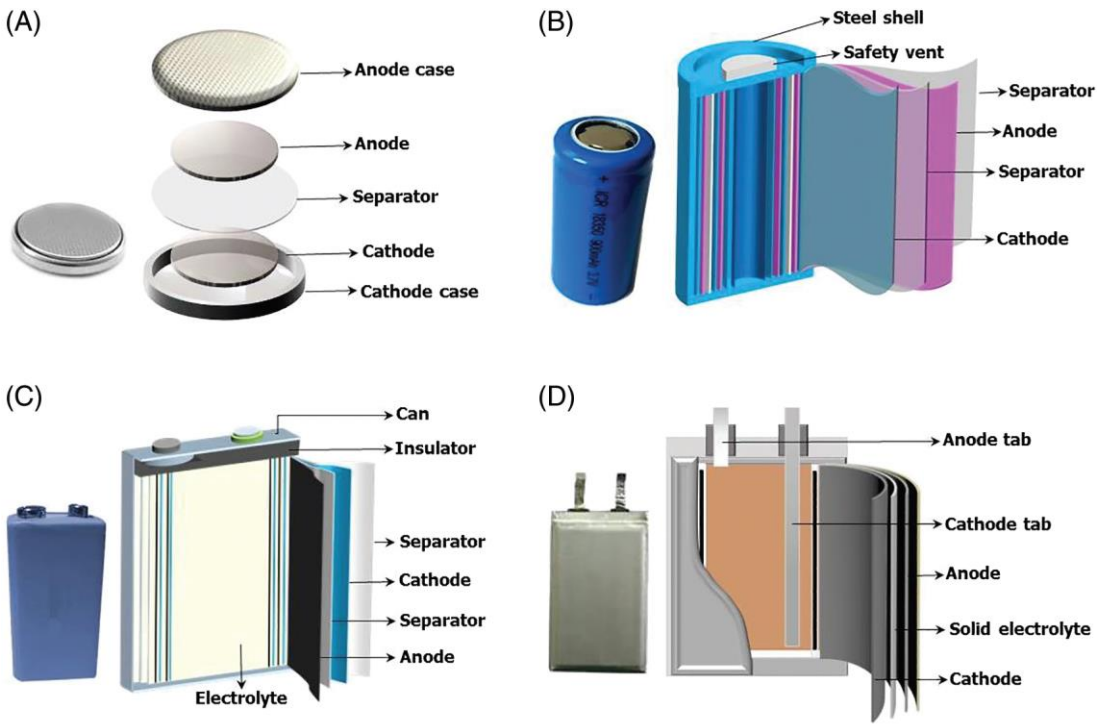

Figure A.3. Types of packaging for Li-ion batteries: (A):Coin, (B):Cylindrical, (C):Prismatic, (D):Pouch [38]

In accordance with the ion chemistry, there are five principal types of Li-ion cells for EVs, i.e., Lithium Nickel Cobalt Aluminum (NCA), Lithium Nickel Manganese Cobalt (NMC), Lithium Manganese Spinel (LMO), Lithium Titanate (LTO) and Lithium-iron phosphate (LFP). These types are based on different combinations of anode and cathode materials. In terms of specific energy, specific power, safety, performance, life span and cost, each type has explicit advantages and disadvantages as shown in Figure A.4 [39].

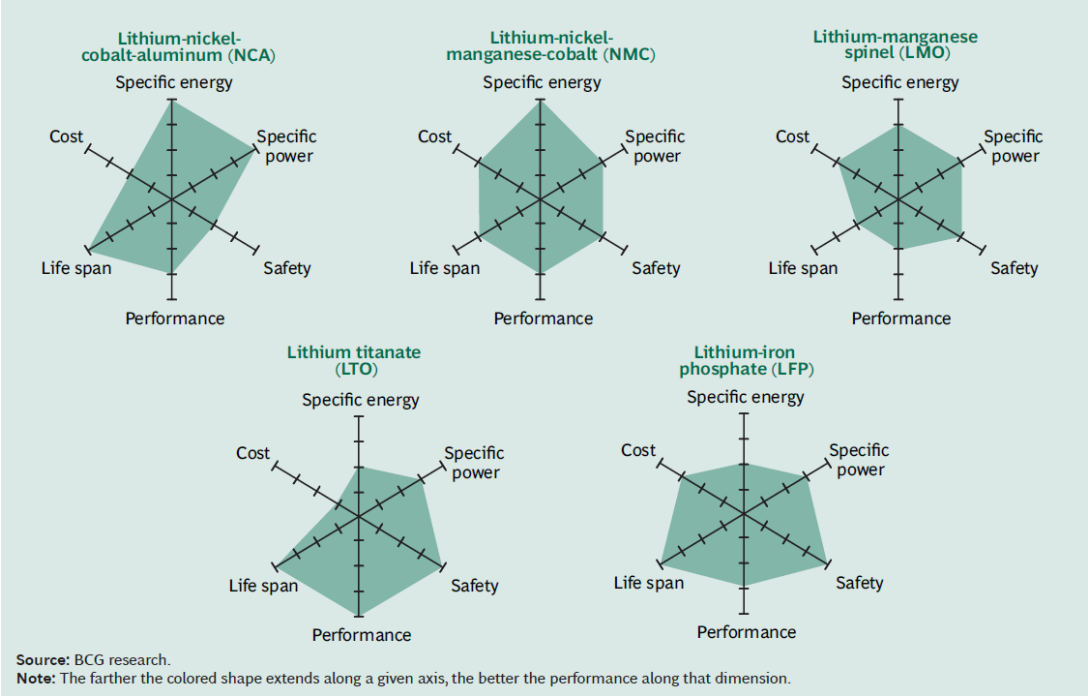

Figure A.4. Tradeoffs among five principal Li-ion battery technologies

Compared to other secondary batteries, Li-ion batteries have

The advantages:

- High specific energy and high load capabilities
- Long cycle and extend shelf-life; maintenance-free
- High capacity, low internal resistance, good coulombic efficiency
- Simple charge algorithm and reasonably short charge times
- Low self-discharge (less than half that of NiCd and NiMH)

The Limitations:

- Require a protection circuit to prevent thermal runaway if stressed
- No rapid charge possible especially at freezing temperatures (<0°C, <32°F)
- Transportation regulations required when shipping in larger quantities

- Degrades especially at high charge and discharge rates and when stored at high voltage and high temperature

Due to above limitations, a battery pack formed by Li-ion cells must be integrated with a battery management system (BMS) that is a technology used to protect the battery and to ensure the operation continues in safe. A BMS monitors the system (temperature, current and voltage), protects the battery, estimates the state of the battery, maximizes the performance of the battery and reports to users and/or external devices [36]. Main state parameters of a battery are state of health (SOH) and state of charge (SOC). A BMS may use any of the direct measurement, the model-based methodology and the data-driven methodology to estimate SOH [40]. Likewise, a BMS may use any of the ampere-hour integral method, looking-up table-based methods, the model-based methods and the data-driven methods to estimate SOC [41]. In addition, a BMS has the functions of charge rate control, thermal management and cell balancing. Thermal management refers to heat or cool the cells by using air or liquid. On the other hand, cell balancing refers to equalize SOC levels between cells connected in series for maximizing the capacity of the battery [36].

Overall, One of the main limitations is degradation. The ageing mechanism must be understood very well to overcome degradation.

Batteries have two main performance parameters: energy capacity and power capability. Power capability depends on the internal impedance. Thus, the degradation mechanisms should be investigated, considering both the capacity fade and the impedance rise. There exist interactions among anode, cathode, separator and electrolyte during charging, discharging and storage. That makes the ageing a very complicated process. But it is still possible to make investigations focusing on the most dominant processes.

Generally, the capacity fade of Li-ion cells is due to a combination of three main processes:

- Loss of Li/loss of balance between electrodes
- Loss of electrode area
- Loss of electrode material/conductivity

The most significant mechanisms for power fade/impedance rise is summarized:

- Surface film formation of both electrodes with low conductivity.
- Loss of electrode area and electrode material leading to a higher local current density.
- Lower diffusivity of lithium ions into active electrode particles and slower kinetics (increased charge transfer resistance) due to surface films
- Reduced conductivity between particles due to both surface films and degradation of binders, possibly in combination with a binder-Li reaction.

In further detail, the ageing mechanisms at negative and positive electrodes can be examined as in Figure A.5 [37].

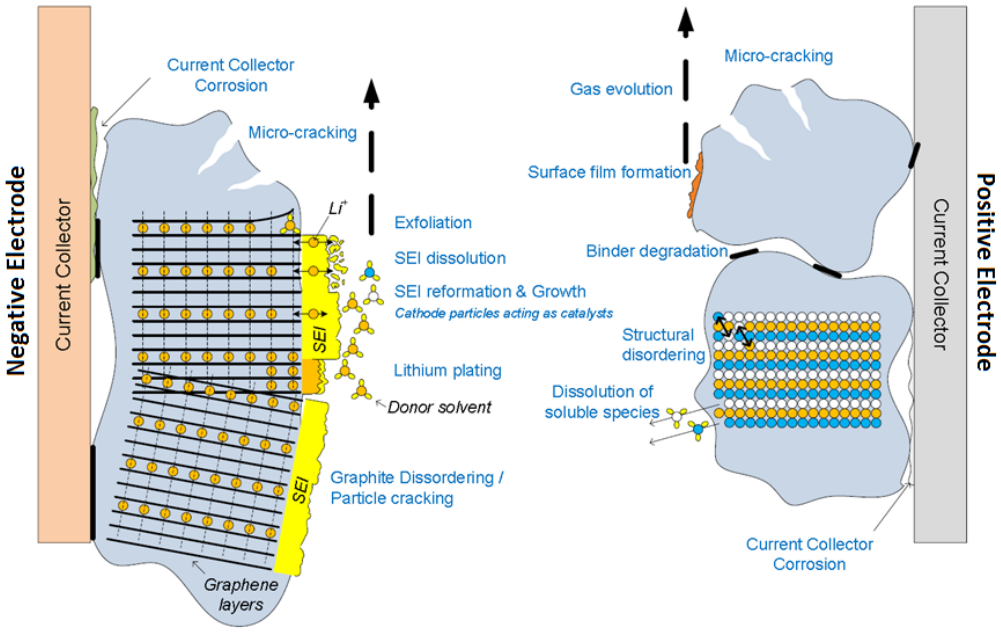

Figure A.5. Main ageing mechanisms occurring at Li-ion battery electrodes [37]

Carbon, in particular graphite, is the most important anode (negative electrode) material in lithium-ion batteries. Thus, the greatest understanding of anode ageing has been accomplished with graphite-based cells. The main ageing factor on graphite electrodes with time is the development of a solid interface on the electrolyte/electrode interface. That is named Solid Electrolyte Interphase (SEI). As the cell is charged for the first time, lithium reacts directly with the graphite to form a thin solid surface film (mainly consisting of Li2CO3, alkyl-carbonates, and polymers). The volume change occurring in the graphite particles upon intercalation / de-intercalation of lithium, which induces graphite exfoliation and creates gas, might lead to micro-cracks in the surface film, which also exposes the graphite to further SEI formation. A high SOC (State Of Charge >80%) should provoke an acceleration of these phenomena as the potential difference between the electrode interfaces and the electrolyte is important. Under high temperatures, the SEI may dissolve and create lithium salts less permeable to the lithium ions, therefore increasing the negative electrode impedance. Low temperatures lead to a decrease in the diffusion of lithium within the SEI and graphite, which can overlay the electrode

with lithium plating. The SEI formation, its development, and the lithium plating are all responsible for the loss of cyclable lithium under conditions of transportation utilization. With time, there is a loss of active surface, increasing the electrode's impedance.

Cause	Effect	Leads to	Reduced by	Enhanced by
Electrolyte decomposition (→SEI) (Continuous side reaction at low rate)	Loss of lithium Impedance rise	**Capacity fade** **Power fade**	Stable SEI (additives) Rate decreases with time	High temperatures High SOC (low potential)
Solvent co-intercalation, gas evolution and subsequent cracking formation in particles	Loss of active material (graphite exfoliation) Loss of lithium	Capacity fade	Stable SEI (additives) Carbon pre-treatment	Overcharge
Decrease of accessible surface area due to continuous SEI growth	Impedance rise	**Power fade**	Stable SEI (additives)	High temperatures High SOC (low potential)
Changes in porosity due to volume changes, SEI formation and growth	Impedance rise Overpotentials	Power fade	External pressure Stable SEI (additives)	High cycling rate High SOC (low potential)
Contact loss of active material particles due to volume changes during cycling	Loss of active material	**Capacity fade**	External pressure	High cycling rate High DOD
Decomposition of binder	Loss of lithium Loss of mechanical stability	Capacity fade	Proper binder choice	High SOC (low potential) High temperatures
Current collector corrosion	Overpotentials Impedance rise Inhomogeneous distribution of current and potential	Power fade Enhances other ageing mechanisms	Current collector pre-treatment (?)	Overdischarge Low SOC (high potential)
Metallic lithium plating and subsequent electrolyte decomposition by metallic Li	Loss of lithium (Loss of electrolyte)	Capacity fade (power fade)	Narrow potential window	Low temperature High cycling rates Poor cell balance Geometric misfits

Figure A.6. Li-ion anode ageing – causes, effects, and influences [42]

Main changes on the cathode (positive electrode):

- ageing of active material
- degradation or changes of electrode components like conducting agents, binder, corrosion of current collector
- oxidation of electrolyte components and surface film formation
- interaction of ageing products with the negative electrode.

To sum up, there exist many ageing mechanisms regarding interaction among anode, cathode, separator and electrolyte during charging, discharging and storage.

REFERENCES

[1] "Tracking Transport – Analysis - IEA." [Online]. Available: https://www.iea.org/reports/tracking-transport-2019. [Accessed: 25-Feb-2020].

[2] A. Bacchini and E. Cestino, "Electric VTOL configurations comparison," *Aerospace*, vol. 6, no. 3, 2019.

[3] (IICEC/SABANCI UNIVERSITY) Üçok, Mehmet Doğan, "Iicec Energy and Climate Research Paper Hydrogen Fuel Cell Vehicles," no. August, 2019.

[4] "Compare electric vehicles - EV Database." [Online]. Available: https://ev-database.org. [Accessed: 22-Aug-2021].

[5] "Types of Lithium-ion Batteries – Battery University." [Online]. Available: https://batteryuniversity.com/learn/article/types_of_lithium_ion. [Accessed: 13-Mar-2020].

[6] "Types of Battery Cells; Cylindrical Cell, Button Cell, Pouch Cell." [Online]. Available: https://batteryuniversity.com/learn/article/types_of_battery_cells. [Accessed: 13-Mar-2020].

[7] "Introduction to Electric Vehicle Battery Systems - Technical Articles." [Online]. Available: https://www.allaboutcircuits.com/technical-articles/introduction-to-electric-vehicle-battery-systems. [Accessed: 25-Feb-2020].

[8] "About Us – Chariot Motors." [Online]. Available: https://chariot-electricbus.com/about/. [Accessed: 25-Feb-2020].

[9] B. Gao, L. Guo, Q. Zheng, B. Huang, and H. Chen, "Acceleration speed optimization of intelligent EVs in consideration of battery aging," *IEEE Trans. Veh. Technol.*, 2018.

[10] S. Sabatini and M. Corno, "Battery aging management for Fully Electric Vehicles," *2018 Eur. Control Conf. ECC 2018*, pp. 231–236, 2018.

[11] O. Teichert, F. Chang, A. Ongel, and M. Lienkamp, "Joint Optimization of Vehicle Battery Pack Capacity and Charging Infrastructure for Electrified Public Bus Systems," *IEEE Trans. Transp. Electrif.*, vol. 5, no. 3, pp. 672–682, 2019.

[12] A. Ostadi and M. Kazerani, "Optimal sizing of the battery unit in a plug-in electric vehicle," *IEEE Trans. Veh. Technol.*, vol. 63, no. 7, pp. 3077–3084, 2014.

[13] A. Babin, N. Rizoug, T. Mesbahi, D. Boscher, Z. Hamdoun, and C. Larouci, "Total Cost of Ownership Improvement of Commercial Electric Vehicles Using Battery Sizing and Intelligent Charge Method," *IEEE Trans. Ind. Appl.*, vol. 54, no. 2, pp. 1691–1700, 2018.

[14] A. Berrueta, M. Heck, M. Jantsch, A. Ursúa, and P. Sanchis, "Combined dynamic programming and region-elimination technique algorithm for optimal sizing and management of lithium-ion batteries for photovoltaic plants," *Appl. Energy*, vol. 228, no. February, pp. 1–11, 2018.

[15] U.S. Department of Energy, "Electrical and Electronics Technical Team

Roadmap," *U.S. DRIVE Partnersh.*, no. October, p. 9, 2017.
[16] I. Husain *et al.*, "Electric Drive Technology Trends, Challenges, and Opportunities for Future Electric Vehicles," *Proc. IEEE*, vol. 109, no. 6, pp. 1039–1059, 2021.
[17] I. Stokes, "Technology Roadmap," *Train. Proj. Manag.*, pp. 241–246, 2020.
[18] S. Grolleau, A. Delaille, and H. Gualous, "Predicting lithium-ion battery degradation for efficient design and management," *World Electr. Veh. J.*, vol. 6, no. 3, pp. 549–554, 2013.
[19] ACEA, "Car emissions testing facts." 2016.
[20] European Commission, "Commission Regulation (EU) 2017/1151 of 1 June 2017 supplementing Regulation (EC) No 715/2007 of the European Parliament and of the Council on type-approval of motor vehicles with respect to emissions from light passenger and commercial vehicles (Euro 5 a," *Off. J. Eur. Union*, no. 692, pp. 1–643, 2017.
[21] "Homepage | UNECE." [Online]. Available: https://unece.org/. [Accessed: 14-Feb-2021].
[22] K. Reif, *Brakes , Brake Control and Driver Assistance Systems: Function, Regulation and Components*. 2014.
[23] B. Ozpineci and Ph.D, "Recent Advances in Electric Drive Technologies for Electric Vehicles," 2016.
[24] J. Schmalstieg, S. Käbitz, M. Ecker, and D. U. Sauer, "From accelerated aging tests to a lifetime prediction model: Analyzing lithium-ion batteries," *2013 World Electr. Veh. Symp. Exhib. EVS 2014*, 2014.
[25] J. Wang *et al.*, "Degradation of lithium ion batteries employing graphite negatives and nickel-cobalt-manganese oxide + spinel manganese oxide positives: Part 1, aging mechanisms and life estimation," *J. Power Sources*, vol. 269, pp. 937–948, 2014.
[26] S. F. Schuster *et al.*, "Nonlinear aging characteristics of lithium-ion cells under different operational conditions," *J. Energy Storage*, vol. 1, no. 1, pp. 44–53, 2015.
[27] "ID.4." [Online]. Available: https://www.vw.com/en/models/id-4.html. [Accessed: 29-Jun-2021].
[28] "Volkswagen ID.4 1st price and specifications - EV Database." [Online]. Available: https://ev-database.org/car/1273/Volkswagen-ID4-1st. [Accessed: 29-Jun-2021].
[29] "Volkswagen ID.4 Features and Specs." [Online]. Available: https://www.caranddriver.com/volkswagen/id4/specs. [Accessed: 29-Jun-2021].
[30] BMW, "Service and Warranty Information 2016 BMW i3," pp. 1–30, 2016.
[31] Jaguar Land Rover Limited, "All-electric Jaguar I-PACE," p. 54, 2018.
[32] R. Quadrelli, "World energy prices," *IEA Energy prices*, 2020.
[33] "İklim: Istanbul - İklim grafiği, Sıcaklık grafiği, İklim tablosu, Su sıcaklığı Istanbul - Climate-Data.org." [Online]. Available: https://tr.climate-data.org/asya/tuerkiye/istanbul/istanbul-715086/. [Accessed: 18-Aug-2021].

[34] D. G. Luenberger and Y. Ye, *Linear and Nonlinear Programming*, 4th ed. .
[35] B. Veronika Henze, "Battery Pack Prices Cited Below $100/kWh for the First Time in 2020, While Market Average Sits at $137/kWh | BloombergNEF." [Online]. Available: https://about.bnef.com/blog/battery-pack-prices-cited-below-100-kwh-for-the-first-time-in-2020-while-market-average-sits-at-137-kwh/. [Accessed: 29-Jun-2021].
[36] D. Andrea, *Battery Management Systems for Large Lithium-Ion Battery Packs*. 2010.
[37] J. Groot, "State-of-health estimation of Li-ion batteries: cycle life test methods," *PhD, CHALMERS Univ. Technol.*, p. 138, 2012.
[38] Y. Liang *et al.*, "A review of rechargeable batteries for portable electronic devices," *InfoMat*, vol. 1, no. 1, pp. 6–32, 2019.
[39] A. Dinger *et al.*, "Batteries for Electric Cars: Challenges, Opportunities, and the Outlook to 2020," *BCG*, 2010.
[40] X. Hu, J. Jiang, D. Cao, and B. Egardt, "Battery health prognosis for electric vehicles using sample entropy and sparse Bayesian predictive modeling," *IEEE Trans. Ind. Electron.*, vol. 63, no. 4, pp. 2645–2656, 2016.
[41] R. Xiong, J. Cao, Q. Yu, H. He, and F. Sun, "Critical Review on the Battery State of Charge Estimation Methods for Electric Vehicles," *IEEE Access*, vol. 6, pp. 1832–1843, 2017.
[42] J. Vetter *et al.*, "Ageing mechanisms in lithium-ion batteries," *J. Power Sources*, vol. 147, no. 1–2, pp. 269–281, 2005.